Modeling of Structural Damage of Older Reinforced Concrete Components

Catherine Ann Pagni

A thesis submitted in partial fulfillment of the requirements for the degree of

Master of Science in Civil Engineering

University of Washington

2003

Program Authorized to Offer Degree:
Department of Civil and Environmental Engineering

Table of Contents

List of Figures v
List of Tables vii
Chapter One: Introduction 1
1.1 Background and Research Impetus 1
1.2 Research Objectives 1
1.3 Thesis Organization 3
Chapter Two: Literature Review 6
2.1 Introduction 6
2.2 Damage Measures 6
2.3 Experimental Data 7
2.3.1 Specimen Design Details 7
2.3.2 Interior Joint Specimens 9
2.3.3 Exterior Joint Specimens 11
2.3.4 Influence Factors for Behavior Variation 13
2.4 Methods of Repair 15
2.5 Predicting Damage as a Function of Demand 17
2.5.1 Fragility Curves 17
2.5.2 Testing goodness-of-fit 18
2.5.3 Distribution Selection 19
2.5.4 Method of Maximum Likelihood 23
2.6 Loss Estimation 24
Chapter Three: Damage Measures 26
3.1 Introduction 26
3.2 Damage Measures 26
3.2.1 Progression of Damage 27
3.2.2 Damage States 27

3.3 Cracking 28
3.3.1 Damage State 0 28
3.3.2 Damage State 1 29
3.3.3 Damage States 2, 3, and 5 29
3.3.4 Damage State 9 30
3.4 Concrete Spalling and Crushing 31
3.4.1 Damage State 6 31
3.4.2 Damage State 8 32
3.4.3 Damage State 10 33
3.4.4 Damage State 11 33
3.5 Joint Failure Mechanisms 34
3.5.1 Damage State 12(a) 34
3.5.2 Damage State 12(b) 35
3.5.3 Damage State 12(c) 35
3.6 Strength-based Damage Measures 35
3.6.1 Damage State 4 36
3.6.2 Damage State 7 36
3.7 Conclusion 38
Chapter Four: Engineering Demand Parameters and Experimental Data 40
4.1 Introduction 40
4.2 Experimental Data 40
4.2.1 Type of Joint 40
4.2.2 Identify Data Points 41
4.3 Engineering Demand Parameters 41
4.3.1 Drift Ratio 42
4.3.2 Number of Cycles 43
4.3.3 Nonlinear Function of the Drift and Cycles 44
4.3.4 Joint Strain 45
4.4 Conclusion 46

Chapter Five: Methods of Repair 47
5.1 Introduction 47
5.2 Repair of Damage Measures 47
5.3 Method of Repair 0: Cosmetic Repair 48
5.3.1 Demolition 48
5.3.2 Finish Work 48
5.4 Method of Repair 1: Epoxy Resin Injection of Cracked Concrete 49
5.4.1 Epoxy Resin 49
5.4.2 Advantages and Disadvantages 50
5.5 Method of Repair 2: Patching of Spalled Concrete 50
5.5.1Cementitious Material 50
5.5.2 Advantages and Disadvantages 51
5.6 Method of Repair 3: Removal and Replacement of Damaged Concrete 51
5.6.1 New Concrete and Formwork 51
5.6.2 Shoring 51
5.6.3 Advantages and Disadvantages 51
5.7 Method of Repair 4: Removal and Replacement of Damaged Rebar 52
5.7.1 New Rebar 52
5.7.2 Shoring 52
5.7.3 Advantages and Disadvantages 52
Chapter Six: Predicting Damage as a Function of Demand 54
6.1 Introduction 54
6.2 Data Sets 54
6.2.1 Data Set One 55
6.2.2 Data Set Two 56
6.2.3 Data Set Three 56
6.2.4 Comparison of Data Sets 56

6.3 Distribution Selection 57
6.3.1 Step-wise CDF 57
6.3.2 Normal Distribution 59
6.3.3 Lognormal Distribution 59
6.3.4 Weibull 60
6.3.5 Beta 61
6.3.6 Best Distribution 62
6.4 Method of Maximum Likelihood 64
6.5 Fragility Curves for Selected EPDs 67
6.5.1 Number of Cycles 68
6.5.2 Nonlinear function of drift and cycles 69
6.5.3 Joint Strain 70
6.5.4 Nonlinear function o f Joint Strain and Cycles 71
6.5.5 Comparison of the EDPs 71
6.6 Uncertainty 72
6.7 Conclusion 74
Chapter Seven: Loss Estimation 75
7.1 Introduction 75
7.2 Cost Framework 75
7.2.1 Labor 75
7.2.2 Equipment 77
7.2.3 Repair Materials 78
7.3 Markups 79
7.3.1 Labor Conditions 79
7.3.2 Mobilization 80
7.3.3 Delays due to the Earthquake 80
7.3.4 Overhead and Profit 80
7.3.5 Uncertainty 80

7.4 Unit Cost per Method of Repair 81
7.4.1 Method of Repair 0 81
7.4.2 Method of Repair 1 82
7.4.3 Method of Repair 2 82
7.4.4 Method of Repair 3 83
7.4.5 Method of Repair 4 83
7.5 Downtime per Method of Repair 84
Chapter Eight: Example 91
8.1 Introduction 91
8.2 Example Building 91
8.2.1 Building Dimensions 92
8.2.2 Joint Dimensions 92
8.3 Demand Parameter 92
8.4 Earthquake Loss Assessment 93
8.4.1 Predicting Damage for Given Demand 93
8.4.2 Markups 94
8.5 Moderate Earthquake Demand 95
8.5.1 Contract Price 96
8.5.2 Downtime 97
8.6 Severe Earthquake Demand 97
8.6.1 Contract Price 98
8.6.2 Downtime 99
8.7 Uncertainty 99
8.8 Conclusion 99
Chapter Nine: Conclusions 101
9.1 Summary 101
9.2 Conclusions 102
9.3 Improvements of the Prediction of the Economic Impact 104
9.4 Projected Use of Model 105

List of References 106
Appendix A Design Details of Joint Specimens 110
Appendix B Joint Strain from Curvature Measurements 113
Appendix C Best Engineering Demand Parameter 115
Appendix D Questions and Answers from Interviews 118
Appendix E Best Distribution 122
Appendix F Modeling of Beam-Column Joints in OpenSEES 124

List of Figures

Figure 1.1: Flowchart identifies the link between the traditional concerns of the engineer with the traditional concerns of the owner..... 2

Figure 2.1: (a) Exterior joint detail demonstrates anchorage of beam rebar bent into the joint. (b) The same joint exhibits shear failure of the beam. (Hakuto 2000)..... 13
Figure 2.2: Detail of exterior joint specimen O7 demonstrates anchorage of beam rebar bent into the column. (Hakuto 2000)..... 13
Figure 2.3: The proper labeling of the width and depth of the beam-column joint..... 15
(Adapted from Pessiki 1990). 15
Figure 2.4: Probability density functions of the Lognormal and Normal distributions. (Haldar and Mahadevan, 2000)..... 21
Figure 2.5: Probability density functions for the Beta distribution for varying values of the beta function parameters. (Haldar and Mahadevan, 2000)..... 23

Figure 3.1: Interior joint specimen PEER 22 exhibits Damage State 1 partially hidden by instrumentation and Damage State 0 from the previous load cycle. (Walker 2001) 29
Figure 3.2: Interior joint specimen CD30 22 exhibits Damage State 5. (Walker 2001)... 30
Figure 3.3: Exterior joint specimen 07 exhibits Damage State 9. (Hakuto 2000)..... 31
Figure 3.4: Interior joint specimen PEER 22 exhibits Damage State 6. (Walker 2001) .. 32
Figure 3.5: Interior joint specimen PEER 14 exhibits Damage State 8. (Walker 2001) .. 33
Figure 3.6: Interior joint specimen C15 14 exhibits Damage State 11. (Walker 2001) ... 34
Figure 3.7: An existing joint in Caracas, Venezuela exhibits Damage State 12 after an earthquake. (Portland Cement Association, 1967) 35
Figure 3.8: Response hysteresis for specimen P8 (Pessiki 1990)..... 37
Figure 3.9: (a) Response hysteresis of specimen P4 (b) Response hysteresis of specimen P7 (Pessiki 1990) 38

Figure 4.1: The damage states are identified on the response hysteresis of specimen PEER 22. (Adapted from Walker 2001)..... 41
Figure 4.1: Typical loading set-up of beam-column joint sub-assemblage. 42
Figure 4.2: Number of cycles counted for the load history of specimen PADH 14. (Walker 2001)..... 44
Figure 4.3: Joint strain is measured by the large shear rig (Alire 2002)..... 45

Figure: 6.1: Scatter plots showing the demand at which each damage state (0-12) occurs for all 25 specimens. (a)Drift Ratio (%) (b)Number of cycles (c) Nonlinear Function of drift and cycles (d) Joint strain 55
Figure 6.2: Results of Kolmogorov-Smirnov test applied to the three data sets. 56
Figure 6.3: The probability of exceeding each of the five repair groups evaluated using the Stepwise CDF. 58

Figure 6.4: Fragility curves for the repair methods 0-4 evaluated using the normal distribution. 59
Figure 6.5: Fragility curves for the repair methods 0-4 evaluated using the lognormal distribution. 60
Figure 6.6: Fragility curves for the repair methods evaluated using the Weibull distribution. 61
Figure 6.7: Fragility curves for the repair methods evaluated using the Beta distribution. 62
Figure 6.8: Kolmogorov-Smirnov test results. (a)Comparison of the test parameters for each distribution and the critical value. (b)Comparison of the probability of the test parameters being less than the critical value..... 63
Figure 6.9: Probability of exceeding the repair method evaluated using the method of maximum likelihood to determine the lognormal parameters. 66
Figure 6.10: Chi-Square test results show that the method of maximum likelihood yields a smaller error and thus will be used to determine the fragility curves. 67
Figure 6.11: Prediction of the method of repair given the number of cycles. 68
Figure 6.12: Prediction of the method of repair for a nonlinear function of drift ratio and number of cycles. 69
Figure 6.13: Prediction of the method of repair given the demand in terms joint strain.. 70
Figure 6.14: Predication of the method of repair given the demand in terms of nonlinear function of joint strain and number of cycles. 71
Figure 6.15: Results of the Kolmogorov-Smirnov test applied to the selected EDPs for data set two. 72

Figure 8.1: The joint demand is linked to a probability of requiring a specific method of repair using the fragility curves. 81

List of Tables

Table 5.1: Damage states assigned to each repair technique. 47

Table 6.1: Stepwise CDF for Method of Repair 0. 58
Table 6.2: The results of the Chi-Square test for Method of Repair 0. 64
Table 6.3: Evaluating the confidence parameters of data set one. 73

Table 7.1: Approximate downtime per joint using the time allotted to each method of repair according to the 2003 National Renovation and Insurance Repair Estimator cost book. 90

Table A.1: Design details for interior joint specimens. 110
Table A.2: Design details for exterior joint specimens. 111
Table A.3: Variation of behavior due to 3 factors. 112

Table C.1: Best EDP. 115
Table C.2: Best EDP. 116
Table C.3: Best EDP. 117

Table E.1: Best Distribution. 122
Table E.2: Best Distribution. 122
Table E.3: Best Method. 123

Acknowledgements

This research would not have been possible without the guidance, advice, and enthusiasm of Professor Laura Lowes. The interest and critique of Professor Stanton and Professor Eberhard improved the quality of this paper. Thank you for serving on my committee.

Interviews with professionals from industry made a significant part of this research possible. Thank you Steve Savage of Coughlin, Porter, and Lundeen; Harvey Coffman and Jugesh Kapur of the Washington Department of Transportation; Roger Runacres of Contech Services, Inc.; Dave Juraszek of Juraszek Concrete Construction; and Jared Cole of T.Y. Lin.

Discussions with other people involved with PEER provided valuable insight and further improved the quality of this research. Thank you to those who gave feedback on the content of poster presentations, to those in 235, and to Steve Walker for his willingness to communicate through email.

Thank you to the Pacific Earthquake Engineering Research center, PEER, and the National Science Foundation, NSF, for the funding for this research.

To my family

Chapter One
Introduction

1.1 Background and Research Impetus

Performance-Based Earthquake Engineering (PBEE) initiates investigation into the development of tools engineers can use to better portray earthquake risk. The design of a structure achieves a specific level of structural performance identified by PBEE for a specific level of earthquake loading. To enable a building owner to evaluate the structural performance of a building of a specific design, the owner requires an estimate of the economic impact associated with each design. For an existing structure, the building owner requires an estimate of the economic impact associated with older design without retrofitting.

The building owner requires information regarding the economic impact of the earthquake in terms of the cost of repair work and the cost associated with downtime. Engineers traditionally have not characterized building performance using economic impact measures, but instead have associated performance with response parameters that are the output of a structural analysis. Thus, engineers require models linking economic impact measures to traditional structural response parameters.

Calculation of the total earthquake loss posed by a particular structural design requires multiple models that can be used to predict economic loss associated with structural, non-structural and contents damage as well as loss of building use. The contribution of structural damage to the total economic impact offers the greatest potential for an accurate and reliable predictive model. Models linking repair cost and time with structural response parameters may be developed using the data from experimental models determine the economic impact due to earthquake induced damage.

1.2 Research Objectives

The objective of the current study is to develop a model linking economic impact with structural response parameters for a structural component with particular design details. Specifically, the current project develops a technique for predicting the economic impact associated with damage to an older reinforced concrete beam-column joint. The technique is developed using the process outlined in the Figure 1.1.

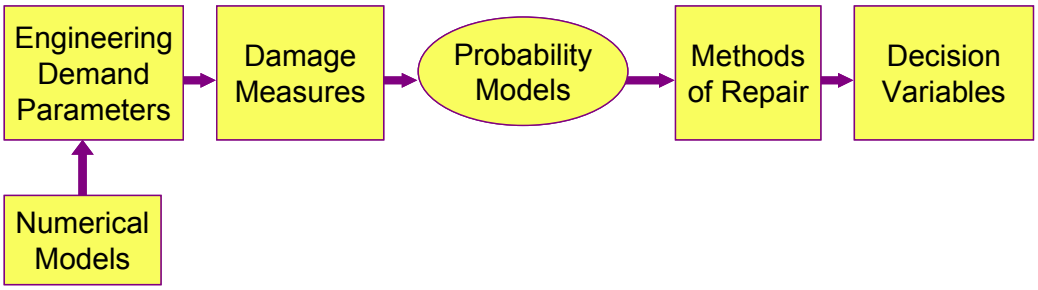

Figure 1.1: Flowchart identifies the link between the traditional concerns of the engineer with the traditional concerns of the owner.

The primary steps of the process are linking the engineering demand parameters to the damage measures to the decision variables. These terms are part of the nomenclature developed by the Pacific Earthquake Engineering Research Center (PEER). An ongoing effort by PEER to improve seismic design and performance of structural components identified these terms and developed simulation software. The numerical models required to generate the structural response parameters is called OpenSees. The application of OpenSees for modeling beam-column joint is currently investigated at the University of Washington.

An engineering demand parameter (EDP) is the measure of earthquake demand on a structural component. The demand on a beam-column joint during an earthquake can be estimated using nonlinear dynamic analysis. The EDP should reflect the deformation and the fatigue sustained by the joint. Possible demand parameters are displacement, number of cycles, and joint strain. The demand parameter most appropriate for the modeling beam-column joints is identified in this report.

A damage measure (DM) is a measure of damage sustained by a structural component. Damage measures are quantified as damage states. The damage states describe the progression of damage sustained by a beam-column joint using experimental investigations of the sub-assemblage performance under seismic loading. The methods of repairing these damage states are investigated and presented. The damage states define the extent of concrete and reinforcement damage in terms of cracking, crushing, and three types of failure mechanisms.

Probability models link the EDP to the damage measure and ultimately, the method of repair. The probability of exceeding the damage requiring a specific method of

repair is modeled in the form of fragility curves. The fragility curves indicate the probability a method of repair will be required for a given demand parameter. The data used to generate the fragility curves is the damage data derived from experimental studies. The damage states are grouped by the method of repair most appropriate for restoring the damaged joint to its original capacity.

A decision variable (DV) is the information regarding building performance required by an owner or insurer. Decision variables are the cost due to repair work and the cost associated with downtime and estimates the economic impact due to earthquake induced damage. Cost estimation is discussed with structural engineers on the West Coast. The job cost of each method of repair is estimated using information from these interviews and from construction cost books and software. The total loss due to earthquake induced damage sustained by beam-column joints is determined for an example building at the end of the report. The technique for predicting the economic impact due to earthquake damage developed here could be applied to develop similar models for other components.

1.3 Thesis Organization

This report presents the predictive tools used to estimate earthquake loss due to damage sustained by beam-column joints and the application of these tools to an existing reinforced concrete building. The thesis is organized as follows:

Chapter 2 identifies the literary sources including experimental studies, interviews, scientific articles, and software referenced for completion of the work presented in this thesis. The sources for determining the damage states, the methods of repair, and the cost estimation are discussed. Information relevant to behavior of beam-column joints under seismic loading and the design details of the selected joint specimens are described. A complete description of the statistical methods used for generating the fragility curves is included.

Chapter 3 defines the damage states for beam-column joints. The damage quantifies the extent of damage in terms of cracking, crushing, and rebar damage. The damage states are presented in order of progression from light to moderate to high

earthquake demand. Experimental investigation are used to determine the correct damage states and progression.

Chapter 4 identifies the engineering demand parameters (EDP) appropriate for quantifying the response of beam-column joints under seismic loading. Demand parameters are inter-story drift, number of cycles, joint strain, and damage indices. The damage data

Chapter 5 defines the methods of repair. The methods of restoring the damaged beam-column joints are specific to the extent of damage defined by the damage states. The methods of repairs are techniques recommended by current concrete repair manuals and used in practice by general contractors and structural engineers. The method description include the labor, materials, and equipment required to complete the work. The damage states are grouped by the methods of repair.

Chapter 6 presents the probability models for a given engineering demand parameter. The models are fragility curves indicating the probability of exceeding damage requiring a certain method of repair. The data used to generate the fragility curves is the repair groups of damage states. The data sets may be organized in three ways. The best data set is defined and selected. The distribution functions previously defined are used to generate the fragility curves. The goodness-of-fit tests determine the best fitting distribution.

Chapter 7 defines the process of estimating the cost and downtime associated with the methods of repair. The approximate monetary values of labor, materials, and equipment evaluated using the information from professionals from industry and the construction cost books.

Chapter 8 demonstrates the technique of predicting economic impact for an existing older reinforced-concrete building. The probability model for the most appropriate demand parameter is used to predict the method of repair. The associated costs for the methods of repair are applied to estimate the total earthquake loss. Local conditions are considered for an accurate estimation of the job cost, contract price, and downtime.

Chapter 9 summarizes the work and the primary conclusions presented in this report and indicates future research that would increase the reliability of earthquake loss prediction.

Chapter Two
Literature Review

2.1 Introduction

The results of an extensive review of literature regarding the seismic response of beam-column joints, current repair techniques for damaged concrete, statistical methods of probabilistic assessment, and current cost estimation procedures and price quotes are presented in this chapter. Background information for these topics are required for development of the predictive model of the economic impact of earthquake induced structural damage.

2.2 Damage Measures

The damage states were determined following extensive literature review of three sources. These sources were previous experimental reports, post-earthquake reconnaissance reports, and post-earthquake repair reports. Four specific experiments; Walker (2001), Pessiki (1990), Clyde (2000), and Hakuto (2000) were selected for the initial review of previous experiments based on load history and sufficient damage descriptions. All these experiments used load histories where the story drifts incremented progressively so that damage could be associated with points along a monotonic envelope. Since loading was applied in two or three cycles per displacement, the number of cycles for all specimens was similar and the order of damage occurrence could be established.

Reconnaissance reports were reviewed for descriptions and photos of existing reinforced concrete buildings damaged during an earthquake. Damage sustained by reinforced concrete and masonry buildings during the 1995 Kobe earthquake is described by Mitchell (1996). The articles consist primarily of failed columns and unrepairable buildings. Shear failure of beam-column joints is discussed and accompanied by dramatic images. The damage shown in the images is more severe than the damage sustained during an experiment. Damage sustained by concrete buildings during the 1967 Caracas, Venezuela earthquake is described in the Portland Cement Association's report (1967). A clear image of damage to the joint is shown in Section 3.5.1.

The third source was post-earthquake repair methods and applications. Repairs used in the 1985 Mexico City earthquake, reported by Jara (1989), are grouped into three categories. The first two categories define increments of crack width appropriate for two different types of repair. For cracks less than two one-hundredths of an inch wide, epoxy resin injections can be used. Concrete cracked to widths greater than this and reinforcement that is bent or exposed makes up the second category where replacement of materials restores component strength and stiffness. Immeasurable cracks, spalling, and hinging about the largest joint crack all qualify for the last category in which jacketing and encasing of the existing component is required. This last category of repair may constitute retrofitting where the strength or stiffness of the component is improved. Sometimes repairs within the first two categories can be considered retrofitting and such repairs are beyond the scope of this project.

2.3 Experimental Data

The data used for the analysis of this research is gathered from previous experimental studies. The nine experimental studies were selected for 1) the design details of the joints tested, 2) loading history, and 3) sufficient data characterizing component damage and demand.

2.3.1 Specimen Design Details

The design details of the selected specimens must be typical of pre-1970s construction. Pre-1970s construction was designed according to the Uniform Building Code (UBC) of 1967 and the American Concrete Institute (ACI) 318 of 1963. The provisions strongly influencing the behavior of beam-column joints are 1) the amount of joint transverse reinforcement, 2) the anchorage lengths, and 3) the nominal joint shear demand ratios. The code provisions are defined as follows:

Joint Transverse Reinforcement

Editions of the ACI code prior to 1971 do not specify if the column ties are to continue through the joint. (Pessiki 1990) As a result, most joint designed during this time do not have transverse reinforcement within the joint. The resistance of the joint to seismic loads was addressed in the mid-1980s when the transverse reinforcement spacing

requirements of the columns were applied to the joint. Currently, the longitudinal spacing should not be less than 4 in. between ties.

Current ACI code allows a reduction of transverse reinforcement requirement of a column through a joint. The confining reinforcement may be reduced by 50% and spacing of the ties or hoops may be increased to 6 in. if all four faces of the column are adjoined by beams ¾ as wide as the column. The beam-column joint sub-assemblages considered in this research have no more than two column faces adjoined by beams and do not qualify for this reduction.

Anchorage Lengths

Anchorage lengths allow the stress to transfer fully between the concrete and the reinforcing steel. If the anchorage length is insufficient, the bond between the steel and the concrete is broken and slip of the rebar occurs. The anchorage length for column splices is defined as early as 1951 to be $20d_b$ or 20 times the column bar diameter. This same year, the anchorage length for non-continuous, embedded beam rebar is defined as 6 in.

Beam longitudinal reinforcement must now be continuous through a support. Current UBC and ACI 318 code require anchorage length of $20d_b$ or 20 times the beam bar diameter. The ratio of the column depth to beam bar diameter, h_c/d_b is the bond strength ratio. Prior to 1967, the average bond strength ratio was 22. (Walker 2001)

Nominal Joint Shear Demand

Nominal joint shear demand varies from 0.03 to 0.37 f'_c for buildings constructed prior to 1967. (Walker 2000). The UBC and ACI 318 editions of the mid-1980s were the first to address limitations of shear stress demand on the joint. The shear stress demand for a beam-column joint is currently limited to $0.2f'_c$ or $15\sqrt{f'_c}$.

The specimens considered from the selected experimental studies meet most of these criteria. In an effort to increase the sample size of the damage data and the reliability of the probability models, some specimens were considered that did contain some joint transverse reinforcement. The design details for the selected specimens are discussed in Sections 2.4.2 and 2.4.3 and are listed in Appendix A.

2.3.2 Interior Joint Specimens

A total of twenty-five interior joint specimens are included in this research. Interior joints are cruciform with a main beam extending through the column in both directions. In addition to the design details defined in the previous section, the joint specimens are considered if the load history simulates seismic loading and the progression of damage is described throughout testing. Seismic loading is simulated using reverse cyclic loading. The load histories of these studies are primarily displacement-controlled and repeat cycles to the same displacement more than once. These twenty-five specimens and the experimental studies are identified by the authors listed below. The original abbreviated labels for each specimen are unchanged for the ease of reference to the test reports.

Meinheit and Jirsa (1977)

This study investigated the effect of confinement of the joint core concrete on joint performance under cyclic loading. Current design recommendations are developed using the results of this study. Eleven joints were tested, seven beam-column sub-assemblages and four with lateral beams as well. Only the data from M II (as labeled by Meinheit and Jirsa) is considered here because the report included detailed information regarding the progression of damage of this joint. The joint contains minimal transverse reinforcement with spacing too large for current seismic codes. The load history used in this study differs from the other because loading consists of only three cycles. The first cycle increases displacement demand until the shear cracking occurs in the joint or half the yield strain of the beam rebar has been exceeded. The second cycle increases displacement demand until the maximum joint shear stress is reached or yielding of the beam bar occurs. The final cycle repeats the previous displacement demand to ensure maximum shear stress of the joint has been reached.

Durrani and Wight (1982)

This study investigated the behavior of beam-column joints designed according to current design practice and the confinement effects of various joint transverse reinforcement. The data from specimens X1, X2, and X3 (as labeled by Durrani and

Wight) are considered here. Specimens X1 and X3 contain 2 ties within the joint spaced more than 4 in. apart. However, specimen X2 contains 3 ties but is still considered because the peak shear stress demand is less than $0.2f'_c$ and the damage progresses similarly as the other joints. The study concludes that joint damage is a function of joint shear stress, the number of layers of joint hoops, and the presence of transverse beams and slabs.

Pessiki, Conley, Gergely, and White (1990)

This study investigates the behavior of existing structures under seismic loading. Eight joints, P2 through P9 (as labeled by Pessiki, Conley Gergely, and White), are considered here. Specimens P5 and P6 have joint transverse reinforcement. The other specimens have none. Specimen P5 contains only 2 #3 ties. Specimen P6 contains 6 but the yield strength of column longitudinal reinforcement is significantly lower than the other specimens. Specimens P7, P8, and P9 have embedded beam longitudinal reinforcement with anchorage lengths of 6 in. and failed due to pull-out of the beam rebar. The study provides substantial data characterizing the damage for eight specimens tested under the same conditions. The study concludes that the beam-column joint failure mechanism depends on the amount of reinforcing steel within the joint. These specimens had column splices located just above the joint and bond strength ratios less than or equal to 16.

Joh, Goto, and Shibata (1991)

The experimental data relevant to this research are reported in two papers in an ACI special publication, “Design of Beam-Column Joints for Seismic Resistance”. The first paper presents the results of a study investigating the influence of joint transverse reinforcement on joint stiffness and beam transverse reinforcement ratio on bond degradation. One joint, JXO-B8-LH (as labeled by Joh, Goto, and Shibata), is considered here. The specimen is designed for transverse reinforcement ratios that are low in the joint and high in the beam. The joint contains 3 #2 ties. The authors conclude that an increase of joint transverse reinforcement will result in decrease of rebar slippage, increase of energy absorption ability, and increase of joint stiffness after cracking.

The second paper presents the results of a study investigating the effect of torsion due to eccentricity on the shear strength of columns and joints. Two joints, JXO-B1 and JXO-B2, are considered here and have the same joint transverse reinforcement as the previous specimen. Additionally, the anchorage lengths are greater than $20d_b$ but the beam to column width ratios are much less than one. The authors conclude joints with this eccentric configuration suffer larger moments of torsion around column axes, narrows the effective joint width, likely reduces the shear cracking stress, and increases the flexibility of the joint.

W*alker, Lehman, and Stanton (2001)*

This study evaluates existing joints and the influence of joint shear stress demand and load history on earthquake response. Data from all of the joint sub-assemblages as part of this study are considered here because the design details for these joints are typical of pre-1970s construction. Two joints, PEER 14 and PEER 22 (as labeled by Walker, Lehman, and Stanton), were tested using increasing increments of displacement. Three joints, CD15 14, CD30 14, and CD30 22, were tested using constant maximum displacement load histories. The last two joints, PADH 14 and PADH 22, were tested using asymmetrical load histories. The authors conclude joints perform best when earthquake demand is limited to 1.5% drift and shear stress demand is less than $10\sqrt{f'_c}$ (psi).

Alire, Lehman, and Stanton (2002)

This study continues the investigation of Walker, Lehman, and Stanton. Three joints, PEER 09, PEER 15, PEER 41 (as labeled by Alire, Lehman, and Stanton), are considered here because failure mechanisms are consistent with those seen in past earthquakes. The authors conclude the joint shear stress demand is most accurate when defined as a factor of the square root of the compressive strength of the concrete.

2.3.3 Exterior Joint Specimens

A total of nine interior joint specimens are included in this research. Exterior joints have a main beam extending through the column in only one direction. The same criteria are required of the selected exterior specimens. These nine specimens and the

experimental studies are identified by the authors listed below. Due to the limited number of specimens, the data gathered is not enough to generate probability models specific to exterior joints. The damage described in these studies aid in the development of the damage states. The original abbreviated labels for each specimen are unchanged for the ease of reference to the test reports.

Uzumeri (1977)

This study investigates the effect of various amount of joint reinforcement and the stress-strain characteristics of that steel on the behavior of the joint. Four joints, U2, U6, U7 and U8 (as labeled by Uzumeri), are considered here. The author concludes ductility of the joint is undesirable and that yielding of the joint transverse reinforcement should be avoided.

Clyde, Pantelides, and Reaveley (2000)

This study investigates the effect of various axial compressive loads on joint behavior at high earthquake demands. Four joints, C2, C4, C5, and C6 (as labeled by Clyde, Pantelides, and Reaveley), are considered here. None of the joints have transverse reinforcement in the joint. The study concludes the higher axial load allows the maximum joint shear stress to reach higher value at lower strain and yielding of the beam longitudinal reinforcement yields at higher displacement demand.

Hakuto, Park, and Tanaka (2000)

This study investigates the effect of retrofitting damaged beam-column joints. The joints are loaded at the top column end with pinned beam end. Reverse cycle loading is applied until the system exhibits extreme damage. No axial load is applied during testing. Two joints constructed with different anchorage of beam longitudinal reinforcement. The first joint contains the detail shown in Figure 2.2 (a) where the longitudinal rebar is bent into the joint core. Note the spacing of the beam transverse reinforcement is large. The failure mechanism occurs in the beam rather than the joint.

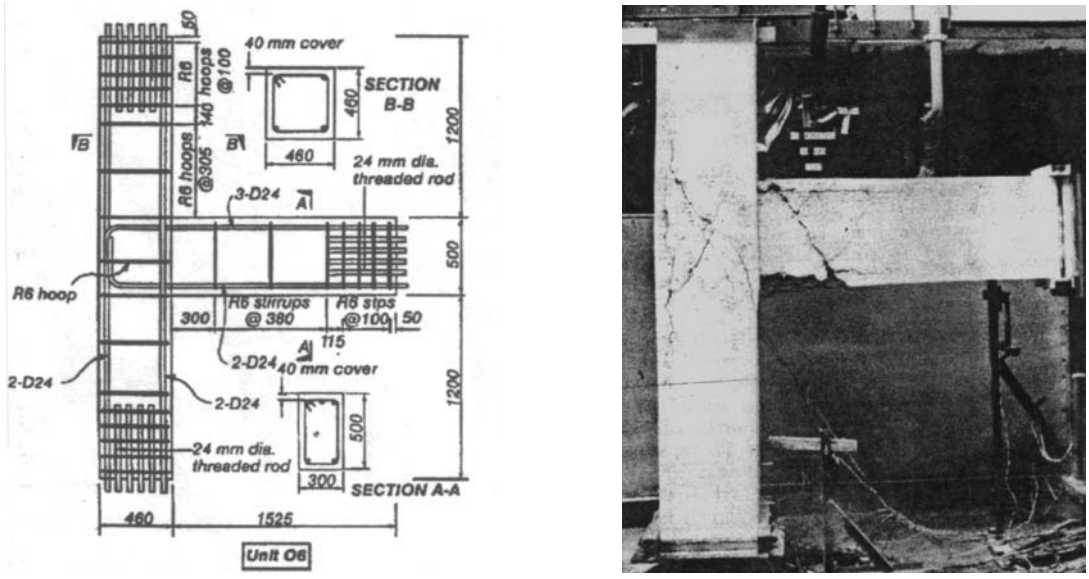

Figure 2.1: (a) Exterior joint detail demonstrates anchorage of beam rebar bent into the joint. (b) The same joint exhibits shear failure of the beam. (Hakuto 2000)

More consistent with the behavior typical of pre-1970s joints, the second joint exhibits concentration of damage within the joint. This joint, O7 (as labeled by Hakuto, Park, and Tanaka) is designed with the detail shown in Figure 2.3. The authors conclude the retrofitting methods tested successfully improve the joint performance.

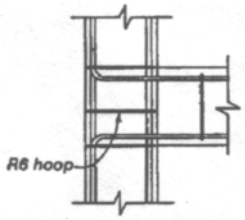

Figure 2.2: Detail of exterior joint specimen O7 demonstrates anchorage of beam rebar bent into the column. (Hakuto 2000)

2.3.4 Influence Factors for Behavior Variation

Despite the similarity of the design details of the selected specimens, variation of the behavior must be explained. The joint specimens have most of the design details typical of pre-1970s construction, but details vary among the experimental studies. Thus, the response among the selected joint specimens will vary. The behavior of the selected specimens is primarily influenced by the peak shear stress demand, the axial load applied

during testing, and the column depth to beam bar diameter ratio. The primary influence factors are presented in Table A.3 in Appendix A.

Shear Stress Demand

An effective way to increase the demand on the joint is to add more longitudinal reinforcement to the beam. More longitudinal reinforcement were added in the beams of three specimens tested at UW to increase the joint shear stress demand to 0.22*f'c. (Walker 2001) The second group of joints tested at the University of Washington had various target joint shear stress demands. These were achieved using different combinations of reinforcing bars, high strength steel and high strength concrete (Alire 2002). The actual peak shear stress demand reached for these specimens is listed in Appendix A.

Axial Load

The set-up of the selected specimens includes an axial load placed and maintained on the top end of the column. The greater the load, the more confined the joint will be and the better it will perform. The majority of the specimens maintained an axial load of 10% of the gross capacity of the column or $0.1*f'c*A_g$. However, some specimens had no axial load (Hakuto 2000). This is expected to highly affect the behavior of these exterior joints.

Embedded Beam Rebar

Three of the eight specimens have detailing unique from that previously discussed. Specimens P7, P8, and P9 have embedded beam longitudinal reinforcement (Pessiki 1990). Embedded reinforcement is non-continuous rebar that relies on the bond strength to resist the tensile forces at the joint. Thus damage state 13, pull-out of the longitudinal reinforcement, defines the failure applicable to these specimens.

Column Splice

A number of the specimens selected have a splice in the top column. The length of the splice should reflect the code prior to 1971. The construction joint was often placed above the floor slab without addressing the confinement of the column longitudinal

reinforcement (Pessiki 1990). The splice lap length ranges from $24*d_b$, where d_b is the bar diameter, to $30*d_b$.

Beam to Column Ratios

Two beam to column dimension ratios affect the demand on the joint. See Figure 2.1 for the correct labeling of the depth and width. The column depth is named the anchorage length and affects the bond performance of the beam longitudinal reinforcement. The ratio of the anchorage length to the beam bar diameter, hc/db, indicates the goodness of the bond between the concrete and the rebar. The ratio must be large enough to maintain the bond so that the coupled forces on either side of the joint do not reduce to one tensile force.

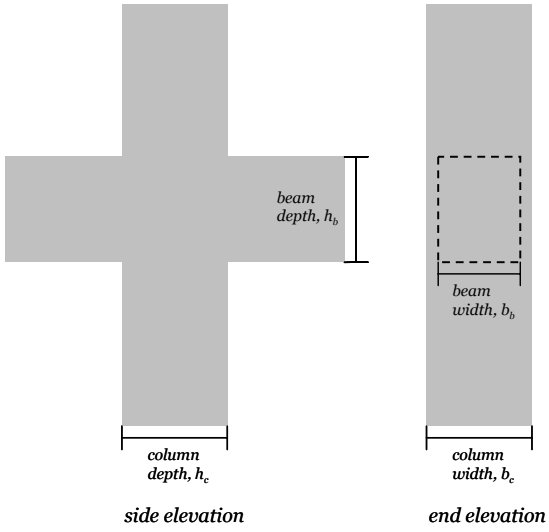

Figure 2.3: The proper labeling of the width and depth of the beam-column joint (Adapted from Pessiki 1990).

The second ratio is the beam width to the column width. The demand on the joint will increase as the width ratio moves closer to one. For the majority of the selected specimens, the width of the beams and columns are equal. Thus, the is not included anticipated to vary the response among the specimens.

2.4 Methods of Repair

The sources for determining the methods of repair are government documents, design codes, previous experiments, and interviews with professionals in the industry. The methods of repair are specific for reinforced-concrete damaged in an earthquake. The

methods of repair of beam-column joints presented in Chapter Five were determined using the information provided in the following sources.

Government documents and repair manuals provide concise instruction for the identification and repair of damaged reinforced concrete. A series of documents regarding repair to earthquake damaged were prepared by the Applied Technology Council (ACT) and funded by the Federal Emergency Management Agency (FEMA) in 1998. Within the series, repair techniques appropriate for various types of buildings are listed. Chapter 4 of FEMA 308, "Repair of Earthquake Damaged Concrete and Masonry Buildings", contains a list of repair techniques similar to those presented in this paper. The repair techniques are categorized as Cosmetic Repair, Structural Repair, and Structural Enhancement. The materials, equipment, and method of execution are provided as well as the limitations for the extent of damage to be repaired.

The American Concrete Institute (ACI) publishes repair manuals defining the materials, equipment, and techniques of mixing and applying epoxy resin to repair cracked concrete. An ACI Special Publication dating back to the late 1960's defines the application process and effectiveness of the repair (ACI SP-21, 1968). The most current method of assessment, material selection, application techniques, and case studies are available in ACI 546R-96 (ACI, 1996).

A number of studies have addressed the repair of reinforced-concrete components damaged as a result of earthquake loading. Testing of joints was performed by Tasai (1992), Filiatrault (1996), and Karayannis (1998). Application of repair techniques after damaging the joints provides information regarding the effectiveness of the repair. Filiatrault and Tasai describe the improvement of the behavior of the joint after epoxy resin injection of cracks. Karayannis defines the properties of the cementitious material for patching of spalled and crushed concrete.

Other studies document repair strategies employed in the field following seismic events. Jara (1989) provides case studies of repairs taking place after the Mexico City earthquake in 1985. The article suggests that various application methods of epoxy resin injection provide restoration of the concrete element to the original strength and

serviceability. The material properties are selected to resist the loading conditions, while the environmental conditions causing corrosion of the exposed resin, are not addressed.

Investigation of the previous sources produced a list of repair materials and application methods considered applicable to the earthquake induced damage of beam-column joints. The list was presented to professionals with experience in repairing damaged reinforced concrete buildings and bridges. A structural engineer from Coughlin, Porter, and Lundeen of Seattle provided insight to the most applicable repair methods and the importance of accounting for non-structural elements for more invasive repair techniques (Savage, 2003). Engineers at the Washington Department of Transportation in Olympia provided information regarding the repair of bridges in the area (Coffman and Kapur, 2003). The limitations of the repair techniques were identified, such as the width of the cracks for epoxy resin injection. A project engineer from T.Y. Lin of San Diego provided a breakdown of the cost estimation for repairing failed joints with buckled rebar (Cole, 2003). The interview transcripts highlighting relevant information discussed during the in-person interviews are provided in Appendix D.

2.5 Predicting Damage as a Function of Demand

The sources used to generate the fragility curves in this report are previous analytical reports and a statistical textbook. In the current study, four probability distributions are considered to model the data and two goodness-of-fit tests are used to evaluate these distributions. The textbook Probability, Reliability, and Statistical Methods in Engineering Design by A. Haldar and S. Mahadevan was used to identify the cumulative distribution functions and the goodness-of-fit tests.

2.5.1 Fragility Curves

Fragility curves indicate the probability of reaching or exceeding a damage measure for a given engineering demand parameter. A report by Saxena et al. (2000) develops the curves for multi-span concrete highway bridges. The paper follows the approach defined by Shinozuka (2000) where “development of vulnerability information in the form of fragility curves is a widely practiced approach.” The vulnerability of a component for seismic damage is defined by both empirical and analytical curves. For

both sources, the peak ground acceleration is the demand. The approach for developing the fragility curves used here is consistent with that used by Saxena and Shinozuka.

2.5.2 Testing goodness-of-fit

Two tests are used commonly to determine the best fitting distribution for a given data set. The first is the Kolmogorov-Smirnov test which numerically confirms the visual indication of the best fit when comparing selected distribution function to the ranking order of the data. The K-S test is defined by Equation 2.1.

$$D_n = \max\left|F_x(x_i) - S_n(x_i)\right| \tag{2.1}$$

where D_n, is the K-S parameter, F_x is the selected distribution function, and S_n is the rank defined by the stepwise CDF. Goodness of fit is determined from the comparison of the K-S parameter, D_n, to the critical value, D_n^{α}, for a selected significance level, α. If the K-S parameter exceeds the critical value, the selected distribution is not appropriate at that significance level. The critical value is determined from a standard mathematical table where the number of data points and the significance level must be known. The probability of the K-S parameter less than or equal to the critical value is related to the significance level in Equation 2.2.

$$P\left(D_n \le D_n^{\alpha}\right) = 1 - \alpha = P^{\alpha} \tag{2.2}$$

where P^{α} is the CDF of the K-S parameter at a selected confidence level, 1-α. The highest probability determines the best fitting distribution. The significance level, α, indicates the number out of one hundred that the selected distribution is not an acceptable model. A commonly used confidence level is 95% where the significance level is 5%. This means for 5 out of 100 data points, the selected distribution is not acceptable. The critical value decreases for increasing number of data points and increasing significance levels.

The second goodness-of-fit test is the Chi-Square test. This test compares the observed frequency with the theoretical frequency. The Chi-Square test requires dividing the sample data into *m* intervals or bins and selecting a confidence level, 1-α. The results of this test are dependent on *m*, the chosen number of bins. The test may yield a range of results and thus is considered arbitrary. The reliability of the results of the test can be improved when data points are equally divided among at least 5 bins.

The Chi-Square test is completed by determining the error value, $E^{\chi 2}$. The error value is compared to the Chi-Square parameter, $c_{1-\alpha,f}$. The error value must be less than the Chi-Square parameter as defined in Equation 2.3 a.

$$\sum_{i=1}^{m} \frac{(n_i - e_i)^2}{e_i} < c_{1-\alpha,f} \tag{2.3 a}$$

$$f = m - 1 - k \tag{2.3 b}$$

The parameter defined in Equation 2.3 b is the degree of freedom, *f*. The *m* bins decreased by the number of parameters, *k*, of the selected distribution and 1. The observed frequency, n_i, is the actual number of times the demand occurs in each interval. The theoretical frequency, e_i, is the expected number of times the demand occurs in each interval. The expected number is the probability of occurrence determined by the selected distribution times the number of data points.

2.5.3 Distribution Selection

The following distributions were selected for evaluation and compared using the tests described previously. The Stepwise CDF is a distribution used primarily comparing other distributions to the given data points. The Lognormal distribution is commonly used as the best fitting distribution in most fragility curve analysis. Normal, Weibull, and Beta are also compared due to the varying boundaries. Each uses a different approach to the data and since the lower and upper bound values are known, all are important.

Stepwise CDF

A useful comparative cumulative distribution is the Step-wise CDF, $S_n(x_i)$. This CDF utilizes the rank of each data point to determine the probability of occurrence. Repeating data values are included in the rank sequence.

$$S_n(x_i) = \begin{Bmatrix} 0, & x < x_1 \\ \dfrac{m}{n+1}, & x_m \le x \le x_{m+1} \\ 1, & x \ge x_n \end{Bmatrix} \tag{2.4}$$

where m_i is the rank of each data point, x_i, and n is the total number of data points in the set. The extreme values, x_1 and x_n, are defined by the range of the data set. When the data set considered is small, rank is normalized by the number of data points plus one, n+1.

Normal Distribution

The normal distribution is similar to the lognormal except the range of data includes negative values.

$$f_x(x) = \frac{1}{\sigma_x\sqrt{2\pi}} \exp\left[-\tfrac{1}{2}\left(\frac{x-\mu_x}{\sigma_x} \right)^2 \right] \quad -\infty < x < +\infty \tag{2.5}$$

This distribution is useful when negative as well as positive data values are used. The normal parameters, μ_x and σ_x, can be evaluated directly from the mean and variance of the data.

$$\mu_x = \frac{\sum_{i=1}^{n} x_i}{n} = E(x)$$
$$\sigma_x = \frac{\sum_{i=1}^{n} (x_i - \mu_x)^2}{n} = Var(x) \tag{2.6}$$

Lognormal Distribution

The lognormal distribution is expressed as

$$f_x(x) = \frac{1}{\sqrt{2\pi}\zeta_x x} \exp\left[-\tfrac{1}{2}\left(\frac{\ln x - \lambda_x}{\zeta_x} \right)^2 \right] \quad 0 \le x < \infty \tag{2.7}$$

Where x is the demand and the lognormal parameters, λ_x and ζ_x^2, are related to the mean and the variation of x. Note the data set must be all positive integers. These parameters can also be called the expected values, or normal parameters, of the ln x.

$$\lambda_x = \ln \mu_x - \tfrac{1}{2}\zeta_x^2$$
$$\zeta_x^2 = \ln\left[1 + \left(\frac{\sigma_x^2}{\mu_x} \right)^2 \right] = \ln\left(1 + \delta_x^2\right) \tag{2.8}$$

The graph in Figure 2.4 compares the probability density functions for the normal and lognormal distributions. The graph is based on a mean value of 100 and a standard deviation of 10. Note the boundaries of the normal distribution extend infinitely in both directions. The lognormal distribution function is zero at X=0 and extends infinitely in the positive direction. The integrating the area under the density curve provides the probability of an event.

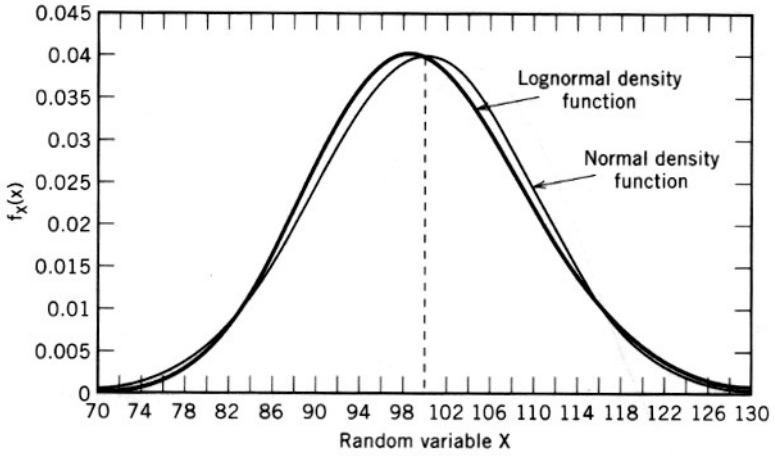

Figure 2.4: Probability density functions of the Lognormal and Normal distributions. (Haldar and Mahadevan, 2000)

Weibull Distribution

The Weibull distribution is considered an asymptotic distribution where the smallest values of the data set are limited to the lower bound, ε. To represent the data considered here, the value of ε is set to zero.

$$f_{x1}(x_1) = \frac{k}{w_1}\left(\frac{x_1}{w_1}\right)^{k-1} \exp\left[-\left(\frac{x_1}{w_1}\right)^{k}\right] \quad x_1 \geq 0 \tag{2.9}$$

The parameters of the Weibull distribution, k and w_1, are evaluated using the mean and variance of the sample data. The Γ is the gamma function.

$$k = \delta_{X_1}^{-1.08} \qquad w_1 = \frac{\mu_{X_1}}{\Gamma\left(1+\frac{1}{k}\right)} \tag{2.10}$$

The gamma function can be evaluated using the polynomial approximation when x of $\Gamma(1+x)$ is greater than or equal to zero and less than or equal to 1. Since k is a positive

value for the data considered here, the criteria for x is met. The polynomial approximation is a fifth order equation.

$$\begin{aligned}&\Gamma(1+x) = 1 + a_1 x + a_2 x^2 + a_3 x^3 + a_4 x^4 + a_5 x^5 + \varepsilon(x)\\&a_1 = -0.575,\ a_2 = 0.951,\ a_3 = -.06999,\ a_4 = 0.425\\&a_5 = -0.101, \qquad |\varepsilon(x)| \le 5\times 10^{-5}\end{aligned} \tag{2.11}$$

Beta Distribution

The Beta distribution is defined by the upper and lower bound limits, a and b. The values of a and b are determined using the smallest and largest data points included in each set. Variations of the parameters, q and r, generate a wide range of PDFs from parabolic to linear to exponential.

$$f_X(x) = \frac{1}{B(q,r)} \frac{(x-a)^{q-1}(b-x)^{r-1}}{(b-a)^{q+r-1}} \quad a \le x \le b \tag{2.12}$$

The beta function, B(q,r,) is calculated using the gamma function. The gamma function may be evaluated using the polynomial approximation as described in Equation 2.11 if the criteria for x are met.

$$B(q,r) = \frac{\Gamma(q)\Gamma(r)}{\Gamma(q+r)} \tag{2.13}$$

The parameters, q and r, are related to the mean and variance of x in Equation 2.14. A modified Newton-Rhapson iteration is used to evaluate the most appropriate positive values of q and r.

$$\begin{aligned}E(x) &= a + \frac{q}{q+r}(b-a)\\Var(x) &= \frac{qr}{(q+r)^2(q+r+1)}(b-a)^2\end{aligned} \tag{2.14}$$

Figure 2.5 shows the impact of the parameters q and r on the probability density function. The probability of an event is the integration of the area under the curve.

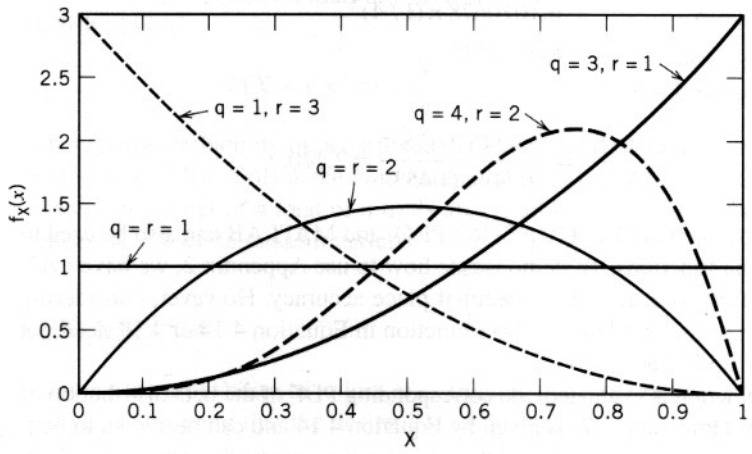

Figure 2.5: Probability density functions for the Beta distribution for varying values of the beta function parameters. (Haldar and Mahadevan, 2000)

2.5.4 Method of Maximum Likelihood

The parameters of the distribution functions presented in the previous section estimated using the method of moments. An alternative to estimating the parameters is the method of maximum likelihood. The alternative method may estimate parameters that represent the population. "A population represents all conceivable observations of a random variable." (Haldar and Mahadevan, 2000) The method of moments depends on the mean and variance to estimate the parameters. The mean and variance are evaluated using the sample data. Since the sample data is only a small portion of the population, a high degree uncertainty is associated with the mean and variance and is carried into the distribution parameters.

Instead, the maximum likelihood uses optimization to predict the parameters of the distribution function for the best fitting curve. This method is in contrast to the method of moments where the first and second moments, i.e. mean and variation are used to evaluate the distribution parameters. The parameters are evaluated using the likelihood function, L, defined in 2.15.

$$L(x_1, x_2, ..., x_n; p) = f_X(x_1, p) f_X(x_2, p) ..., f_X(x_n, p) \tag{2.15}$$

where f_X is PDF of the selected distribution and p represents all the parameters associated with the selected distribution. Note X indicates the entire data set and x indicates a single data point. Section 6.3 demonstrates the application of this method to distribution function selected for this research.

2.6 Loss Estimation

Various sources were sought providing information regarding developing the framework and determining the monetary values for calculating the cost associated with the repair methods. The sources are articles regarding the application of loss estimation to reinforced-concrete structures, estimation software developed for use by general contractors, and in-person interviews with professional form the industry. Some sources may overlap with those used for determining the methods of repair. The loss estimation applied to damaged reinforced-concrete beam-column joints is presented in Chapter Seven.

Providing information regarding the framework of cost estimation is the article by Shiohara (1999). The economic loss is defined as a sum of three parts: the distribution of damage in a component, the amount of damage, and the unit cost of repairing work. Additionally, loss should include "the loss to compensate the time the building does not function". A framework reflecting these parts is introduced where the cost per component is D x S x U x C. Where the D is the type of damage, S is the size of member, U are the factors considering nonuniform distribution of damage, and C is the unit cost of repair.

The cost data in the 2003 National Renovation and Insurance Repair Estimator are assembled from the cost and productivity records of over 700 companies that are active in the renovation and insurance repair industry. The publication is described in the May 2000 issue of Cost Engineering magazine as having "a practical application for both the loss adjuster retained by an insurance company and a general contractor who is bidding for work in the field. The publication is a useful tool for estimating." The cost data is available on the website, "www.costbook.com", for updating on a quarterly basis. An adjusting factor applied to the total job cost is included in the software to account for changes in cost due to location. The average adjustment for California of 17% was used for the quotes used in this paper.

Cost estimates for three retrofit alternatives for the seismic upgrading of the Asian Art Museum in San Francisco by Rutherford & Chekene, Consulting Engineers (1992) are investigated for price quotes and markup factors. The study report contains the cost estimates for construction on an existing building. The prices quoted in the estimates

provide information unavailable in the other sources, but most importantly demonstrate the application of markup to the total job cost.

The interviews with professionals from the industry were conducted on the phone and/or in person. The professionals included structural engineers, project engineers, general contractors, and companies producing the materials used in the repair of damaged reinforced-concrete components. The transcripts of the in-person interviews are available in Appendix E.

Chapter Three
Damage Measures

3.1 Introduction

Damage measures provide a description of the extent of damage sustained by a component during an earthquake. The extent of damage is characterized by damage states. The results of experimental investigation provide the basis for identifying the damage states that best characterize the seismic response of reinforced-concrete beam-column joints. Damage states are linked to specific repair techniques and models are developed defining the probability of a joint exceeding a specific damage level for a given earthquake demand. Thus, identifying the appropriate damage states represents the first step for developing the prediction model for the economic impact due to earthquake induced damage.

Damage states describing joint damage are observable either visually or by instrumentation. Section 3.2 presents the damage states and how the states are measured during loading. Damage states measured by visual observation are characterized in terms of cracking, concrete spalling and crushing, and joint failure in Sections 3.3 through 3.5. Damage states measured using instrumentation are described as strength-based and are discussed in Section 3.6.

3.2 Damage Measures

Results of an experimental investigation of the earthquake response of reinforced-concrete beam-column joints are used to identify the damage states. The damage states are measured by two means. The first measure of damage is visual observation. The observable damage states are extents of cracking, concrete crushing, and bond degradation. These damage states are quantified as crack width, area of missing concrete, or amount of exposed reinforcing steel. The majority of the damage states presented in this research are visually observable.

Two damage states are not visually observable but must be measured using instrumentation. These are strength-based damage states indicating a reduction of capacity of a portion of the joint. Strength-based damage states are particularly valuable

in predicting economic loss as a function of engineering demand parameters, EDPs. Few researchers provide unabbreviated data and detailed discussion of damage, however all researchers present a measure of shear capacity and yielding of the reinforcing steel.

The damage states presented in this section describe the damage sustained by both interior and exterior joints. However, some damage or failure mechanisms may be more common in exterior rather than interior joints. Using the images provided by reconnaissance reports by Mitchell (1996) or the Portland Cement Association (1967), the failure of exterior joints is analyzed. Failure is characterized by exposure and buckling of the column longitudinal reinforcement and the concrete appears to have sheared on a steep diagonal. Exterior joints fail with portions of the core concrete intact whereas interior joints experience concrete crushing that extends through the core, hollowing out a round area in the center.

3.2.1 Progression of Damage

The damage measures presented in this paper are the result of analysis of the progression of damage recorded in the nine experimental reports presented in Section 2.4. The initial order of progression is determined using the most detailed damage reports and compared against the damage reported in the remaining selected specimens. The progression of the damage measures is essential to the relationship between the damage evident through inspection and the damage evident through instrumental read-outs.

The probability models could be generated for each damage state. However, the prediction of economic impact requires the cost due to the damage. The cost is related to the damage through the repair work. Thus, the probability models are generated for each method of repair. Since more than one damage state is repairable by the same method, the damages states are divided into repair groups. The progression of damage is important when determining the repair groups.

3.2.2 Damage States

The damage states sustained by a beam-column joint in order of increasing earthquake demand are:

0. Initial cracking at the beam-column interface
1. Initial cracking within the joint area

2. Crack width is less than 0.02 in. (5 mm)
3. Crack width is greater than 0.02 in. (5 mm)
4. Beam longitudinal reinforcement yields
5. Crack width is greater than 0.05 in. (1.3 mm)
6. Spalling of at least 10% joint surface concrete
7. Joint shear strength begins to deteriorate
8. Spalling of more than 30% joint surface concrete
9. Cracks extend into the beam and/or column
10. Spalling of more than 80% joint surface concrete
11. Crushing of concrete extends into joint core
12. (a) Buckling of longitudinal steel reinforcement
12. (b) Loss of beam longitudinal steel anchorage within the joint core
12. (c) Embedded beam longitudinal steel reinforcement pull-out

3.3 Cracking

The first indication of damage in the joint is cracking of the concrete. The joints are non-ductile and under seismic loading respond to shear forces by cracking diagonally through the joint. The crack widths are measured at the maximum displacement demand. High earthquake demand may cause permanent displacement of the building, the beams and columns may not return to their original positions, and the cracks may not close. Cracks due to moderate earthquake demand are more likely to close. However, the experimental studies more consistently report the maximum crack width.

Initial characterization of the progression of cracking defined the increasing crack widths. The maximum crack width grows as the cyclic loading continues. However, investigation of the repair of concrete cracking revealed the smallest repairable widths is 1/16 in. and the largest is ¾ in. (Runacres, 2003). Damage States 2, 3, and 5 would all be in the same repair group. These damage states are retained to provide more information for future use of this research.

3.**3.1 Damage State 0**

Damage State 0 is cracking between the joint and the beam. These cracks are the first to appear when the loading starts at a low demand. The cracks form before any other

cracks within the joint area. The crack may initiate from the joint corners and progress vertically as seen in Figure 3.1.

3.3.2 Damage State 1

Damage State 1 is initial cracking with the joint. The crack width is hairline or immeasurable. Structural engineers are not alarmed by cracks of this width (Savage, 2003 and Coffman and Kapur, 2003). These cracks may appear as those seen in Figure 3.1. Note the cracks highlighted at the seam between the beam and the joint. In the center of the joint and behind the shear measurement instruments are the initial diagonal cracks.

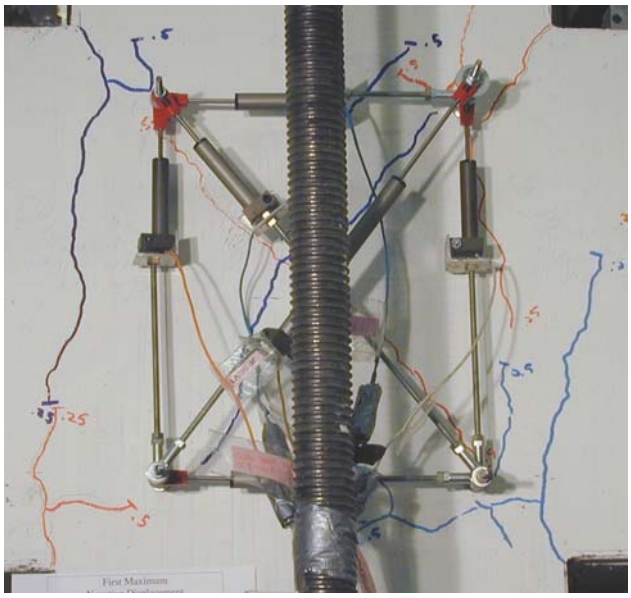

Figure 3.1: Interior joint specimen PEER 22 exhibits Damage State 1 partially hidden by instrumentation and Damage State 0 from the previous load cycle. (Walker 2001)

3.3.3 Damage States 2, 3, and 5

Damage States 2, 3 and 5 are increments of crack widths. Defining the increments of cracks appeared important when investigating the repair of cracked concrete. Cracks in damaged reinforcement concrete buildings after the Mexico City earthquake were repaired based on the width of the cracks. (Jara 1989) The cracks smaller than 0.02 in. were not repaired. Similarly, ACI 318-95 defines cracks having a width less than 0.013 in. for exterior and 0.016 in. for interior components as appropriate for no repair. Crack widths greater than 0.016 in. are at risk for corrosion of the reinforcing steel or will not

allow transfer of stresses through the aggregate. These sources of repair determined the cracks widths of Damage State 2, 3, and 5 seen in Figure 3.2.

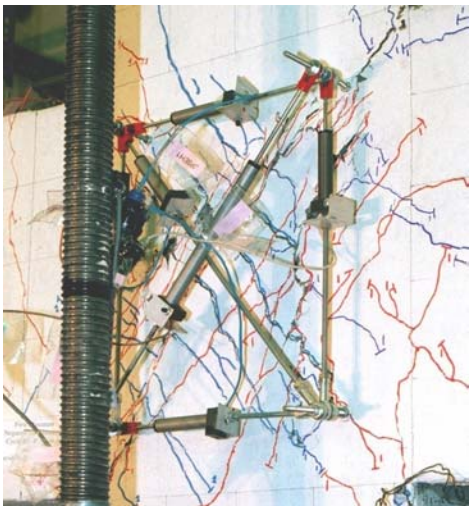

Figure 3.2: Interior joint specimen CD30 22 exhibits Damage State 5. (Walker 2001)

3.3.4 Damage State 9

Damage State 9 describes the damage initiating within the joint but progressing outside the joint core. Cracks that begin within the joint extend into the adjacent beams or columns. The crack progresses along the reinforcement and may be considered bond splitting. An exterior joint, specimen O7, exhibits bond splitting up and down the column at the end of the test in Figure 3.3. While most common in exterior joints, three selected interior joint specimens exhibit this damage prior to failure.

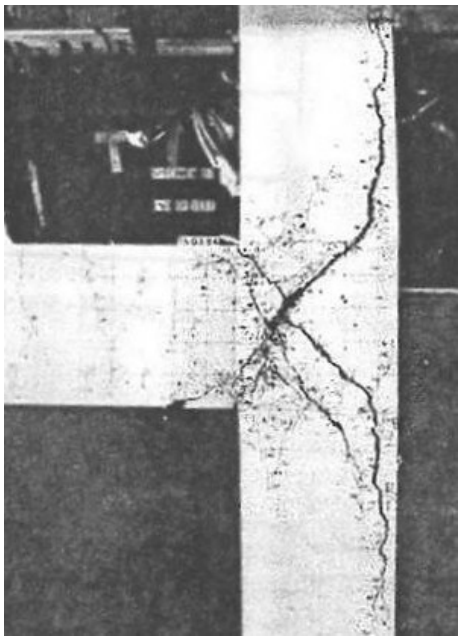

Figure 3.3: Exterior joint specimen 07 exhibits Damage State 9. (Hakuto 2000)

3.4 Concrete Spalling and Crushing

Damage States 6, 8, 10, and 11 are descriptions of damage to the joint concrete. Concrete spalling is the breaking of the outer most concrete away from the remaining solid concrete. Flaking of the concrete is also present when the cover concrete is broken but remains on the specimen. Experimental studies approach the flaked concrete in two ways resulting in a higher degree of uncertainty when determining progression from a smaller area to a larger area of spalling as defined in Damage States 6, 8, and 10. The flaked concrete may be removed by gently brushing the surface and thus more spalling would be assumed. Alternatively, the flaked concrete is left intact and not included in the description of spalling. Including the flaked concrete in the spalled area is preferred to the alternative in this research. Comparing the damage description and the photos of the damage decreases the uncertainty.

3.4.1 Damage State 6

Damage State 6 defines the transition from cracking to spalling. Cracking is no longer measurable where the smooth surface has broken and fallen away. Spalling begins in the center of the joint and must cover to an area of 10% of the joint surface area. This amount of damage to the surface area means crack widths can not be measured. Figure

3.4 is an example of the small area of exposed aggregate surrounded by flaked sections of cover concrete.

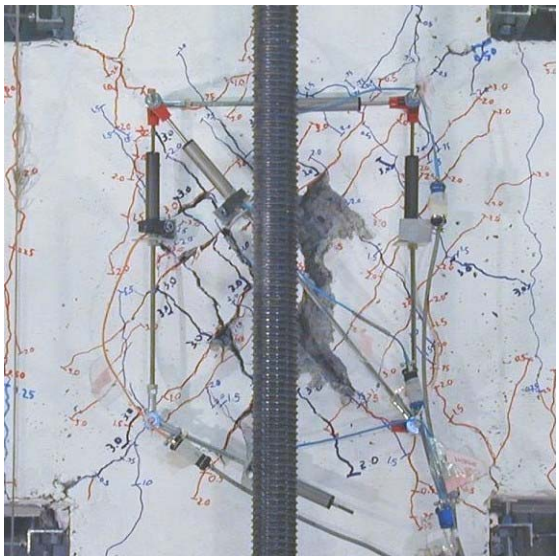

Figure 3.4: Interior joint specimen PEER 22 exhibits Damage State 6. (Walker 2001)

3.4.2 Damage State 8

Damage State 8 describes spalling of more than 30% of the joint surface area. Thicker sections of cover concrete break and fall away from the center of the joint exposing the center column longitudinal reinforcement. At the same time, the area of exposed aggregate grows bigger but remains concentrated in the center of the joint surface. The amount of surface area expose is important for the application of the method of repair.

Figure 3.5: Interior joint specimen PEER 14 exhibits Damage State 8. (Walker 2001)

3.4.3 Damage State 10

Damage State 10 defines spalling of more than 80% of the joint surface area. Both the depth and the width of the area of spalling continue to grow, exposing the corner column longitudinal reinforcement.

3.4.4 Damage State 11

Damage State 11 defines crushing of the concrete extending into the joint core. Spalling of more than the cover concrete is considered crushing. Breaking and falling away of concrete thicker than the cover leads to exposure of the interior aggregate and large sections of the rebar. The steel reinforcement is in danger of damage where no concrete is present to prevent buckling. Damage of this extent indicates compressive failure may be inevitable but requires a different repair than more extensive damage.

Figure 3.6: Interior joint specimen C15 14 exhibits Damage State 11. (Walker 2001)

3.5 Joint Failure Mechanisms

Damage States 12(a, b, c) define three types of failure commonly observed in older reinforce-concrete joints. Despite the numbering, these states are not progressive but would occur for the same high earthquake loads. These failure mechanisms should be expected where the design details of these joints do not confine the joint core. The first, and most common among the selected joints, is the buckling of the longitudinal steel reinforcement. Plastic deformation or hinging of the beam, rather than the joint or the column, is the current design target. However, damage to joints may not allow transfer of the stresses into the beam and result in movement within the joint.

3.5.1 Damage State 12(a)

Damage State 12(a) is the failure due to loss of gravity load capacity within the joint. Inevitable after crushing of the core concrete, only the longitudinal reinforcement is available to resist the gravity load. During or even after the earthquake motion has ceased, buckling of the rebar occurs.

Figure 3.7: An existing joint in Caracas, Venezuela exhibits Damage State 12 after an earthquake. (Portland Cement Association, 1967)

3.5.2 Damage State 12(b)

Damage State 12(b) is defined as the loss of beam longitudinal steel anchorage with the joint. The beam appears to pull away from the joint and move without resistance against the lateral loading. The bond between the beam and the joint is lost when a significant amount of the concrete is crushed. Interior joints, specimens J-B1, X3, P4 and P3 all exhibit this failure. "The north beam [of specimen P3] pulled away from the beam-column joint, pivoting about [a large] crack and offering decreasing resistance with increasing displacement." (Pessiki 1990)

3.5.3 Damage State 12(c)

Reinforcement details of some interior joint specimens reveal the beam longitudinal reinforcement is non-continuous through the joint. The rebar ends are embedded only 6 in. into the joint. Similar to the previous damage state, Damage State 12(c) defines bond failure for these embedded specimens. "Failure of the [specimen P9] was attributed to pullout of the embedded positive beam reinforcement from the beam-column joint, accompanied by significant damage to the top and bottom columns." (Pessiki 1990)

3.6 Strength-based Damage Measures

Strength-based damage is measured using instrumentation. Inclusion of the damage states is influenced by the damage progression chronicled by L. Zhang and J.

Jirsa (1982) for compressive failure of ductile joints. Between the concrete at the state of resisting only compressive loads and the state of crushing at the joint core, Zhang lists the "deformation reaches a value that corresponds to the ultimate strength of concrete under compressive loading". Indicating that as the joint progresses toward compressive failure, there is a point at which damage can not be observed and yet, the onset of significant damage leading to failure is inevitable. Assuming the same point exists for shear and bond failures, a state must be defined for the onset of significant shear or bond damage. Analysis of the measured response of the specimen will provide information regarding the onset of impending damage. This becomes especially important when the previous damage states are not described in the study or the loading is halted prior to failure. The Damage States 4 and 7 provide additional information where damage descriptions are insufficient.

3.6.1 Damage State 4

Damage State 4 is yielding of the beam longitudinal reinforcement.. Strain gauges measure the elongation of the reinforcement during loading. One method of attaching the strain gauges to the rebar is by cutting a groove into the steel to minimize interference due to the surrounding concrete. (Alire 2002) Other tests do not cut into the reinforcement and obtain reliable results. The damage state has occurred once the measured strains exceed the yield strain. Yielding of the reinforcement reduces the bending capacity of the beam close to the joint. After the rebar yields, the bond strength between the concrete and the steel deteriorates. Elongation of the rebar causes the bar diameter to decrease and the slip of the bar to increase. The ability of the rebar to transfer stresses is significantly decreased.

3.6.2 Damage State 7

Damage State 7 is the onset of shear strength degradation. The shear capacity of the joint will peak during loading prior to occurrence of the failure mechanism. The peak joint shear strength is identified on the response hysteresis. The onset of shear strength degradation occurs when the peak strength is followed by a significant reduction of strength. Commonly, a significant reduction is defined as 20% of the peak shear demand. However, many of the tests included in this research do not share this definition and

while shear demand reaches a peak, a 20% drop may not occur for a few more cycles, if at all before the test is terminated. Thus, only the specimens reporting the occurrence of the peak shear demand followed by a significant reduction in the resistance are included.

This is clearly demonstrated by the following three selected specimens tested by Pessiki (1990). The response hysteresis of classically loaded specimens shows the shear demand versus the displacement. Note the plots are labeled "drift (in)" where the drift is not normalized by the column height. For example, 2" on the plot is 1.5% drift ratio. Specimen P8 is an example of peak shear demand corresponding to an appropriate onset of shear strength degradation. The response hysteresis of specimen P8 is shown in Figure 3.8.The author reports the peak shear demand of 31.4kips at 1.42% drift ratio and cycle 14. The subsequent cycles resist a demand of approximately 25kips, a reduction of slightly more than 20% of the peak demand.

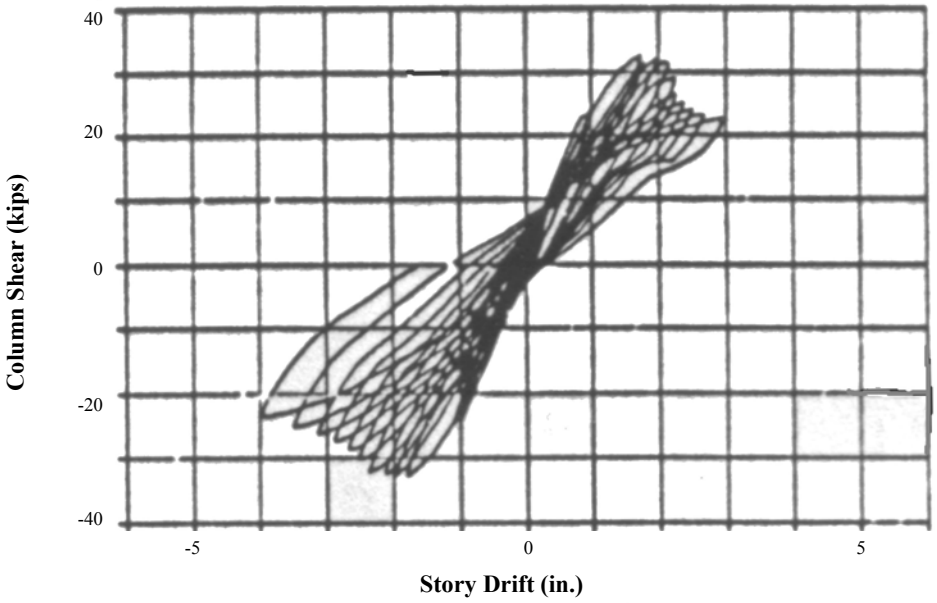

Figure 3.8: Response hysteresis for specimen P8 (Pessiki 1990)

Compare the response hysteresis of specimen P8 to those of specimens P7 and P4, each deviating from the appropriate definition of Damage State 7. The response of specimen P7 in Figure 3.9(b) is characterized by a slow decrease of the shear demand after the peak occurs at 1.75% drift ratio and cycle 16. Despite a slightly smaller reduction than the required 20% occurring in each of the following cycles, the specimen is considered to have achieved onset of shear strength degradation. Alternatively

specimen P4 in Figure 3.9(a) is not considered to have achieved Damage State 7. The peak shear demand is followed by one cycle of nearly the same demand of 42kips. Then the test is terminated due to Damage State 12(b), beam pulling away from the joint.

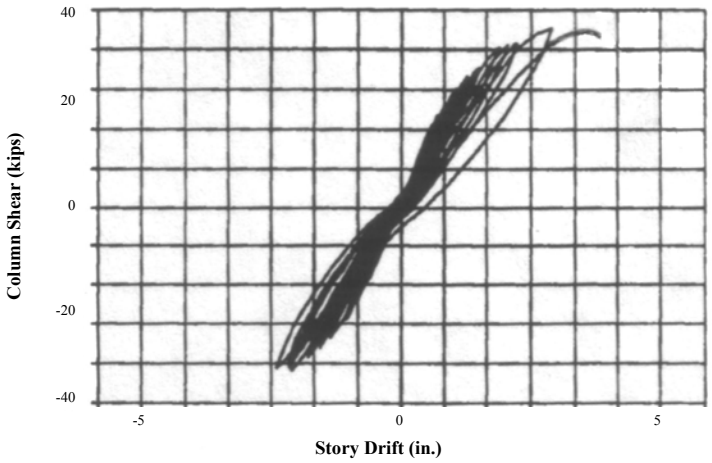

(a)

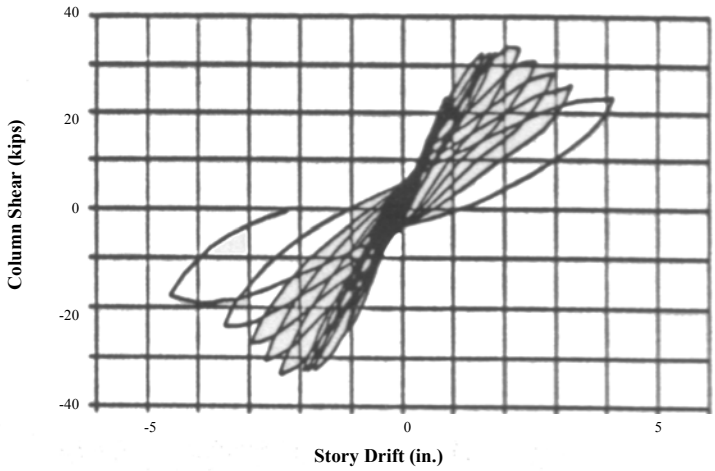

(b)

Figure 3.9: (a) Response hysteresis of specimen P4 (b) Response hysteresis of specimen P7 (Pessiki 1990)

3.7 Conclusion

The selected experimental studies describe the damage sustained by joints subjected to earthquake loading. The damage measures are defined in terms of cracking, crushing, and joint failure. Six damage states characterize the location and width of the cracks. Investigation of current repair techniques identifies the widths significant for repair. Four damage states characterize the amount of concrete spalled and crushed

within the joint. Two strength-based damage states are not visually observable but are strong indication of damage. Three types of joint failures are described for different types of beam bar detailing.

Chapter Four
Engineering Demand Parameters and Experimental Data

4.1 Introduction

Engineering demand parameters define the earthquake demand for component-specific behavior. Investigation of the engineering demand parameters used commonly in seismic modeling determines the best EDP for the modeling of beam-column joints based on the data gathered from previous experiments. Engineering demand parameters are linked to the damage measures by probability models generated based on this experimental data. Thus, identifying the appropriate engineering demand parameters represents the second step for developing the economic impact for a given earthquake demand..

This chapter discusses the identification and definition of engineering demand parameters that are appropriate for use in predicting economic loss associated with earthquake induced damage to older beam-column joints. Section 4.2 discusses the criteria for selection of the experimental studies and the joint specimens and identification of the empirical data. Section 4.3 defines the engineering demand parameters appropriate for the seismic response of beam-column joints.

4.2 Experimental Data

Experimental studies are the source of the empirical data used to generate the probability models. The probability models will be used to predict the damage for a given engineering demand parameter which is the output of numerical models. To ensure that probability model is applicable to the modeled beam-column joints, the experimental joint specimens must meet the specified criterion.

4.2.1 Type of Joint

The criterion for the experimental studies are 1) design details are typical of pre-1970s construction, 2) load history and set-up are consistent with the other studies and 3) sufficient information regarding the damage progression is provided. The experimental studies that meet this criterion are listed in Section 2.4. The joint specimens considered from each study are also identified. The design details of joints built according to the

Uniform Building Code (UBC) 1967 and American Concrete Institute (ACI) 318-63 primarily do not have joint transverse reinforcement. These older joints have insufficient confinement of the joint core, anchorage lengths, and column to beam strength ratios. The damage states described in Chapter 3 are specific to these types of joints.

4.2.2 Identify Data Points

One criterion for selecting the experimental studies was the study must include sufficient information regarding the progression of damage during testing. The progression of damage describes the demand at which a measure of damage is observed. The Damage States 0-12 defined in Chapter 3 characterize these observable measures of damage. For each joint specimen, the observation of a damage state is recorded for used in the development of the economic impact prediction model. The damage states recorded for specimen PEER 22 are shown on the response hysteresis in Figure 4.1.

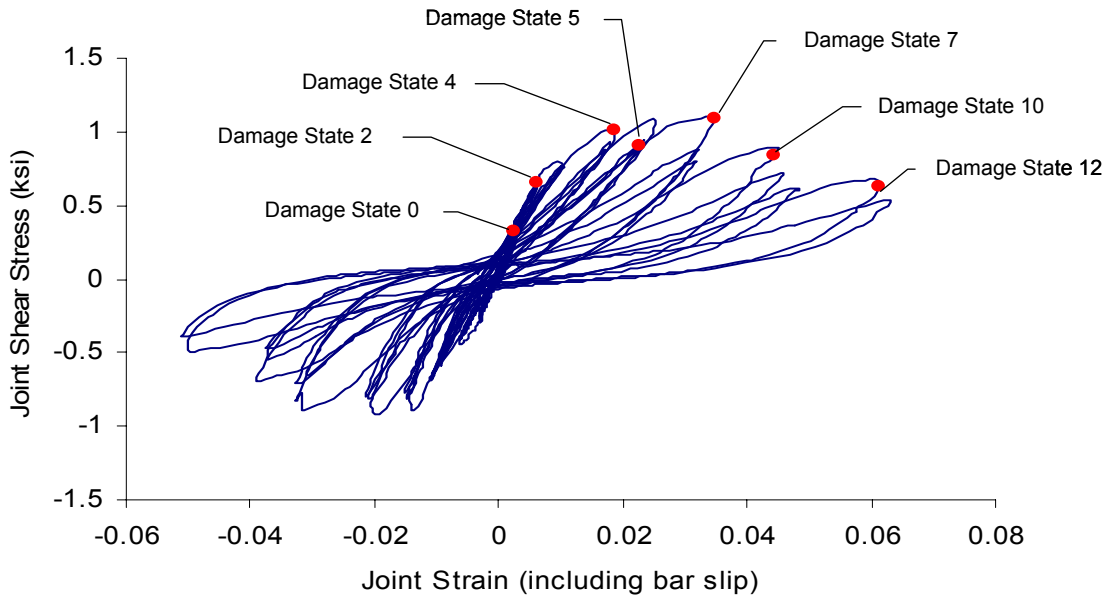

Figure 4.1: The damage states are identified on the response hysteresis of specimen PEER 22. (Adapted from Walker 2001)

4.3 Engineering Demand Parameters

Four engineering demand parameters are considered for beam-column joints. Consideration of these parameters is based on indication of damage for the structural response specific to beam-column joints. The engineering demand parameters are

identified from the load history and set up of the selected experiments. The demand at which a damage state is observed can be recorded in terms of as many engineering demand parameters as available in the experimental study. The last considered engineering demand parameter is only available for two experimental studies and ten joint specimens.

4.3.1 Drift Ratio

Inter-story drift ratio is a simple and common measure of the deformation of the beam-column joint. The ratio is easily calculated from information that is readily available in the selected experimental studies. Many of the beam-column joint sub-assemblages are set up in the experimental studies with the load applied at the end of the top column shown in Figure 4.1.

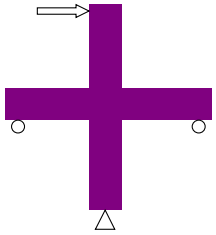

Figure 4.1: Typical loading set-up of beam-column joint sub-assemblage.

Drift ratio is the lateral displacement, Δ_{column}, of the column ends divided by the length of the column, ℓ_{column} as shown in Equation 4.1. In order to isolate the joint, the column is measured from the mid-point of the bottom column to the mid-point of the top column. For the purposes of this research, the drift ratio is given in terms of percent.

$$\frac{\Delta_{column}}{\ell_{column}} \times 100\% \tag{4.1}$$

Other experimental studies load the beam-column joint sub-assemblage at the beam ends. The displacement of the beams, Δ_{beam}, are summed and divided by the length, ℓ_{beam}. The lengths of the beams are measured from the center of the joint to the beam end. The drift ratio is calculated using Equation 4.2.

$$\left(\frac{\Delta_{beam1} + \Delta_{beam2}}{\ell_{beam1} + \ell_{beam2}} \right) \times 100\% \tag{4.2}$$

The method of calculating this parameter may vary from experiment to experiment depending on the loading and response information provided. For example,

Pessiki (1990) provides the lateral displacement at the top column end for the positive and negative half cycles. Since the damage states are reported as occurring at the cycle as a whole, the author requests that the drift be calculated using an average of these lateral lengths. The resulting displacement is divided by 133.5 in., the height of the column.

4.3.2 Number of Cycles

Damage indices developed in the past suggest the number of cycles is an important indicator of damage. The number of cycles accounts for the fatigue sustained by a component similar to the measurement of energy dissipation. A complete cycle is four parts. Loading the component to the target demand is part one. Part two is unloading the component back to the initial position. Loading and unloading in the opposite, or negative, direction are parts three and four.

The method of counting the number of cycles must account for the variety of load histories. This is done by weighting the cycle number with the magnitude of the displacement demand for that cycle. The simple cycle-counting algorithm proposed by Lowes (1999) was modified for use in this study. This algorithm defines the cycle counts as shown in Equation 4.3

$$\sum_{i=1}^{n} \frac{\left|\Delta u_i\right|}{4u_{\max}} \tag{4.3}$$

where the u_{max} is the historic maximum displacement, Δu_i is the current displacement increment, n is the number of displacement increments. This algorithm weighs cycles on the basis of the ratio of maximum displacement demand of the cycle to the maximum historic displacement demand. Lowes (1999) concludes that the results of experimental testing of reinforced concrete components suggests that cyclic loading to displacement demands that are less than the historic maximum displacement demand are less damaging and this approach to cyclic counting is appropriate.

The algorithm proposed by Lowes (1999) was developed for use with arbitrary displacement histories where Δu_i is the arbitrary displacement increment. The load histories used in the selected experimental studies consist of full or half cycles simulating seismic demand. The displacement increment, Δu_i, becomes the maximum displacement of the half cycle, $u_{half\text{-}cycle}$. Equation 4.4 shows the modified algorithm.

$$\sum_{i=1}^{2} \frac{\left| u_{i\,half-cycle} \right|}{2u_{\max}} \tag{4.4}$$

The modified algorithm is applied to the load histories of the selected joint specimens. Where the maximum displacement demand of the half cycle is either equal to or greater than the previous cycle, the algorithm does not change the cycle count. However, some specimens were tested using load histories that vary the maximum displacement demand throughout the test. Application of the modified Lowes algorithm is very effective in providing a more consistent engineering demand parameter. For example, the algorithm is applied to the asymmetrical load history of specimen PADH 14 tested at the University of Washington shown in Figure 4.2.

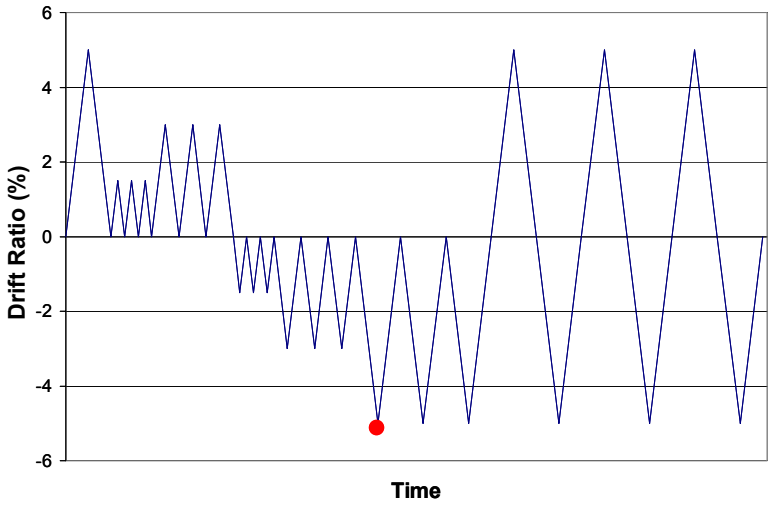

Figure 4.2: Number of cycles counted for the load history of specimen PADH 14. (Walker 2001)

The first half cycle has a magnitude of 5% drift ratio. Description of the damage in the study report identifies Damage State 5 occurring at 5% drift and cycle number ½. The next description of damage is Damage State 6 occurring at the dot shown in Figure 4.2. Applying the modified Lowes algorithm, the cycles are counted using the maximum historic displacement demand, u_{max}, of 5% drift ratio. The cycle count becomes 7.

4.3.3 Nonlinear Function of the Drift and Cycles

Combining the first two engineering demand parameters, drift ratio and number of cycles, into a nonlinear function yields a more robust engineering demand parameter.

Both the displacement demand and the impact of fatigue are accounted for. The nonlinear function is designed using a general nonlinear formula defined in Equation 4.5

$$f(drift, cyles) = a \times drift^{b} + c \times cycles^{d} \tag{4.5}$$

The coefficients *a, b, c,* and *d* optimize the function to reduce the scatter of the damage data. Great dispersion is associated with the engineering demand parameters for each method of repair. A scatter plot showing the dispersion is Figure 6.1. The values of *a, b, c,* and *d* are 7.7, 0.85, 0.87, and 0.8, respectively. The optimization code in MATLAB is used to evaluate these coefficients. The minimum value was set to 0.25 to avoid optimizing the function for only one EDP, i.e. the drift ratio.

4.3.4 Joint Strain

Joint strain defines the demand sustained only by the joint. The displacement demand characterized by drift includes the contributions of the beam bending, beam-end rotation due to bar slip, column bending, and finally joint shear deformation. (Bonacci 1996) Since the performance of strictly the joint is important for this research, joint strain becomes a valuable EDP.

Measurement of the joint strain is possible using two methods. The first is a configuration of linear variable differential transformers (LVDT) over the surface of the joint called a shear rig. Two shear rigs, one small and one large, were mounted on the face of the joints tested by Walker (2001) and Alire (2002). The instruments are arranged in four triangles and shown Figure 4.3. According to the recommendation of the author of the study, the large shear rig is selected for the most reliable data and is used to generate the probability models developed in Chapter 6.

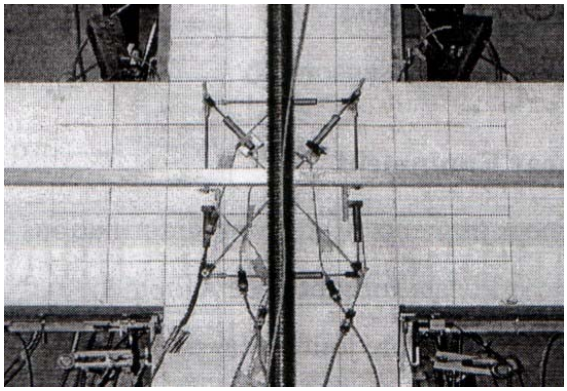

Figure 4.3: Joint strain is measured by the large shear rig (Alire 2002).

The second method of determining the joint strain is derived from the four contributing sources of displacement. The contributions of beam and column bending are removed from the drift demand. The curvature or bending is measured with instrumentation attached to the beams and columns. The process of deriving the joint strain from these demand measures is described in Appendix B. The curvature instrumentation is not considered as reliable as the shear rigs and is not applied for generation of a probability model in this report.

4.4 Conclusion

The results of previous experimental investigations of the earthquake response of beam-column joints were evaluated to identify the damage data and determine the appropriate engineering demand parameters. Four demand parameters were identified; inter-story drift ratio, number of cycles, nonlinear function of drift ratio and cycles, and joint strain. Damage is predicted well by the nonlinear function of drift ratio and cycles. However, inter-story drift includes the influence of the beam and column inelastic deformation. Joint strains provide indication of joint demand without error associated with the inclusion of beam and column deformation.

Chapter Five
Methods of Repair

5.1 Introduction

For the current study, repair costs and downtime associated with repair define economic loss due to earthquake induced structural damage. This chapter defines a series of progressively extensive repair techniques that can be used to restore a damaged reinforced concrete structural component to its original, pre-earthquake strength and ductility capacity. These repair techniques are included in the repair manuals, identified in Section 2.4, used in field following recent earthquakes on the west coast of the United States.

The proposed repair techniques are organized into five methods of repair progressing from the most minimal type of repair, Cosmetic, to the most substantial, Replacement of the Rebar. The methods of repair are assumed to be comprehensive and, with the exception of the Method of Repair 0, mutually exclusive. Given the damage state sustained by a component, the information presented in this chapter links damage to repair to enable the progression from component damage to economic loss.

5.2 Repair of Damage Measures

The methods of repair appropriate for the earthquake induced damage sustained by beam-column joints are number 0 through 5. Each of the 12 damage states described in Chapter 3 is repaired by one of the methods shown in Table 5.1.

Table 5.1: Damage states assigned to each repair technique.

#	Method of Repair	Extent of Damage	Damage States
0	Cosmetic Finish	Minor Cracking	0 and 1 +2-12
1	Epoxy Injection	Cracking	2, 3, 4, and 5
2	Patching	Spalling	6, 7, and 8
3	Replacement	Crushing	9, 10, and 11
4	Replacement	Rebar Damage	12 a, b, and c

The method of repair is linked to a cost that is used to determine the economic impact of the damage. The damage state describes the amount of the joint requiring

repair. The most severe damage state associated with each method of repair is used to determine the amount of materials and time required to complete the repair work. Spalled concrete, characterized by Damage States 6, 7, and 8 require Method of Repair 2. The spalled concrete associated with Damage State 8 covers more of the joint than that seen in Damage State 6. Since neither Damage State 6 nor 8 would require removal of undamaged concrete, either would be representative. However, Damage State 8 would require more material and would provide a more conservative estimate of loss and it is used to represent Method of Repair 2 when the cost per joint is calculated.

5.3 Method of Repair 0: Cosmetic Repair

Cosmetic repair is required when damage is sustained by the finish. Removal and replacement of the damaged finish materials define this method of repair. Upon removal of the material covering the joint, the damage sustained by the joint is assessed. While Damage States 0 and 1 require only this method, all damage states require cosmetic repair in addition to the following methods.

5.3.1 Demolition

The existing damaged finish material must be removed from the joint and the building. The process required for removal is characterized as demolition. Demolition is required to gain access to the damage joint prior to any repair work. Demolition involves removal of the materials covering the joint and disposal of the resulting debris.

Additionally, lifelines may inhibit access to the damaged joint. Replacement of the lifeline is not included in the repair. Since the presence of lifelines and the necessity of removing them are specific to each situation, the impact of the work associated with lifelines is not included in this report.

5.3.2 Finish Work

Finish work is matching, installing, and painting or texturing the finish material. The type of finish will vary from low end to high end. The low end material selected in this research is drywall. Drywall is a common material that general contractors have experience in installing and texturing. Estimating will cost of this type of finish will be easier due to the wide use. The high end finish may be a variety of expensive materials,

including wood, stone, or marble. Due to the variety, an exact estimate will be difficult to determine.

5.4 Method of Repair 1: Epoxy Resin Injection of Cracked Concrete

Low to moderate earthquake demand will crack reinforced concrete. The cracks are wide enough to be repaired with epoxy resin. An exterior joint tested by A. Filiatrault was repaired by this method after loading up to 1.4% drift and yielding of the beam longitudinal rebar. Numerous cracks are distributed over the surface of the joint. First, holes are drilled for ports. Then the surface is sealed with a quick-setting viscous epoxy. The low viscous epoxy resin is injected starting at the lower ports and moving up. (Filiatrault 1992)

This repair technique is recommended when the cracks in the concrete significantly reduce the earthquake resistance of the component. Application of epoxy resin injection may be used for crack widths as small as two one-thousands of an inch and for crack widths as large as three-fourths of an inch. (Runacres, 2003) The width a shear crack must be before requiring repair varies among the sources investigated. Cracks width greater than 0.013 in. for exterior and 0.016 in. for interior components are defined by ACI 318-95 to require repair. The reason listed is to prevent steel reinforcement corrosion or to allow transfer of stresses through the aggregate. For beam-column joints, a more practical minimum crack width is one-thirty seconds of an inch or one-sixteenths of an inch. (Savage, 2003)

5.4.1 Epoxy Resin

The parameters considered in application of this method is the sealant applied to the joint surface, the viscosity of the resin, the pressure under which the resin is applied, and for how long until the entire crack is filled. The bond between the reinforcement and the concrete may be restored, but such restoration is not recognized by rehabilitation guidelines. (Newman, 2001) The tensile and compressive strengths of the epoxies used in lab tests (Tasai, 1992 and Filiatrault, 1992) are 7.2 to 8.7ksi (50 to 60 MPa) and 6.4 to 13.3ksi (44 to 92 MPa), respectively. The low-pressure injection requires a sealant on the component surface. This high viscosity adhesive has a quicker setting time and a lower strength than the injectable epoxy. The tensile and compressive strengths of the sealant

used in lab tests are 4.6ksi (32MPa) and 10.6ksi (73MPa), respectively. This is usually a temporary sealant and should be removed after the epoxy resin has set. The resin sets for up to four weeks.

5.4.2 Advantages and Disadvantages

The injection of epoxy resin has been around for decades and the process has undergone some changes. Most importantly is the risk of trapping air pockets while filling up the cracks. The disadvantage of epoxy injection is the risk and the extra time that must be taken to reduce risk.

The advantage is the highly common use of this method of repair. All concrete repair crews have had significant experience in applying epoxy injection and are highly skilled. The risk of trapping air pockets within the concrete is obviated by the skilled use of injection equipment.

5.5 Method of Repair 2: Patching of Spalled Concrete

Experimental investigation of joint response shows that the concrete covering column longitudinal reinforcement in the joint core will spall under moderate earthquake loading of the joint. (Clyde 2000) Spalled concrete will fall away from the joint during loading or will be brushed away prior to repair exposing the aggregate and the rebar underneath. The exterior joints tested by Karayannis were loaded until spalling occurred at 3.6% drift. The “loose concrete fragments” were repaired with a cement paste.

5.5.1Cementitious Material

The cement paste used in the repair of the exterior joint specimens has low shrinkage, high strength, and rapid hardening properties. (Karayannis 1998) The tensile strength of the material used in the experiments is 3800psi. Compare this to the modulus of rupture, f_r, of the original concrete approximated as $7.5\sqrt{f'_c}$ by the ACI code. The compressive strength of the paste is also more than twice the original concrete compressive strength, f'_c. Adhesive materials are added to the mixture to ensure adhesion to the exposed aggregate. The paste may also be called a mortar.

5.5.2 Advantages and Disadvantages

The advantage of patching the spalled concrete is no equipment must be rented. The contractor hired for the repair work owns the tools needed to mix and apply the small amounts of cementitious material.

5.6 Method of Repair 3: Removal and Replacement of Damaged Concrete

If earthquake loading of the joint is severe, concrete damage may extend beyond the cover concrete, with significant loss of concrete in the joint core resulting in exposure of the column and/or beam longitudinal reinforcement. The concrete may separate from the component via severe cracking that breaks up joint core concrete. The broken concrete must be removed. The remaining intact concrete must be jack hammered out. New concrete will replace the entire joint area. (Savage, 2003)

5.6.1 New Concrete and Formwork

This repair technique is distinct from the previous because the concrete is intentionally removed by chipping and/or jack hammering. The concrete is removed to improve the bond of the new material to the existing steel and remaining concrete. Once the original concrete is removed, the repair is essentially new construction. Formwork must be installed on the front and back of the joint. New concrete is mixed and poured. The compressive strength is reached in twenty-eight days.

5.6.2 Shoring

During repair, the compressive strength of the joint is compromised. A temporary support must be installed to relieve the joint of the existing gravity load.

5.6.3 Advantages and Disadvantages

The advantage of removing remaining concrete is negating the need for a cementitious material similar to that used in the previous method. The repair manuals require a procedure more complicated than either methods of repair 2 or 3. If the depth of concrete broken off is greater than 6 in., additional modes of adhesion are required. These include an epoxy adhesive or a mechanical device, such as epoxy coated dowels, used to bond the new material to the original concrete. (FEMA 308, ACI 546R)

The disadvantage of removing the remaining concrete is the process also removes the remaining compressive strength of the joint. Shoring must be used, adding significant time and expense.

5.7 Method of Repair 4: Removal and Replacement of Damaged Rebar

This loss of concrete may result in redistribution of loads and additional loads being applied to the column and beam longitudinal reinforcing steel. Load redistribution due to loss of concrete has results in the column reinforcing steel carrying most of the column axial within the joint and has yielded, buckled and possibly fractured under the loading.

5.7.1 New Rebar

The damaged reinforcement and crushed concrete is removed and replaced. New steel is held in place with a mechanical connection. The mechanical connection may be a sleeve, splice, or threaded couplers. Skilled application of connection must ensure the proper length of the original and new steel as well as correct material properties for devices requiring grout. (FEMA 308) The new concrete material must have the same properties at the original to ensure proper bond.

5.7.2 Shoring

The compressive strength of the joint is significantly reduced when the damage reaches the reinforcing steel. The axial load demand on the rebar must be removed prior to repair. Temporary support, shoring, must be installed immediately to relieve the joint of the existing gravity load.

5.7.3 Advantages and Disadvantages

The advantage of installing a mechanical connector is that recent advancement in the technology has reduced the degree of skill required for installation. New products like Zap Screwlock® couplers can be installed efficiently. Detailed instructions accompany the devices upon delivery from the manufacturer obviating the need for especially skilled labor and inspectors.

The disadvantages of replacing the rebar and concrete in an existing joint is the combined cost of the repair work and downtime may exceed the cost of demolishing the entire building.

5.8 Conclusion

Five methods of repair were identified to restore the damaged joint to pre-earthquake condition; Cosmetic, Epoxy Resin Injection, Patching, Removal and Replacement of Concrete, and Removal and Replacement of Rebar. Repair techniques for concrete damage identified in repair manuals are verified by structural engineers and general contractors for application to the specific damage sustained by older beam-column joints. The relationship is considered deterministic between damage states and methods of repair.

Each method of repair defines the labor, material, and equipment required to complete the repair work. For some damage states, multiple methods are required for complete restoration of the joint. For example, Method of Repair 0 is applicable to the nonstructural damage associated with low levels of structural damage. The nonstructural damage is sustained by the finish material covering the joint. Repair of this material would be required for all levels of damage after Damage States 0 and 1.

Spalled concrete is repaired by Method of Repair 2. This method is intended for the cover concrete that has fallen away from the joint and must be replaced. The progression of damage described in Chapter 5 suggests that significant cracking will occur before spalling. Thus, it is assumed that a joint requiring Method of Repair 2 will also require Method of Repair 1.

Shoring is required for Methods of Repair 3 and 4 and is included in Sections 5.6 and 5.7. Large pieces of equipment are required for shoring where the entire gravity load demand on the joint must be relieved. A significant amount of the labor and equipment of these methods is due to shoring.

Chapter Six
Predicting Damage as a Function of Demand

6.1 Introduction

Component-specific probability models provide the link between the engineering demand parameter and the earthquake induced damage sustained by the component. The probability models consist of fragility curves generated from the damage data in collected from the experimental studies. Fragility curves indicate the probability of reaching or exceeding a damage state as a function of an engineering demand parameter. The deterministic relationship between the damage states and the methods of repair extends the prediction directly to a method of repair. Section 6.2 defines the sets of damage data. Section 6.3 and 6.4 described the selected distribution functions and determines the best for the data using the goodness-of-fit tests. Section 6.5 presents the fragility curves based on the appropriate engineering demand parameters.

6.2 Data Sets

Three sets of data were devised from the observed damage state occurrences in the twenty-five interior beam-column joints. The observed damage states are grouped according to the method of repair each requires. Since at least two or more damage states are contained in each repair group, three options are available for gathering the data sets. Figure 6.1 shows the scatter of the all the data points for four considered engineering demand parameters. The y axis is the Damage States 0-12 as defined in Chapter 3. These damage states are group into the method of repair as defined in Chapter 5.

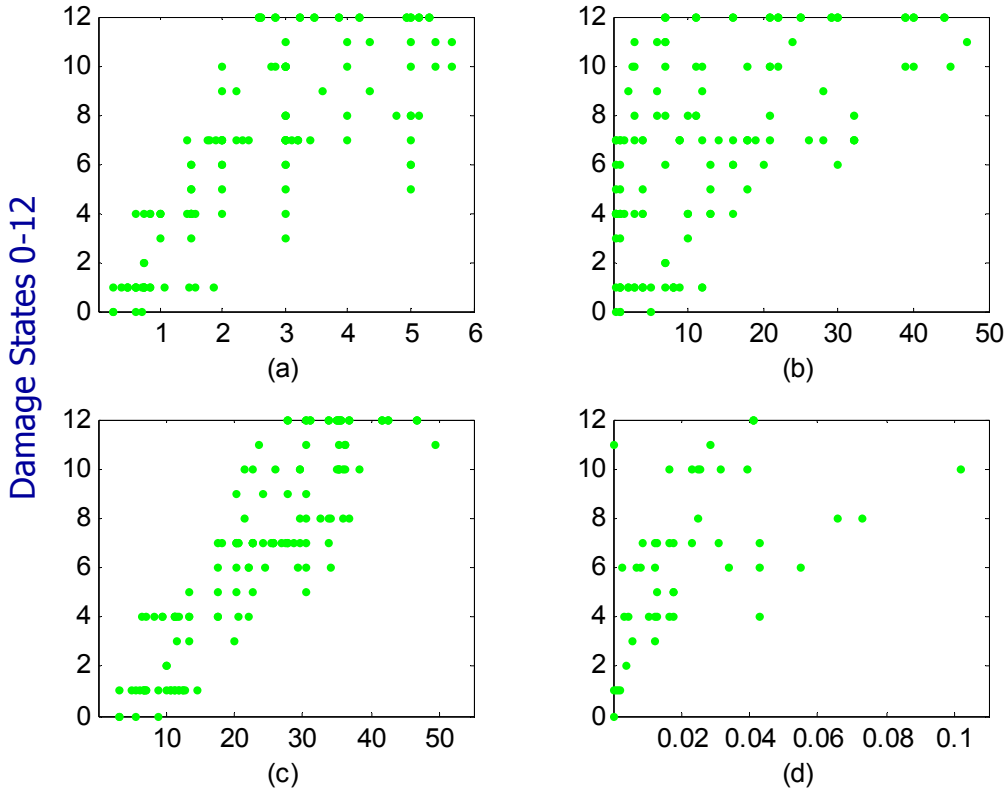

Figure: 6.1: Scatter plots showing the demand at which each damage state (0-12) occurs for all 25 specimens. (a)Drift Ratio (%) (b)Number of cycles (c) Nonlinear Function of drift and cycles (d) Joint strain

The three data set for gathering the data points into sets are labeled Data Set One, Data Set Two, and Data Set Three. For completeness all three sets are defined in this section and are compared to find the most suitable option.

6.2.1 Data Set One

Data Set One includes, in each repair group, all of the damage states associated with the repair method. However, one specimen can not provide more than one data point per repair group. For each specimen, the lowest damage state associated with the repair group is selected and any subsequent damage states reported for the same specimen are removed. Thus, the data set will include no more data points than the total number of specimens, twenty-five.

6.2.2 Data Set Two

Data Set Two is similar to Data Set One except that more data points are included in each group. The set begins with the data included in Data Set One. If a specimen did not exhibit any damage state included in the repair group, a data point may be added for a damage state requiring a higher method of repair. The data set contains no more data points than the twenty-five selected specimens.

6.2.3 Data Set Three

Data Set Three includes, in each repair group, only the lowest, or trigger, damage state. The trigger damage state is the first state of the damage progression qualifying for the method of repair. For example, Method of Repair 2 is patching of spalled concrete and would be required at the first signs of significant spalling. This is damage state 6 where at least 10% of the joint surface has spalled. Thus, only the specimens reporting this damage state are included in the group resulting in a very limited sample size.

6.2.4 Comparison of Data Sets

The goodness-of-fit test is applied to the three data sets. The K-S parameter is compared to the critical value to determine the most reliable data set in Figure 6.2.

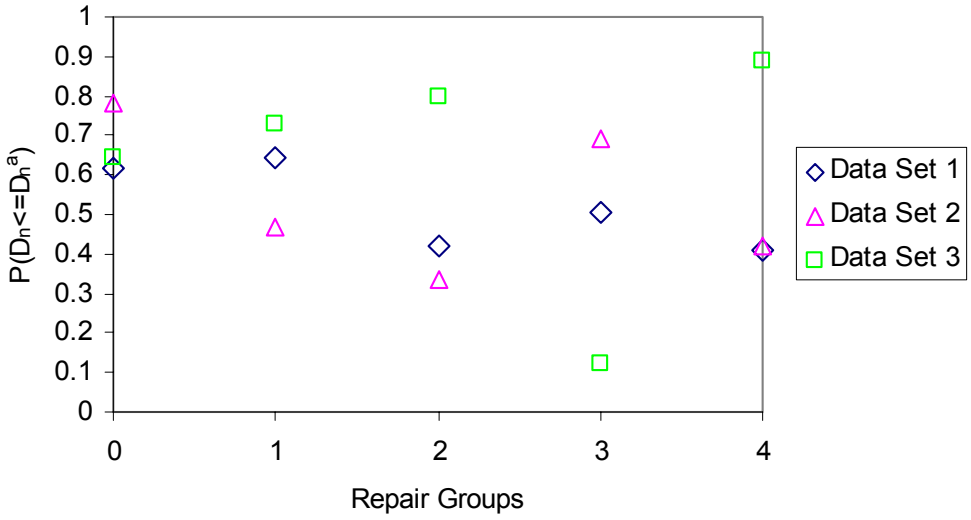

Figure 6.2: Results of Kolmogorov-Smirnov test applied to the three data sets.

However, the sample size interferes with the results. As noted in Section 2.5.2, the critical value will increase as the sample size decreases. Thus, the data set with the

smallest number of data points, Data Set Three, will demonstrate the highest probability of being less than the critical value. This is confirmed in the Figure 6.2 above. Instead, the best data set is determined by comparing the impact of each set on the probability model. Reliability of the model increases with the larger data set, eliminating Data Set Three. Additionally, Data Set Two will generate a model shifted to higher demands where the higher damage states of the additional data points are observed. Thus, Data Set One provides the best collection of data points and is used for the fragility curves presented in this chapter.

6.3 Distribution Selection

The fragility curve must be evaluated using the best fitting curve. The Kolmogorov-Smirnov and Chi-Square tests are used to determine the distribution that provides the best fitting curve. The distributions are selected based on their parameters and the upper and lower limits. The data sets are the data points at each damage state and grouped according to the appropriate repair method. Four distributions were selected for comparison with the Step-wise CDF. The considered distributions are lognormal, normal, Weibull, and Beta and are discussed in detail in Section 2.4.

6.3.1 Step-wise CDF

The Step-wise Cumulative Density Function (CDF) characterizes the probability model for the given demand and data set. The CDF is a function of the rank of the data point defined in Equation 2.4. The distribution applied to Data Set One for percent drift is shown in Figure 6.3 as a scatter plot. The curves represent the probability of exceeding the requirements for each of the five methods of repair. The methods of repair are identified by number in the legend.

Since more than one data point may have the same demand value, often a single point on the plot can represent more than one occurrence of damage. The rank of the data set for Method of Repair 0 is shown in Table 6.1. The effect of the sample size on the reliability of the damage prediction is discussed in Section 6.6.

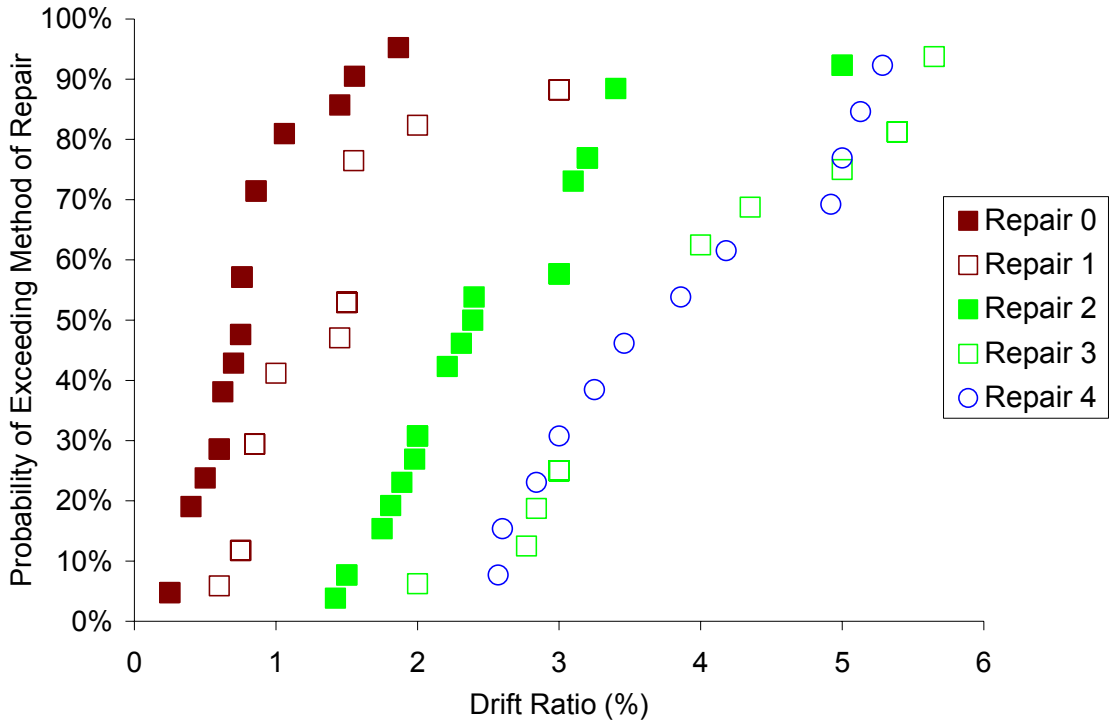

Figure 6.3: The probability of exceeding each of the five repair groups evaluated using the Stepwise CDF.

Table 6.1: Stepwise CDF for Method of Repair 0.

Drift	Rank	P
0.25	1	4.76%
0.25	1	4.76%
0.25	1	4.76%
0.4	4	19.05%
0.5	5	23.81%
0.6	6	28.57%
0.6	6	28.57%
0.63	8	38.10%
0.7	9	42.86%
0.75	10	47.62%
0.75	10	47.62%
0.76	12	57.14%
0.76	12	57.14%
0.76	12	57.14%
0.86	15	71.43%
0.86	15	71.43%
1.06	17	80.95%
1.45	18	85.71%
1.55	19	90.48%
1.87	20	95.24%

6.3.2 Normal Distribution

The upper and lower limits of the normal distribution extend infinitely. The normal distribution provides equal probability to data occurring on either side of the mean. For example, the average demand at which the damage requiring Method of Repair 1 provides just as much chance that Method of Repair 1 would be required as Method of Repair 0. This is not conservative, especially when compared to the lognormal distribution. The lognormal distribution will weigh, at least slightly, in favor of the greater repair technique. Note the curves shift slightly to the higher demand in Figure 6.4 than Figure 6.5.

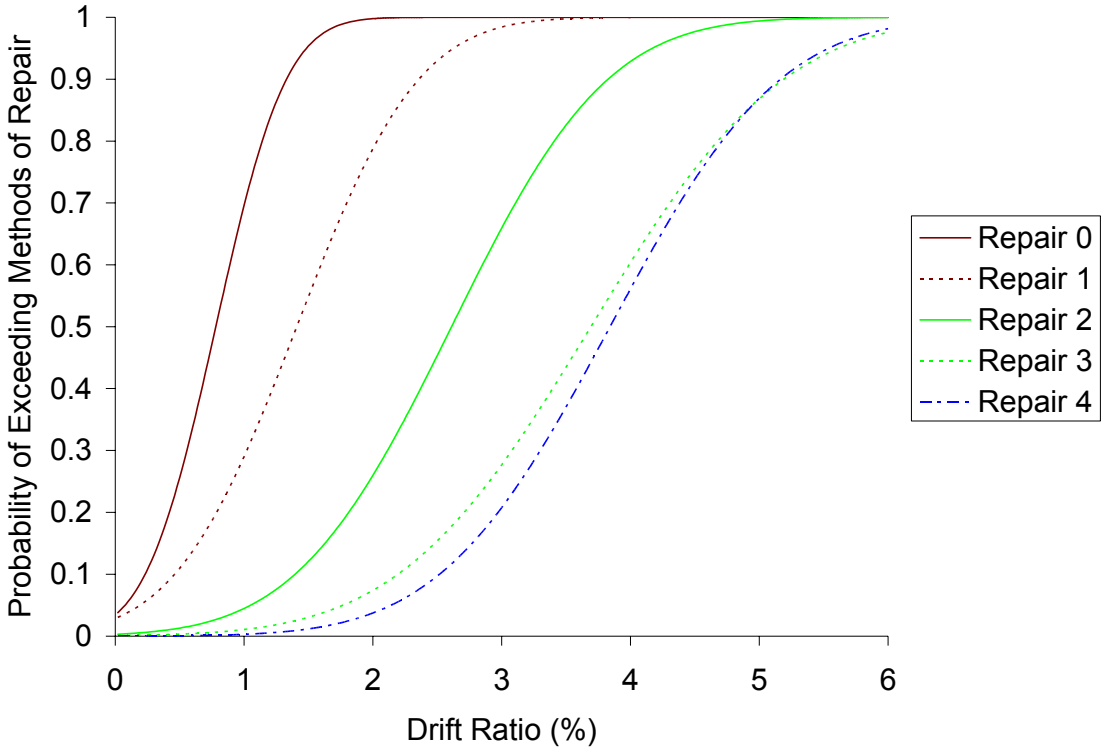

Figure 6.4: Fragility curves for the repair methods 0-4 evaluated using the normal distribution.

6.3.3 Lognormal Distribution

The lognormal distribution is commonly used for evaluation of fragility curves. The lognormal parameters are evaluated using the first and second moments, E(x) and Var(x) as defined in Equation 2.6.

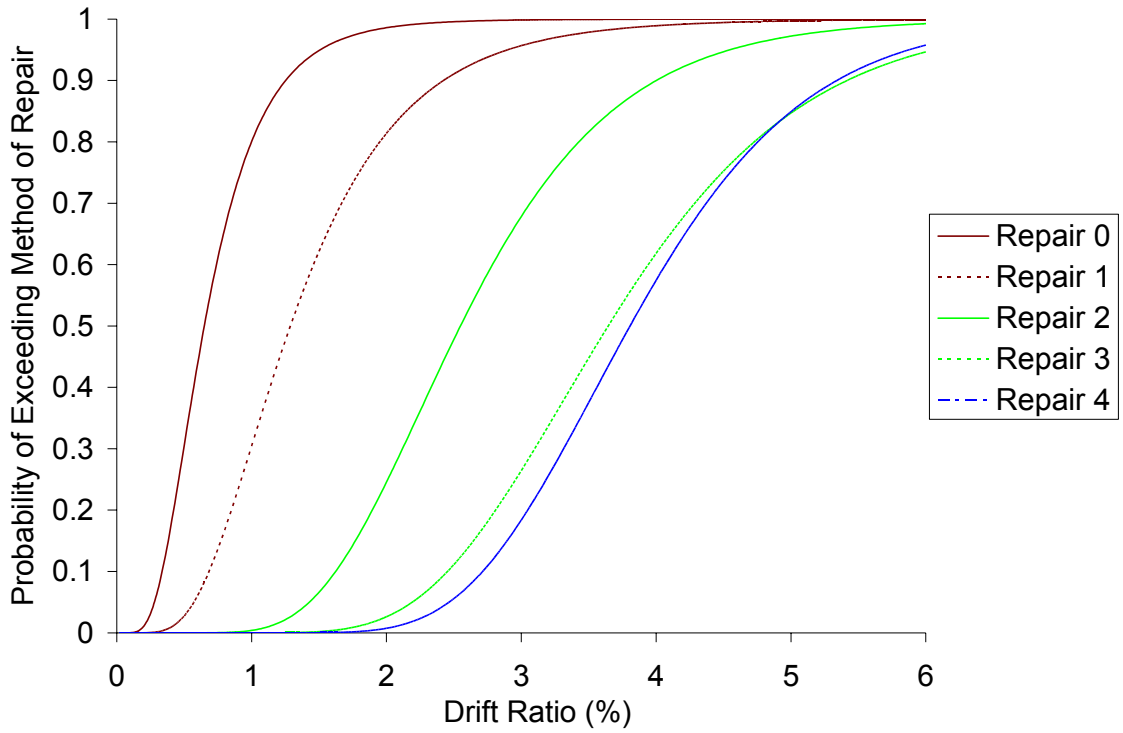

Figure 6.5: Fragility curves for the repair methods 0-4 evaluated using the lognormal distribution.

6.3.4 Weibull

The Weibull distribution allows for a stronger influence from the extreme values of the data set. Where the smallest values of demand are of greatest importance to this research, this is a potentially useful distribution. The parameters, k and w_1, are evaluated using Equation 2.10 for the sample data. The fragility curves generated for this distribution are shown in Figure 6.6.

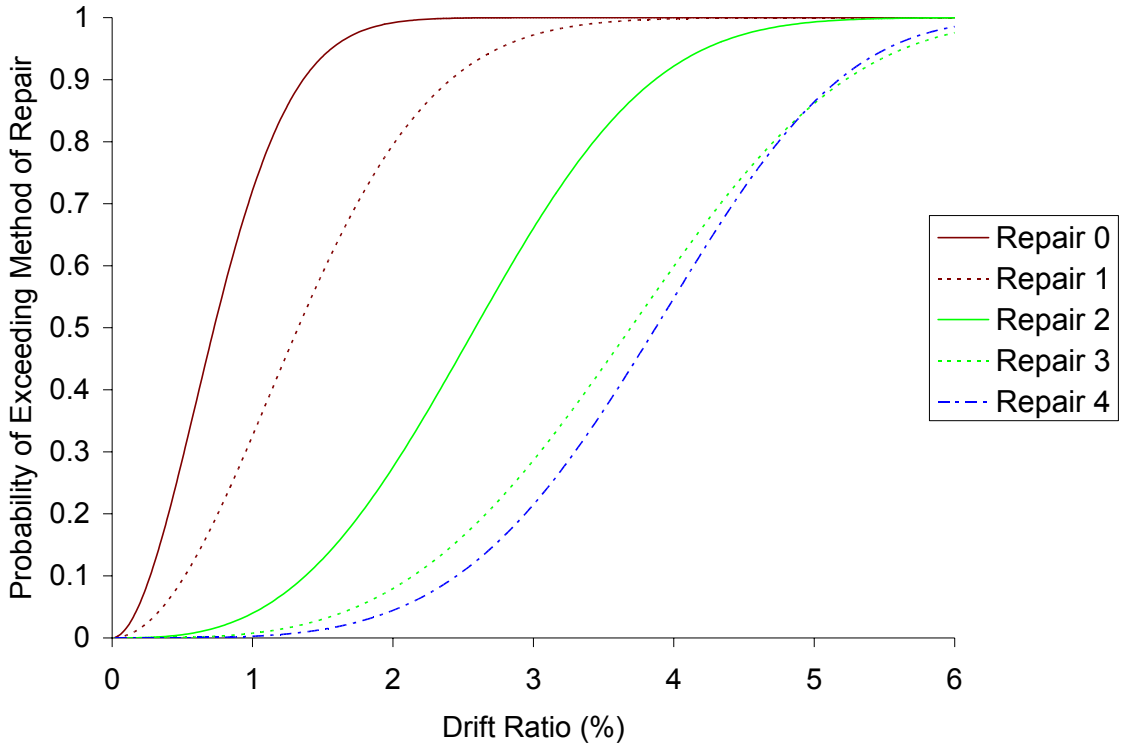

Figure 6.6: Fragility curves for the repair methods evaluated using the Weibull distribution.

6.3.5 Beta

The Beta distribution is defined by lower and upper limits, *a* and *b*. The smallest and largest data points are used for these values. The resulting curves indicate the benefits of the bounds do not out weigh the complexity of evaluation as seen in Equations 2.13 and 2.14. The probability density function requires that both the gamma and beta functions be evaluated, introducing more uncertainty into the distribution. The results of the goodness-of-fit tests confirm this. The fragility curves generated for this distribution are shown in Figure 6.7.

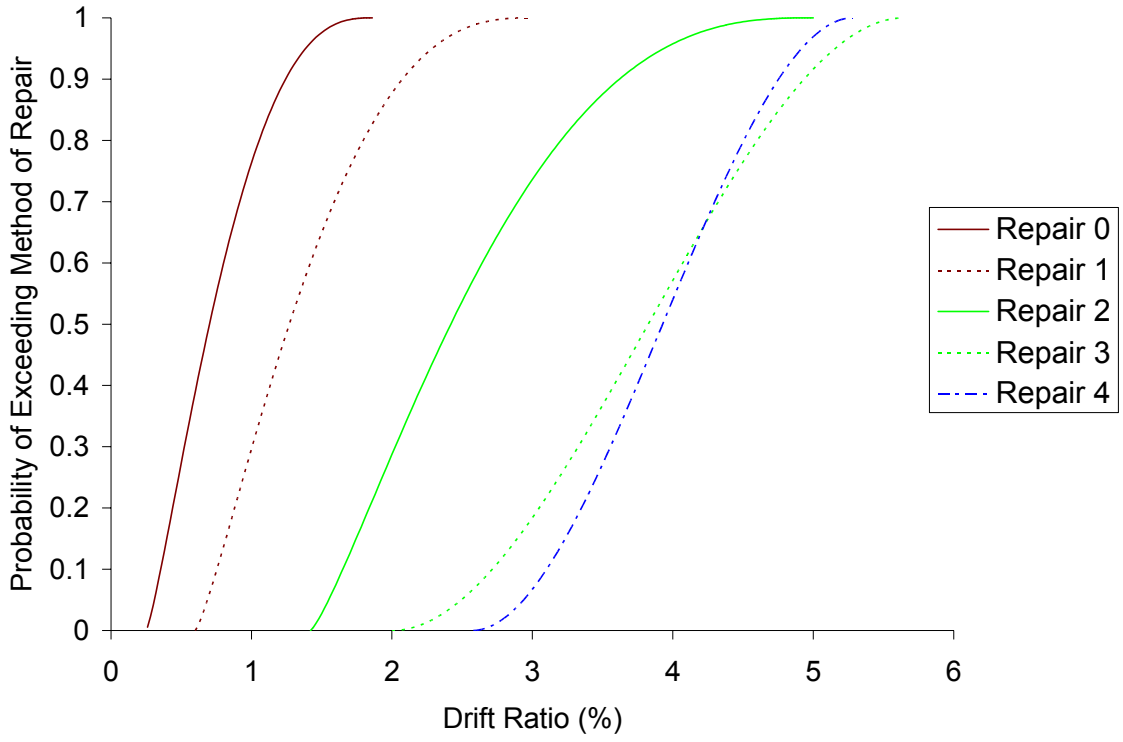

Figure 6.7: Fragility curves for the repair methods evaluated using the Beta distribution.

6.3.6 Best Distribution

The best fitting distribution is determined using the Kolmogorov-Smirnov test. The K-S parameter, D_n, is defined in Equation 2.1 as the maximum difference between the selected distribution values and the Step-wise CDF value. The K-S parameter may be called the error. The error is compared to a critical value, D_n^{α}, for the selected significance level. The distribution providing the greatest probability the error will be less than the critical value is considered the best fitting.

For each of the five repair groups, the error values may be compared to the critical values in Figure 6.8(a). The associated probability of the error being less than the critical value is shown in Figure 6.8(b). The complete results of the K-S test for each of the previously defined distributions are available in Appendix D. The lognormal and the normal distributions are shown to provide the most acceptable probabilities when compared to the critical values for each repair group. Thus, indication from the plots shown that the lognormal and the normal distribution functions generate the best curves

is verified. Determining the most appropriate distribution between the lognormal and the normal is next.

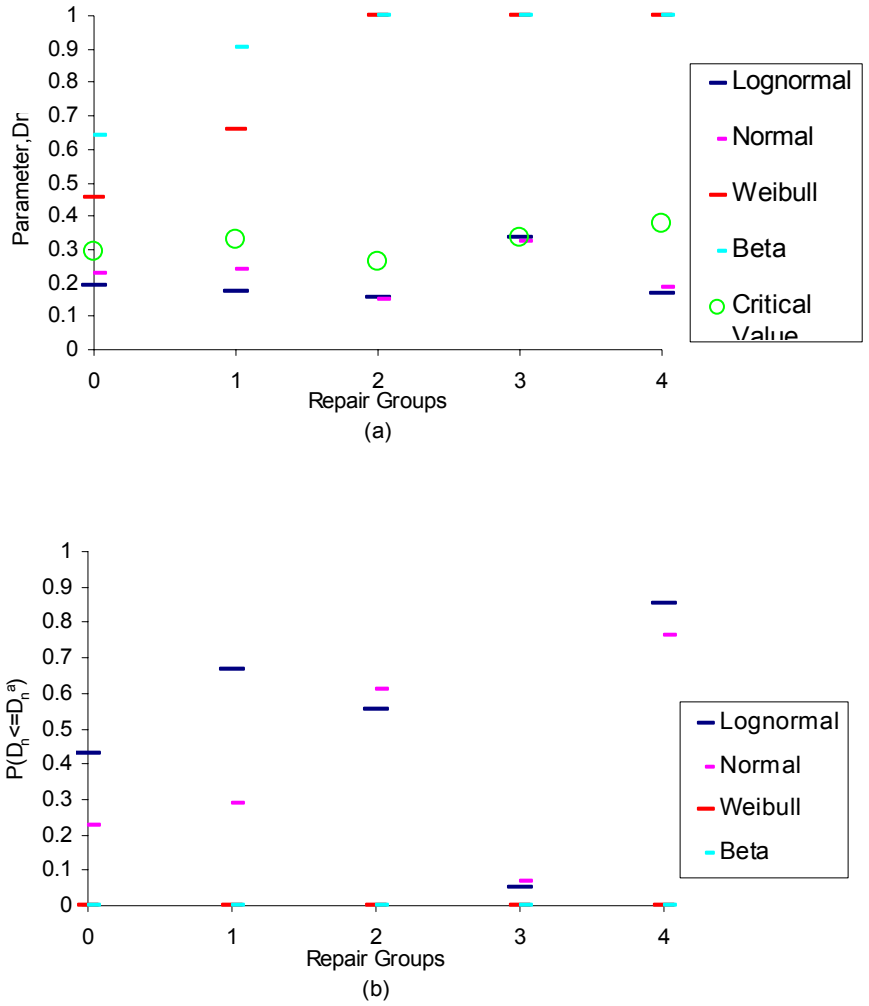

Figure 6.8: Kolmogorov-Smirnov test results. (a)Comparison of the test parameters for each distribution and the critical value. (b)Comparison of the probability of the test parameters being less than the critical value.

In order to determine which of the lognormal and normal distribution provide the best fitting curve, the Chi-Square test is used. The results of this second goodness-of-fit test can be seen below in Table 6.2. Data set one is used for this demonstration. Remember this set is defined by the engineering demand parameter of the story drift where only the specimens reporting the required damage states are included. Thus, only twenty specimens are associated with Method of Repair 0. Compare the error evaluated

for both the lognormal and the normal distributions to the chi-square distribution value, $c_{1-\alpha,f}$, of 5.991. This value is determined based on the degrees of freedom, *f*, and a significance level of 5%. The degrees of freedom, *f*, for five bins and two distribution parameters are 2.

Table 6.2: The results of the Chi-Square test for Method of Repair 0.

Bin Range EDP=drift	Observed Frequency	Expected Frequency for Lognormal	Expected Frequency for Normal	Error $(n_i-e_i)^2/e_i$ Lognormal	Error $(n_i-e_i)^2/e_i$ Normal
< 0.5	**5**	**6.12**	**5.12**	**0.204**	**0.003**
{0.5; 0.86}	**11**	**8.06**	**6.35**	**1.075**	**3.404**
{0.86;1.06}	**1**	**2.44**	**3.39**	**0.851**	**1.683**
{1.06;1.45}	**1**	**2.22**	**3.96**	**0.669**	**2.214**
> 1.45	**2**	**1.17**	**1.17**	**0.596**	**0.583**
Total	**20**	**20**	**20**	**3.395**	**7.887**

Despite individual bin error for the normal distribution being sometimes less than that of the lognormal, the total error for this repair group is significantly smaller for the lognormal distribution. Comparison to the Chi-Square value proves the normal distribution is not acceptable at this significance level. Note this distribution was acceptable for this significance level of 5% for the Kolmogorov-Smirnov test.

6.4 Method of Maximum Likelihood

The parameters of the distribution function described previously have been derived using the Method of Moments. The Method of Moments evaluates the mean and variance of the sample data. With some error, the mean and variance of the sample data represent the mean and variance of the population. As defined in Section 2.5.4, the alternative method to avoid error from evaluating parameters from the mean and variance is the Method of Maximum Likelihood. The likelihood function, Equation 2.15, is set equal to the selected distribution function, the lognormal distribution, in Equation 6.1.

$$L = \prod_{i-1}^{n} \frac{1}{\sqrt{2\pi}\zeta_x} \exp\left[-\tfrac{1}{2}\left(\frac{\ln x - \lambda_x}{\zeta_x} \right)^2 \right] \tag{6.1}$$

where L is the likelihood function and λx and ζ_x are the parameters of the lognormal distribution. The equation is minimized with respect to each parameter. The values of the parameters are evaluated as functions of the data set values, x_i.

$$\frac{\partial L}{\partial \lambda_X} = \tfrac{1}{2}\sum_{i-1}^{n} 2\left(\frac{\ln x_i - \lambda_x}{\zeta_x} \right) = 0; \qquad \lambda_x = \frac{\sum_{i-1}^{n} \ln x_i}{n} \tag{6.2}$$

$$\frac{\partial L}{\partial \zeta_X} = -\frac{n}{\zeta_x} + \tfrac{1}{2}\sum_{i-1}^{n} 2\left(\ln x_i - \lambda_x\right)^2 * \frac{2}{\zeta_x^2} = 0; \qquad \zeta_x^2 = \frac{\sum_{i-1}^{n} \left(\ln x_i - \lambda_x\right)^2}{n} \tag{6.3}$$

Deriving the equation for the parameter λ_x yields the sum of the natural log of the sample data divided by the sample size. Deriving the equation for the second parameter ζ_x yields the sum of the natural log of the sample data divided by the sample size. Essentially, the mean and variance of the natural log of the data is calculated. Thus, these parameters are most simply evaluated as E(ln x) and Var(ln x), respectively. Figure 6.9 shows the fragility curves generated using the lognormal distribution and the parameters calculated using Equations 6.2 and 6.3.

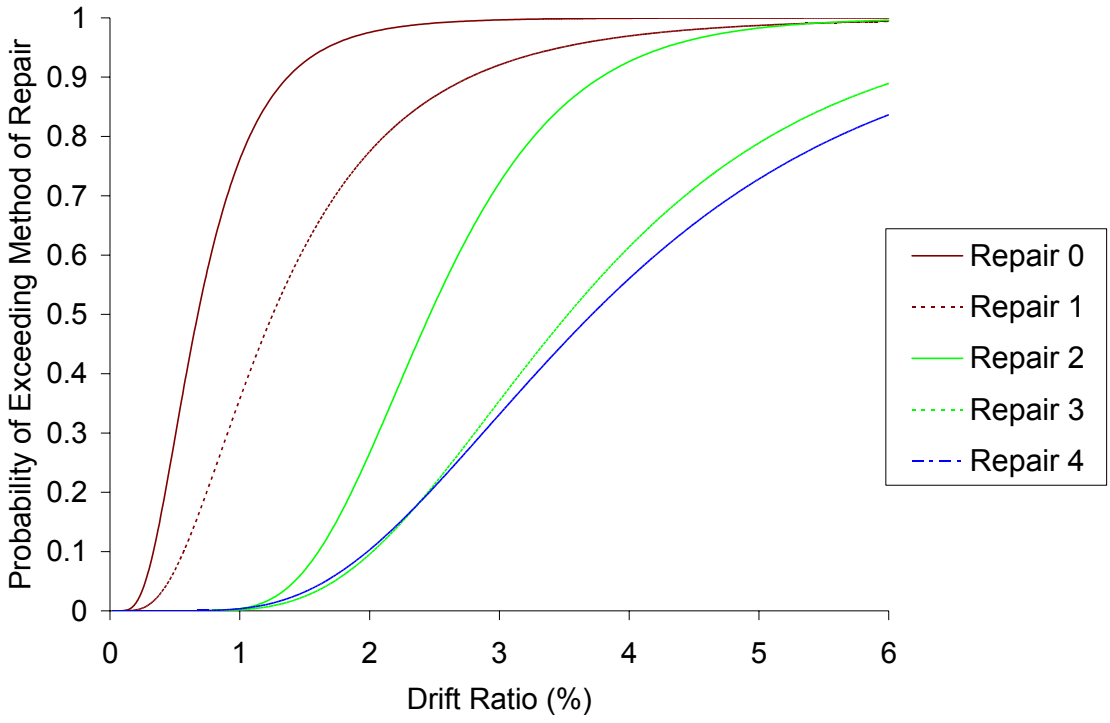

Figure 6.9: Probability of exceeding the repair method evaluated using the method of maximum likelihood to determine the lognormal parameters.

The goodness-of-fit tests are used again to determine any improvement in the curves. Again, the better distribution will have a greater probability of the error being less than the critical value. Since the curves for Methods of Repair 3 and 4 reflect the largest change, those will be the most critical groups to check for goodness of fit.

The goodness of fit of the lognormal distribution via the Method of Moments versus the Method of Maximum Likelihood is evaluated using the Kolmogorov-Smirnov test. The results of the K-S test do not clearly indicate the better method. Specifically for Methods of Repair 3 and 4, neither is consistently more reliable. Further analysis using the Chi-Square test determines the better of the two methods. The Chi-Square parameter is evaluated using Equation 2.3. Figure 6.10 compares the parameter for each method to the tabulated critical error value for each repair group.

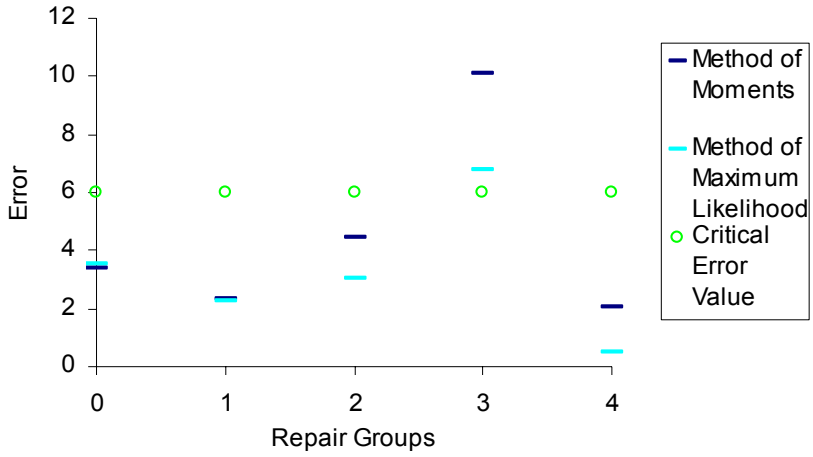

Figure 6.10: Chi-Square test results show that the method of maximum likelihood yields a smaller error and thus will be used to determine the fragility curves.

The Chi-Square parameter should be smaller than the critical error value. Here the Method of Maximum Likelihood is consistently lower than the critical error value and the parameter of the Method of Moments. The best distribution and accompanying method are determined to be the lognormal distribution where the parameters are evaluated using the Method of Maximum Likelihood.

6.5 Fragility Curves for Selected EPDs

The probability models demonstrating the distribution functions in the previous sections are based on the drift demand. The inter-story drift is calculated from the displacement of the beam or the column ends using Equation 4.1 or 4.2. This is the most common demand parameter for seismically loaded components and is readily available in the experimental studies. The other engineering demand parameters considered for beam-column joints in Chapter 4 are the number of cycles, the nonlinear function of drift and cycles, the joint strain, and the nonlinear function of joint strain and cycles.

The probability models for the demand defined by these engineering demand parameters are generated using the lognormal distribution function as determined in Section 6.3 by the goodness-of-fit test. The two distribution parameters are determined using the Method of Maximum Likelihood.

6.5.1 Number of Cycles

The engineering demand parameter of the number of cycles defines the demand as a function of fatigue. This EDP is important to account for the impact of fatigue on joint performance. The number of cycles are counted using Equation 4.3. The fragility curves based on the number of cycles is shown in Figure 6.11. Even though the curves are generated with the same damage data as for Figure 6.7, a significant change in the probability of exceeding each method of repair. For a given number of cycles, the probability of a repair is far more difficult to determine.

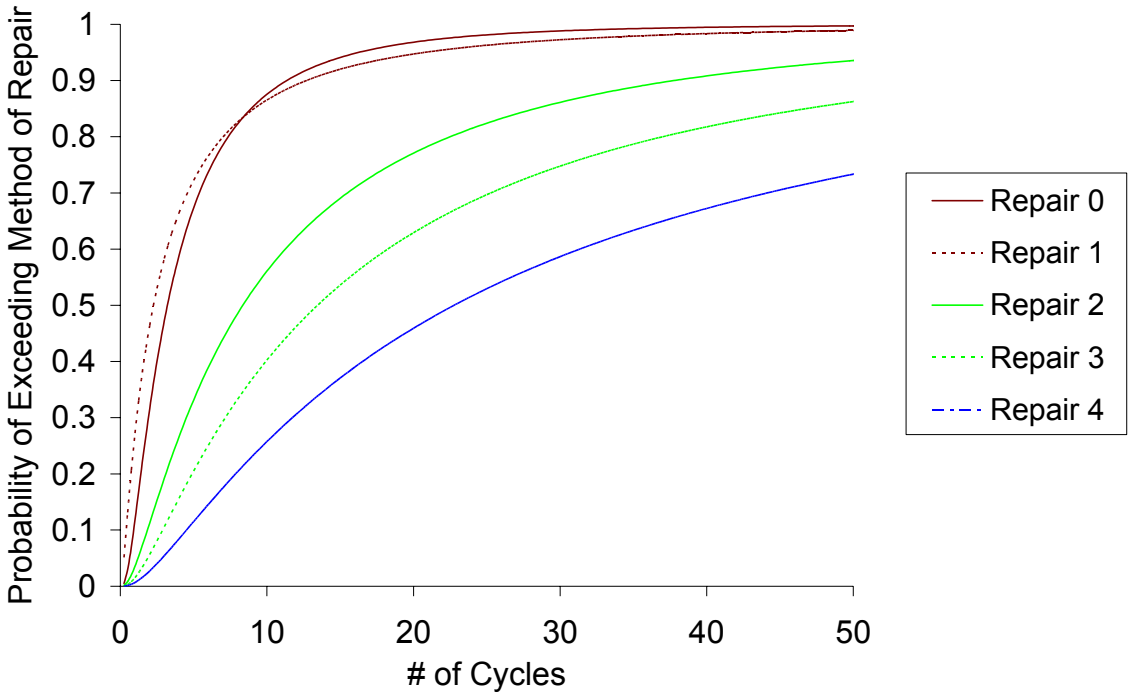

Figure 6.11: Prediction of the method of repair given the number of cycles.

6.5.2 Nonlinear function of drift and cycles

The engineering demand parameter of the function of drift and number of cycles accounts for both the magnitude and the frequency of the load history. The function is defined in Equation 4.5. A better representation of the earthquake demand is anticipated prior to evaluation of the probability model because more information decreases the dispersion of the damage data. The fragility curves based on this nonlinear function is shown in Figure 6.12 and confirms the improvement of dispersion. The curves for each method of repair are distinct and determining the appropriate repair is easiest of all the probability models.

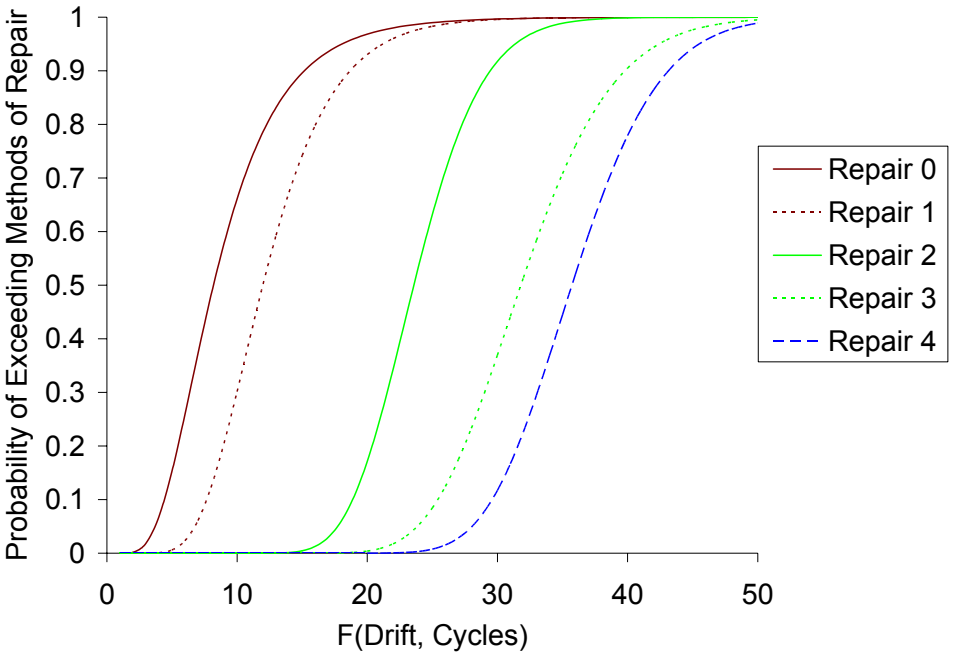

Figure 6.12: Prediction of the method of repair for a nonlinear function of drift ratio and number of cycles.

6.5.3 Joint Strain

The engineering demand parameter of joint strain describes the demand on the joint without influence the beams and columns. The data set for this EDP is limited to the damage data of ten specimens. The experimental studies of Walker (2001) and Alire (2002) provide the data to make this possible. However, the measurements yield a wide range of strain values due to the error associated with the instrumentation. The resulting probability model shown in Figure 6.13 appears very different from the models based on other EDPs.

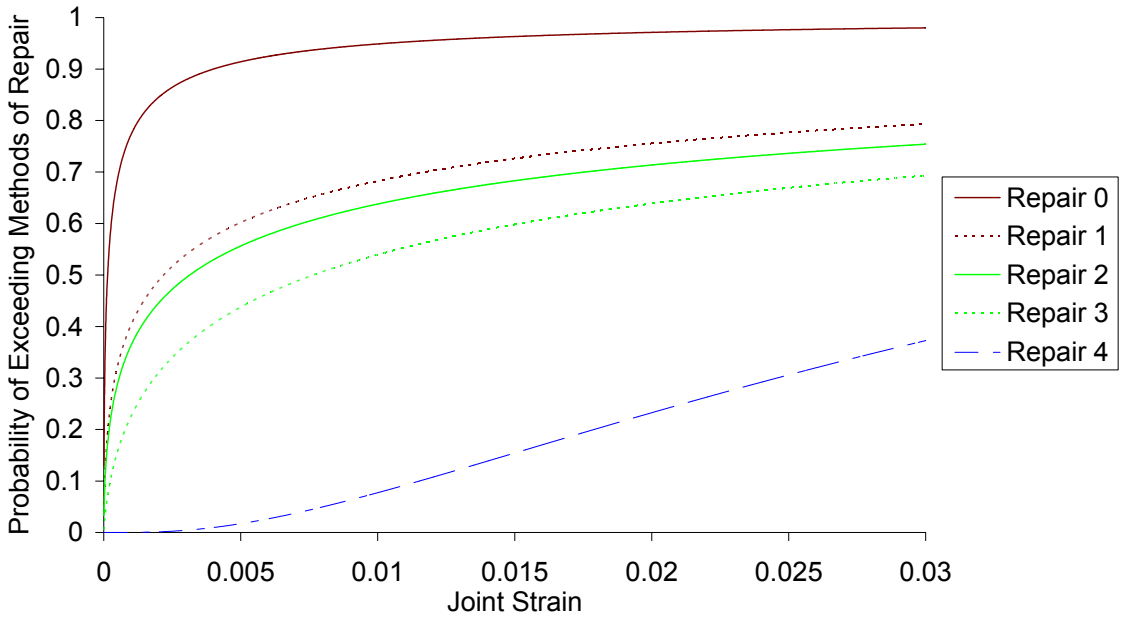

Figure 6.13: Prediction of the method of repair given the demand in terms joint strain.

6.5.4 Nonlinear function o f Joint Strain and Cycles

The nonlinear function used to combine the drift ratio and the number of cycles is used to combine the joint strain and number of cycles. Equation 4.5 is applied to the data set for joint strain and number of cycles. Only ten specimens provide demand in terms of joint strain. The coefficients a, b, c, and d are 20, 0.25, 7.12, and 0.36, respectively. Note the upper and lower limits for optimizing the equation were 0.25 and 20. Combining the joint strain and number of cycles dramatically improves the curves of the fragility curves shown in Figure 6.13. The better, more distinct curves are shown in Figure 6.14.

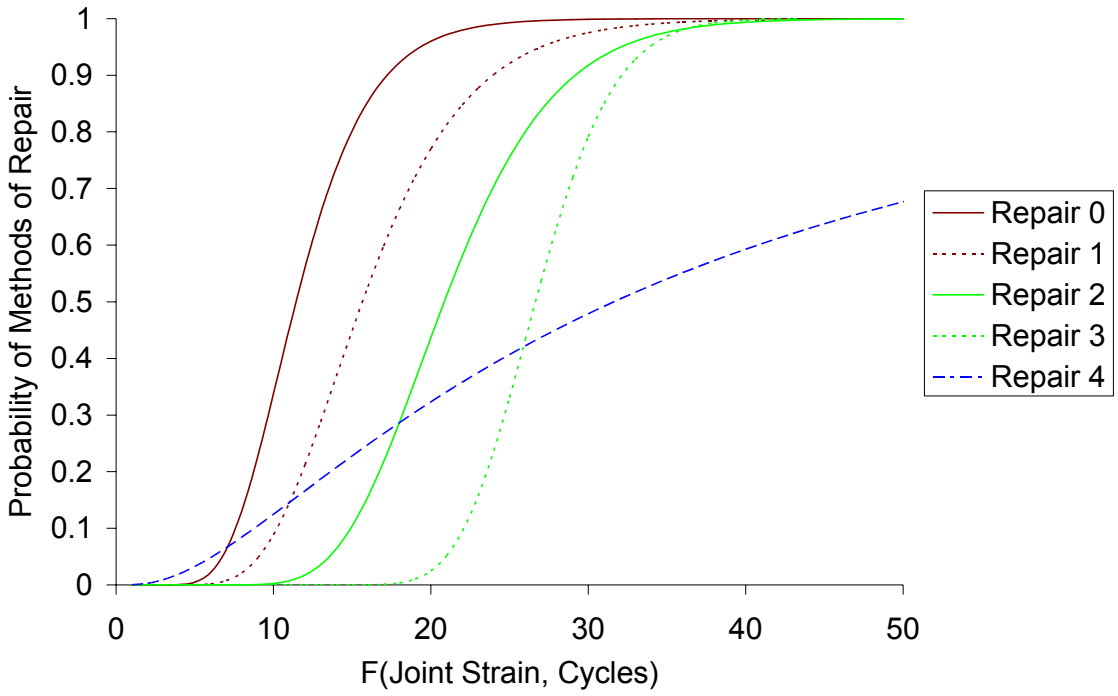

Figure 6.14: Predication of the method of repair given the demand in terms of nonlinear function of joint strain and number of cycles.

6.5.5 Comparison of the EDPs

The engineering demand parameter providing the best indicator of damage for beam-column joints is determined using the goodness of fit tests. The fragility curves generated for each demand parameter are compared. Using the K-S test, the greatest probability that the K-S parameter for the selected curve will be less than the critical

value will indicate the best engineering demand parameter. The results of this test of shown in Figure 6.15.

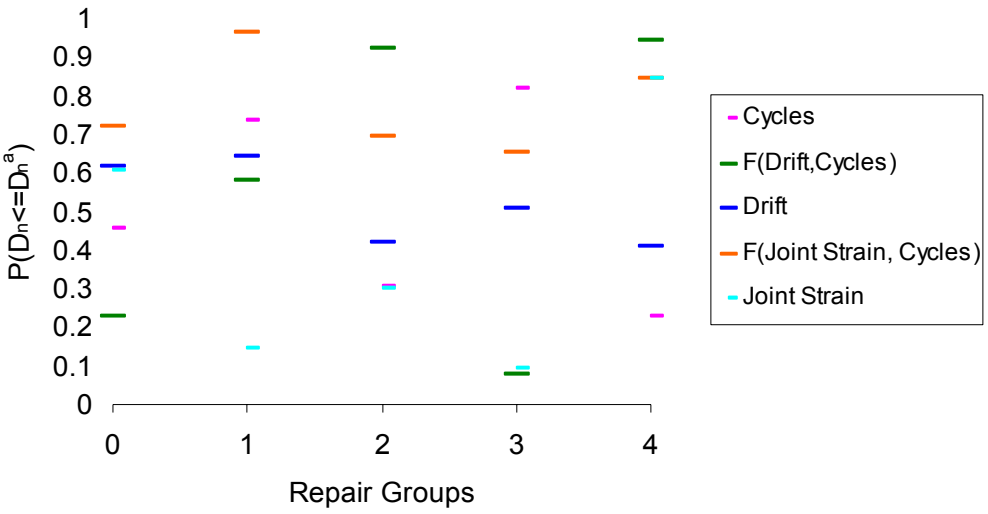

Figure 6.15: Results of the Kolmogorov-Smirnov test applied to the selected EDPs for data set two.

The greatest probability is shared between the nonlinear function of drift and cycles and the inter-story drift by itself. The data sets for Methods of Repair 0 and 3 indicate that including the number of cycles in the demand parameter significantly reduces the reliability.

6.6 Uncertainty

The prediction based on these fragility curves must consider two areas of uncertainty. The first is the error associated with the data points. The error due to lack of adequate damage occurrence description lends to assumptions. Where the damage may occur at any point during the test after the previously reported damage state and the demand at which the damage state in question is observed and recorded.

The second area of uncertainty is the inadequate number of data points. Only twenty-five specimens reviewed were found to have the non-ductile design and the damage descriptions required in this research. Thus no more than twenty-seven data points are available for each curve development.

Several statistical parameters are used to estimate the confidence associated with a data set. These parameters are derived using the sample size and the first and second moments. Indicators of how good the sample mean value is with respect the actual mean value are the confidence level and confidence interval. Choosing a typical confidence level of 95% and a confidence interval of ±1% of the sample mean yields a required sample size of magnitude 100.

The results of the confidence parameters are summarized in Table 6.3. Only the damage states having at least a fifth of the total sample size, 25, were included. The confidence level is evaluated assuming the deviation from the mean as 5% of the mean. The confidence interval is evaluated assuming α is 5%, thus the confidence level is 95%.

Table 6.3: Evaluating the confidence parameters of data set one.

Damage State	Sample size, n	Confidence Level (1- α) for $<\mu>_{1-\alpha} = 5\% * \bar{x}$	Confidence Interval (% of μ) for (1- α) = 95%
1	**21**	**36**	**21**
4	**16**	**36**	**21**
5	**5**	**16**	**50**
6	**8**	**22**	**34**
7	**24**	**60**	**12**
8	**8**	**44**	**17**
10	**12**	**38**	**19**
11	**6**	**43**	**17**
13	**5**	**31**	**24**

The results show a disappointing confidence level of no more than 60% and averaging 36%. Compare this to typical confidence level of 95%. Therefore, the analysis associated with this data set must be interpreted considering the lack of a decent sample size.

6.7 Conclusion

The probability model consists of fragility curves indicating the likelihood of requiring a method of repair for a given engineering demand parameter. The fragility curves are generated for multiple data sets, distribution functions, and engineering demand parameters and goodness-of-fit tests determine the most appropriate approach for developing the model for linking the demand parameter to a damage states and method of repair.

Three ways of grouping the damage data by method of repair produce three sets of data. Data Set Three appears to be the best when the K-S test is applied. However, the sample size of this set is too small. Data Set One is selected because the maximum sample size can be used without compromising the reliability of the probability model.

Four distribution functions are considered for generating the fragility curves. Plotting the fragility curves generated for each distribution using Data Set One and applying two goodness-of-fit tests determines the lognormal distribution function fit best to the damage data. The Chi-Square test confirms the Method of Maximum Likelihood evaluates parameters giving the most reliable lognormal distribution. These parameters are evaluated directly from the sample data and do not incur more error by relying on the mean and variance of the sample data.

Four engineering demand parameters are considered appropriate for beam-column joints. Using Data Set One, fragility curves indicating the likelihood of requiring a method of repair for a given demand in terms of these parameters are compared for the best fit to the data. The nonlinear function of a deformation demand and the number of cycles is favored because the function provides a more robust indication of the seismic demand. The hypothesis that combining two engineering demand parameters creates a better indicator of damage is confirmed visually by the fragility curves in Figure 6.12 and 6.14 and the by goodness-of-fit tests. Joint strain is a more desirable engineering demand parameter because the fragility curves would be applicable to building frames of different configurations and it is a popular output for numerical models. However, the sample size of the joint strain data is so small that the fragility curves based on this EDP do not indicate a unique method of repair.

Chapter Seven
Loss Estimation

7.1 Introduction

Loss estimation is the prediction of the economic impact on a building owner resulting from earthquake induced structural and non-structural damage. This information may be used by a building owner to choose appropriate performance objectives for retrofitting within the context of performance-based earthquake engineering. Here, a technique is developed for predicting the economic impact of repairing damaged reinforced-concrete beam-column joints to original pre-earthquake conditions. Economic impact is defined by both the cost of completing the repair and the loss of or reduction in operational capacity of the structure during repair (i.e. downtime). This chapter provides a structure for computing cost of repair work and estimating downtime, and provides preliminary cost estimates for the repair techniques described in Chapter IV.

7.2 Cost Framework

The economic impact resulting from earthquake damage is defined, in part, by the contract price of the repair work. The cost of repair work is evaluated using a framework similar to that defined by Shiohara (1999) and described in Section 2.6. The cost per component is a function of the damage state, the size of the damaged joint, and the unit cost of repair. Markups, such as mobilization, overhead, and profit, are applied on the total job cost for the entire building in this paper. See Section 7.3 for further discussion of markup. The contract price is the cost quoted by a general contractor after the markups have been added to the total job cost.

The unit job cost is the total unit cost for (a) labor, (b) equipment, and (c) materials. The prices quoted in this chapter of from the National Estimator 32 cost books, unless referenced otherwise. The breakdown for these items for each method of repair is defined in this Section. The base rate for the labor, material, and equipment are available for the most part as units per SF. The total job cost per component is the sum base rate of

the labor, material, and equipment times the appropriate joint dimension. The median size of the selected interior joint specimens is used in Section 7.4. Additionally, a minimum charge for most repair work is quoted in the cost book. The total job cost using the base rate is compared to the minimum charge and the higher estimate is used for the total job cost per joint.

7.2.1 Labor

For each of the methods of repair, the cost labor for the completed repair is defined. The crew of laborers skilled for the specific type of work required is identified and an accompanying starting estimate is provided using the 2003 National Renovation and Insurance Repair Estimator Costbook. Note this cost book specifies costs for repair work where much of the work is done by skilled laborers, even that which under new construction conditions would done by unskilled labor. The increased cost of the skilled labor is accounted for in the quotes presented here.

The quoted labor costs do not include markups such as the location factor, but do include taxes, insurance, vacation, and pension. For an approximate estimate of labor cost in California, at least 17% should be added. Additional markups are described in Section 7.3. The cost per crew is presented on an hourly basis.

Method of Repair 0: Cosmetic repair of damaged finishes requires a laborer experienced with the type of finish to be repaired. The types of finish are categorized as low end and high end. Low end finish will require a drywall crew. The minimum charge depends on the extent of the repair. Patching requires a drywall hanger working 1.42 hours resulting in a crew cost of $61.30. Replacing requires a drywall hanger, a hanger's helper, and a drywall taper working 6.4 hours resulting in a crew cost of $251. High end finish will require a finish carpenter at $42.70 per hour. A carpenter's helper is not specified but would cost an additional $31.60 an hour. The minimum charge for high end finish work is the one man crew working approximately 1 hour resulting in a crew cost of $46.10.

Preparing the work site will required additional laborers and hours for each method of repair. Since all damage beyond that extent requiring method of repair 0 will

also require repair 0, the cost associated with the site preparation will be included in method of repair 0. Prep work includes removing the damaged materials by a demolition laborer costing $28.40 an hour. The minimum charge for demolition is the one laborer crew working 3 hours resulting in a crew cost of $85.

The subsequent methods of repair are repairing and restoring the damaged concrete. Estimation of repair of concrete may be no lower than the minimum charge for concrete repair work listed in the cost book. For each of the three types of repair for damaged concrete, a minimum cost is available. The minimum specifies the crew size, hours of labor, and the cost of materials and equipment. Once the estimate exceeds each and all of these minimums, the cost may be based on the most appropriate crew, materials and equipment. For an existing building damaged in an earthquake, the minimum may be anticipated to be exceeded. The example presented in Chapter Eight will demonstrate the comparison between the minimum and the per dimension cost. For comparison, the required minimum for concrete repair will be provided within the quotes for each method of repairing concrete, 1 through 4.

Method of Repair 1: Repair of cracked concrete requires a concrete finisher at $42.90 an hour. A concrete finisher's helper is not specified but would cost an additional $35.40 an hour. The minimum for epoxy resin repair using pressurized injection is a crew of one concrete finisher working for a minimum of approximately 3 hours resulting in a crew cost of $126.

Method of Repair 2: Repair of spalled concrete also requires a concrete finisher. The minimum for patching the spalled concrete is a crew of one concrete finisher working for a minimum of 1 hour resulting in a crew cost of $42.90.

Method of Repair 3: Repair of crushed and fallen concrete requires a crew of a concrete form installer working at $43.10 per hour and a concrete laborer working at $30.90 per hour. The minimum charge for concrete repair work is a 4 man crew working 9 hours at an average of $38.10 per hour resulting in a crew cost of $343. Additional personnel are required to operate the demolition equipment, specifically the concrete core drill. The concrete saw operator costs $38.80 per hour.

Method of Repair 4: Repair of a failed joint with damaged reinforcing steel requires both concrete and rebar repair. A crew consisting of a concrete finisher and helper, a concrete form installer, and a concrete laborer can complete the job. The minimum charge for just the concrete repair serves as a starting quote to which 0.015 hours are added for each linear foot of new rebar and 0.25 hours for the placement of the rebar with a mechanical splice device.

Supervising personnel may be required during and after the repair is complete to check the quality of the repair. The cost of a two engineer crew is estimated at $400 per hour. (Cole 2003)

7.2.2 Equipment

For each of the methods of repair, the cost of the equipment required to complete the repair is defined in this section. The cost of the equipment is the cost of pieces of equipment not normally owned by the construction crew performing the repair. The crew should be equipped with tools such as "worm-drive saw, miter box, compressor, nail guns, and so forth" (National Estimator 32). The cost of these tools is included in the labor cost. The cost of equipment listed here is for unusual or large machinery such as cranes, dump trucks, concrete core drills, and jack hammers. The quotes are provided from the 2003 National Renovation and Repair Insurance Estimator Costbook.

Equipment cost is one instance in which the number of damaged components will affect the unit cost. The greater number requiring the same repair will reduce the per component cost since the same equipment can be used over and over again. It is more efficient to bring fewer pieces of equipment to the site that are used for a longer time. The repair recommendation of the structural engineer may be affected by these conditions. (Savage, 2003)

Method of Repair 0: Cosmetic repair of damaged finishes requires equipment appropriate for the type of finish. For low end finish, the drywall equipment required is taping tools, texture applicator, and drywall lifter if crew consists of only one laborer. Minimum charge per day for this equipment is $40 or $0.22 per SF. Equipment required to complete high end finish is most likely owned by the contractor.

Since preparation of the site is included in this repair, removal of the damaged materials requires hauling. A chute for moving the materials out of the building is $12.70 per linear foot, if plywood is acceptable. The chute may cost as much as $26.10 LF if steel is required. A dumpster may cost as little as $100 per week for 3CY and as much as $340 per week for 30CY. Note that 25 – 30SF of floor space becomes 1CY of debris. (2003 California Heavy Construction Costbook) Finally, a dump truck and driver cost $450 per day. The truck is able to haul as much as 22CY and 8 tons of debris per day.

Method of Repair 1: Pressurized epoxy injection repair of cracked concrete requires the rental of a pressurized pot. The cost is $181 per day. The cost is broken down to $1.51 per LF for a one man crew working at the pace of 1LF every 6.6 minutes. No additional equipment is listed in the cost book.

Method of Repair 2: Patching repair of spalled concrete requires no additional equipment to be rented.

Method of Repair 3: Repairing crushed and fallen concrete requires many pieces of equipment as described in Section 5.6. Removal of the existing concrete will require a jackhammer costing $195 per day, a concrete core drill costing $93 per day, and additional hauling by the dump truck.

Replacement of the concrete requires a pump truck costing $130 per hour and plywood formwork costing $0.76 per day per SF. The truck must be rented for the number of days it takes to pour all the concrete. In an 8 hour workday, 146LF of concrete can be poured (based on the construction of a grade beam). The cost of all this equipment may be included in the material cost. An estimate for concrete used in new construction $350 to $500 per CY because the formwork and pumping of the concrete are included. (Cole 2003)

Method of Repair 4: Repairing a failed joint with damaged rebar requires the equipment for repair method 3. The equipment for removing, cutting, and setting the reinforcing steel should owned by the repair crew.

Shoring: Temporary support of the gravity load demand on the damaged joint is required for methods of repair 3 and 4. Removal of columns in the retrofitting of the

Asian Art Museum also required shoring. The unit job cost of shoring was estimated as $1M for each column. (R&C, Consulting Engineers 1992)

7.2.3 Repair Materials

The cost of the repair materials for each of the methods of repair are defined in this section. The quotes are provided from the 2003 National Renovation and Repair Insurance Estimator Costbook. The market value of the materials may increase from the time of the quote to the time of actual construction. The estimates provided to Rutherford & Chekene included a 20% markup to account for the increase. This may be only applicable to large scale jobs. (R&C, Consulting Engineers 1992)

Method of Repair 0: Cosmetic repair of damaged finishes requires matching the original materials of the same quality. The materials may range from the inexpensive drywall and texture finish to the very expensive architectural finishes. The range of materials is categorized as low and high end finishes.

Low end finish is defined as installation and finishing of drywall. Drywall cost depends on thickness and ranges from $0.31 for 1/2in to $0.38 for 5/8in. Drywall nails are $50 per box containing enough to cover 32,000SF and drywall taping materials costs $0.04 per SF. Drywall texture costs $15.20 per 50lb box. Depending on the type of texturing, each box covers as much as 190SF or as little as 77SF.

For high end finishes, the material cost is more difficult to determine. The minimum charge for finish carpentry materials is $20 per hour of work. A total job cost for the high end finish is defined in Section 7.4.

Method of Repair 1: Epoxy repair of cracked concrete requires epoxy resin costing $0.72 per linear foot.

Method of Repair 2: Patching of spalled concrete requires a cementitious mortar or paste costing $0.83 per SF.

Method of Repair 3: Replacing crushing and fallen concrete requires new concrete costing $89.10 to $98 per CY for extents of strength ranging from 2500psi and 5000psi, respectively. Calculating the amount of required concrete must account for 6% waste.

Method of Repair 4: Removing and replacing the damaged rebar in a failed joint requires new concrete and reinforcing steel. The rebar costs $0.55, $0.74, and $0.97 per LF for #6, #7, and #8 bars. Calculating the amount of required steel must account for 4% waste.

A mechanical device will permanently bond the new steel to the existing rebar. The standard Zap Screwlock® is a coupler that meets the requirements set by ACI 318-02, Section 21.2.6 for a mechanical splice. The cost of each Screwlock® coupler is $24, $32, and $45 for the sizes appropriate for linking #7, #8, and #10 bars. These prices are quoted for bulk orders of less than 100 and do not include the contractor markup. Installation instructions are provided to the repair crew obviating the need for a special inspection.

7.3 Markups

Markups are intended to cover the other costs involved with completing the repair job. These other costs include overhead, profit, contingency, mobilization, labor conditions, and delays due to the earthquake. The impact each of these items on the job cost is defined in terms of percentage in this section. The order in which the factors are applied in very important when calculating the contract price for the repair job. Labor conditions increase or decrease the amount of time required to complete the job and the factor representing these conditions is applied to the time estimate prior to totaling the job cost. Profit and overhead are applied to the total job cost after mobilization has been added. Contingency is applied after the other factors have impacted the total job cost. The resulting price is the contract price as quoted by a general contractor bidding for the repair job.

7.3.1 Labor Conditions

The conditions under which the repair must be preformed will impact the time required to complete the repairs. As mentioned before, the quotes provided by the 2003 National Renovation and Insurance Repair Estimator Costbook account for the increase in cost due to work in an existing building versus constructing a new building. In addition

to adjusted cost per hour for labor, there are other conditions specific to the repair of beam-column joints that affect the labor time. These conditions are accessing the joint, moving materials to and from the joint, repeating the same repair on many joints, and small repair jobs. The factors defined for each condition is provided by the National Estimator 32 unless otherwise noted.

Accessing the joint is inherently difficult. The joint is the connection between the column and the beam at the level of the floor slab. The joint must be accessed from below or above the floor slab requiring ladders and/or time spent in a congested area. These conditions qualify for the recommended 15% to 25% increase. For magnitude of difficulty in accessing joints in earthquake damaged building, an increase of 25% is appropriate.

Lifting materials above ground level increases the cost by 1% for every 10 feet. For simplicity, each story on which the repair must be performed will incur a 1% increase.

Repeating a method of repair on many joints for many days will decrease the time associated with each repair by 10% to 20%. For application to joints, at least 20% of the joints within the building must require to same repair to incur a reduction of 10%. (Savage, 2003) Method of Repair 0 is anticipated to be required on all damaged joints and will inevitably incur a reduction as much as 20%.

Small repair jobs incur an increase of 30% to 50% when the following conditions exist. Matching the existing materials is more costly on a per SF basis where a larger percentage of the bulk material will be unused. Note the material costs defined in Section 7.3 accounts for a 4-6% waste of the material. The percentage of waste would greatly increase for smaller jobs where the materials can not be ordered in small quantities. Additionally, repair of the few damaged joints will not require closing down the entire building. Therefore, care must be taken to protect the surrounding areas and not disrupt the building occupants. The tolerance level of the occupants will affect the factor of increase. Some tolerance for odors and noise will allow the contractor to pursue alternatives developed to create a more harmonious environment for the occupants and the construction crew. For example, a low odor epoxy resin is available and work may be

done during normal business hours. However, a lower level of tolerance will require the work to be performed during hours the building is unoccupied. Labor cost will increase by time and a half. (Savage, 2003) Note the increase in the labor cost may be offset by eliminating the loss associated with closing the building during the day. The loss due to downtime is further defined in Section 7.5.

7.3.2 Mobilization

Mobilization, moving all the equipment, materials, and personnel, results in an increase of the total job cost. At least 10% of the job cost or $50,000 per building is added to the total, depending on which is more. (Cole, 2003)

7.3.3 Delays due to the Earthquake

Delays due to the earthquake are due to acute demand for skilled labor, equipment, and materials. Start-up and mobilization costs will increase. Obstructions after an earthquake include water from sprinkler systems and damaged lifelines. For example, damage to the Starbuck's building in Seattle after the Nisqually Earthquake prevented occupation of the building and delayed assessment of the structural components. This added at least a few weeks to the total downtime. (Savage, 2003)

The delay affects all aspects of the job cost after mobilization and start-up factors are applied. An increase of 25% to 50% is added after these totals are calculated.

7.3.4 Overhead and Profit

Overhead covers the cost of management personnel, administration, and general business expenses. Profit is set by the contractor and may be dependent on the volume of contracts he already has. The average percentage of the total job cost is 10% for overhead and 8% for profit.

7.3.5 Uncertainty

The proposed repair cost and downtime model was developed using data from the National Estimator 32 cost books and from interviews with practicing engineers and contractors (Cole, Coffman and Kapur, Runacres, and Savage) . All of the professionals

who were interviewed commented on the high degree of uncertainty associated with the loss estimation of damaged structural components. The uncertainty introduced into the economic impact model comes from two sources; unforeseeable costs incurred during repair work and the deterministic approached used to evaluate quotes for all non-ductile joints. The first source of uncertainty is accounted for in the general contractor's markup as contingency. The second must be accounted for in the application of the cost estimates for each method of repair.

Contingency is the uncertainty due to the changes in market values of materials, labor, and equipment as well as fluctuations in downtime and total repair time. Contingency is 10% of the total cost after overhead and profit in the estimates provided by Rutherford and Chekene, Consulting Engineers when estimating the cost of retrofitting the existing Asian Art museum in San Francisco. Jared Cole of T.Y. Lin also estimates contingency as 10% for new construction. The National Estimator 32 provided an estimate as low as 2% and notes the large variation among the repair jobs reviewed in over 740 communities throughout the United States and Canada.

An amount of uncertainty is associated with the deterministic approach to evaluating the loss for beam-column joints designed for non-ductile response. A deterministic approach requires the quantities and prices to be known and complete. It is possible that some items incurring additional cost were overlooked despite extensive effort to confirm the methods of repair, the associated extents of damage, and the cost of the repair work.

7.4 Unit Cost per Method of Repair

The unit cost, dimensions of joint to be repaired, and an estimate for the job cost of each method of repair is presented in this section. The estimate is evaluated using the framework and base rates defined in Section 7.2 and are factored by the mark-ups defined in Section 7.3. More than one estimate may be available and the highest one will be used. Application of these total loss estimates are used in the example in Chapter Eight.

The unit job cost is evaluated by summing the unit cost of the labor, equipment, and materials. The unit cost of the labor is increased by the markup for accessing the

damaged joints as defined 7.3.1. The unit cost of materials is increased by the percentage of waste, usually 6% unless otherwise specified in 7.3.2. This unit price is then multiplied by the damaged dimension of the joint.

7.4.1 Method of Repair 0

The unit job cost of replacing the finish is $2.72 per SF for low end finish and $19.56 per SF for high end finish (R&C, Consulting 1992). Two different estimates are provided for the different materials and skilled labor associated with the different types of finishes. The breakdown for the low end finish is both the removal and replacement of the existing drywall and adjacent ceiling tiles. The median surface area of the selected interior joint specimens is 3.75SF. Limiting repair of the finish to just the surface area of the joint is highly unlikely in an existing damaged building. For a more practical estimate, 3 times the surface area is more likely. Using this larger dimension, the cost estimate for low end finish is as follows:

Low End Finish:	High End Finish:
Labor, Material, Equipment $30.60	Labor, Material, Equipment $220.05
Total Job Cost per Joint $30.60	Total Job Cost per Joint $220.05
Overhead and Profit (18%) $5.52	Overhead and Profit (18%) $39.60
Contingency (10%) $3.60	Contingency (10%) $25.98
Contract Price per Joint $39.72	Contract Price per Joint $285.63

The minimum charge for patching of drywall results in a total job cost of $103.13. The surface area per joint is not enough to exceed this minimum. However, the finish can be completed on many joints and the minimum charge is not an appropriate estimate per joint.

Additional charges for the removal of damaged finish materials from site are dependent on the location of the damage joint and the number of joints. A chute is required to move the material out of the building and adds a unit costs $71.34 per LF,

including installation. A 10CY dumpster adds a cost of $230 per week and a dump truck and driver add a unit cost of $20.50 per CY.

7.4.2 Method of Repair 1

The unit job cost of pressurized epoxy injection repair of cracked concrete $8.18 per LF. This unit price is confirmed by Jugesh Kapur of the Washington DOT who estimates $10 per LF. The cracks are induced by shear forces and cross the joint surface area diagonally. The dimension of damage should be at least twice the length of the diagonal to allow for cracks in both directions. The median diagonal length of the selected interior joint specimens is 3.33LF and twice that is 6.66LF. Using this dimension, the cost estimate is as follows:

Labor $39.63

Materials $5.09

Equipment $10.06

Total Job Cost per Joint $ 54.77

Overhead and Profit (18%) $9.86

Contingency (10%) $6.46

Contract Price per Joint $71.09

However, the minimum charge for epoxy injection results in a total job cost of $322.52. The dimension per joint is not large enough to exceed this minimum. The contract price is recalculated using this minimum.

Labor, Materials, and Equipment $322.52

Total Job Cost per Joint $322.52

Overhead and Profit (18%) $58.05

Contingency (10%) $38.06

Contract Price per Joint $418.63

7.4.3 Method of Repair 2

The unit job cost of patching spalled concrete is $1.32 per SF. The extent of damage is defined by damage state 8 where 30% of the joint surface area has spalled off.

The median joint surface area of the selected interior joint specimens is 3.75SF. Using the dimension of 30% of 3.75SF or 1.125SF, the cost estimate is as follows:

Labor $0.55

Materials $1.00

Equipment $0.00

Total Job Cost per Joint $1.55

The minimum charge for patching results in a job cost of $96.45. The dimension per joint is not enough to exceed the minimum charge. The contract price is recalculated using this minimum unit cost.

Labor, Materials, and Equipment $96.45

Total Job Cost per Joint $96.45

Overhead and Profit (18%) $17.36

Contingency (10%) $11.38

Contract Price per Joint $125.19

7.4.4 Method of Repair 3

The unit job cost of removing the crushed is $119.58 per CY and replacing new concrete is $316.26 per CY . The units for the labor, materials, and equipment that make up the job cost are in terms of one, two, and three dimensional units. The job cost was calculated using the median dimensions the selected interior joint specimens for a total per joint cost. The per joint cost was divided by the volume of the joint for the unit job cost. The estimate provided by Cole is higher than that calculated using the cost book, so $500 per CY will be used for the new concrete unit cost. The entire unit job cost is $619.58 per CY.

The extent of damage is defined by damage states 10 and 11 where more than 80% of the joint surface area is crushed and crushing extends into the joint. Since additional concrete is removed during this repair, the maximum volume of concrete is the volume of the joint. The median joint volume of the selected interior joint specimens is 0.42CY. Using this dimension, the cost estimate is as follows:

Labor $153.80

Materials $73.5

Equipment $32.92

Total Job Cost per Joint $260.22

Overhead and Profit (18%) $46.84

Contingency (10%) $30.71

Contract Price per Joint $337.77

If shoring is required, an additional $1M should be added per joint. Note a significant reduction is available when the equipment is reused for multiple joints.

7.4.5 Method of Repair 4

The unit job cost of repairing a failed joint is $1381.86 per CY. The job cost is the sum of the concrete repair and the rebar repair. The cost of repairing the concrete is the price defined for method of repair 3.

The extent of damage is defined by failure of the joint the concrete is crushed and the rebar is damaged. The median joint volume of the selected interior joint specimens is 0.42CY and the median number of column longitudinal #8 rebar is 8. Using these dimensions and numbers, the cost estimate is as follows:

Labor $352.80

Materials $636.78

Equipment $32.92

Total Job Cost per Joint $1022.50

Overhead and Profit (18%) $184.05

Contingency (10%) $120.66

Contract Price per Joint $1327.21

If shoring is required, an additional $1M should be added per joint. Note a significant reduction is available when the equipment is reused for multiple joints.

The total job cost of repairing failed joints in an existing building should be compared to the cost of demolishing the entire building. The unit demolition cost for an entire reinforced concrete building is $5.74 per SF. (2003 California Heavy Construction Costbook)

7.5 Downtime per Method of Repair

Downtime is the sum of the time required for mobilization, demolition, repair work, and replacing finishes. The cost of the labor is presented in Section 7.4 and the corresponding labor time is presented in this section. Using the markup for post-earthquake conditions, the time for completion of each method of repair is approximated. The time presented is the hours for which the area of the damaged joints can not be used. If the building is occupied during repair, the markup factor defined for *small jobs* in Section 7.3.1 should be applied to the time estimate.

Mobilization after an earthquake requires up to 50% more time than under normal conditions. The time estimate for mobilization is 10% of the time required to complete the method of repair.

Demolition requires a minimum of 3.75 hours per repair job, based on the minimum charge provided by the 2003 National Renovation and Insurance Repair Estimator cost book.

Repair work is dependent on the method of repair required. Based on the cost estimates defined Section 7.4, the corresponding time is presented in Table 7.1.

Replacing finish is dependent on the type of finish and includes removal of the debris. The estimate for low end finish and removal of debris is presented in the table.

Table 7.1: Approximate downtime per joint using the time allotted to each method of repair according to the 2003 National Renovation and Insurance Repair Estimator cost book.

#	Repair Labor	Estimated Time	Estimated Time for Minimum Charge
0	Remove and replace damaged finish.	1 hour per joint	1hour
Debris Removal	Install chute for debris	2hr/LF	N/A
1	Pressurized epoxy injection	1hr per joint	3.68 hours
2	Patching spalled concrete	1min per joint + setting time	1.25 hours
3	Removal and replacement of damaged concrete	1.5 per joint + setting time	9 hours
4	Removal and replacement of damaged concrete and rebar	7hr per joint + setting time	N/A

Chapter Eight
Example

8.1 Introduction

This chapter presents a demonstration of the technique of predicting economic impact. The previous chapters describe the development of the technique. The economic impact is defined in terms of the contract price and the amount of downtime required for completion of the repair work.

8.2 Example Building

The economic impact predictive tools developed in this report are used to assess the earthquake risk of an older reinforced concrete located in Van Nuys, California. The building was designed in accordance with the Los Angeles City Building Code of 1964. The design detailing of the building is inadequate for current seismic design codes. In particular:

- Beam-column joints have no transverse reinforcement and anchorage length for embedded beam longitudinal reinforcement is too small.
- Column longitudinal reinforcement is spliced above the joint with splice lengths too short.
- Columns have insufficient transverse reinforcement to carry the shear load at the top and bottom.

The inadequate design details contribute to damage accumulation during earthquake loading. The Van Nuys building has sustained damage from two large earthquakes. The 1971 San Fernando earthquake, magnitude 6.6, caused moderate damage and was repaired using epoxy resin injection. The 1992 Northridge earthquake, magnitude 6.7 caused shear failure of the joints and required new shear walls.

The model of the Van Nuys building is based on the design details prior to the Northridge earthquake. Beam-column joint modeling was done by Adam Theiss. The model included properties adjusted for the damage accumulated during the San Fernando earthquake. The inelastic beam-column joints represent explicitly using inelastic

rotational spring elements to connect the beam and column elements. Additional details of the model and calibration of joint elements is in Appendix F.

8.2.1 Building Dimensions

The building is seven stories high and is 66,000 SF. A column-beam frame defines the perimeter of the building. This frame consists of three bays in the North-South direction and eight bays in the East-West direction. The perimeter frames are designed to carry lateral loads. The interior frames of the building are column-slab systems designed to carry gravity loads. The predictive tools developed here are not appropriate for this type of frame. Thus, the interior frames are not included in the assessment. The perimeter frames in the East-West direction are assessed for earthquake risk in this chapter. Each floor of each frame contains nine joints. The portion of the building assessed in this chapter contains 126 joints.

8.2.2 Joint Dimensions

The dimensions of each joint are used to evaluate the cost per joint. The unit costs for each method of repair are in terms of linear or square feet or cubic yards. The column and beam depths and widths are used to calculate the length of the diagonal, the surface area, or the joint volume when required. The dimensions of the joints differ between the first story and the stories above because the beam depth is larger at the base of the building. The beam depth of the first story is 30 in. The beam depth of the stories above is 22.5 in. The column dimensions are 14 in. deep and 20 in. wide. The beam width is constant at 16 in.

8.3 Demand Parameter

The results of a push-over analysis provide the demand for the prediction of earthquake demand on beam-column joints. The joint demand for two levels of earthquake damage, one moderate and one severe, is considered. The demand is in terms of joint strain. This engineering demand parameter, described in Section 4.3.4, is most appropriate because the damage states and methods of repair are specific to the behavior of the joint. The joint strain, unlike inter-story drift ratio, does not include the flexural response of the beams and columns. The probability model generated in Section 6.5.3,

shown in Figure 8.1, is used to determine the probability of requiring a method of repair for the given joint strain demand.

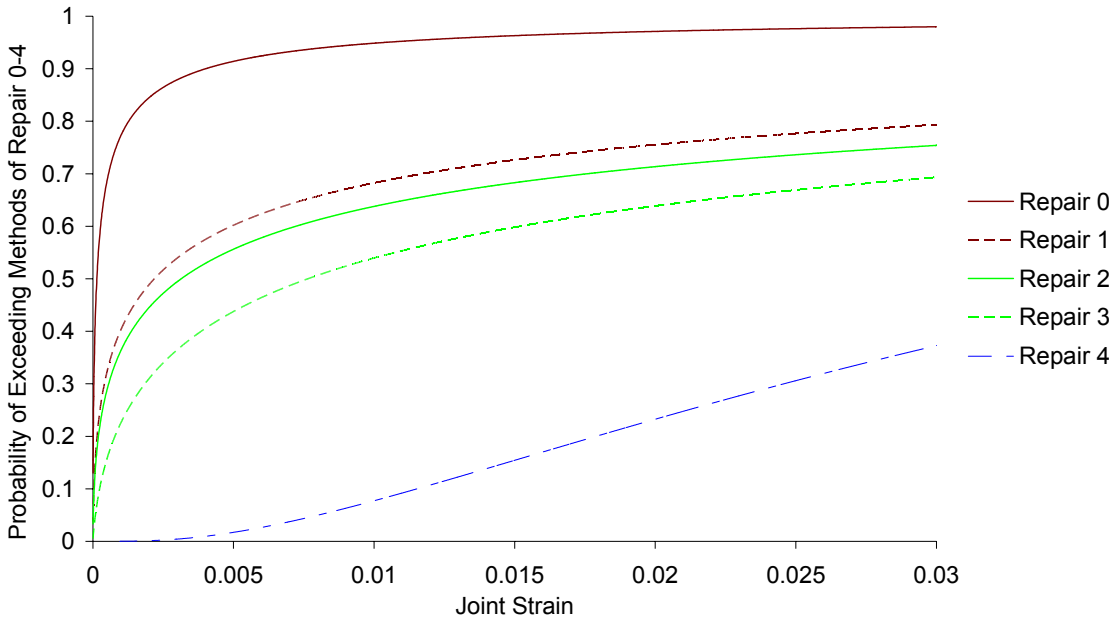

Figure 8.1: The probability model for a given demand in terms of joint strain.

8.4 Earthquake Loss Assessment

The economic impact is the cost and time associated with the method of repair required to restore the damaged joint to the original capacity. This earthquake loss is estimated per method of repair in Chapter 7. The methods of repair are defined for a specific group of damage states in Chapter 5. The damage states are described in Chapter 3. The experimental data described in Chapter 4 is the damage state versus demand data used to generate the probability models in Chapter 6. Thus, the economic impact is the loss estimate linked to the method of repair linked to the demand via the probability models.

8.4.1 Predicting Damage for Given Demand

The probability of exceeding the damage requiring a method of repair for a given joint strain demand is identified on the fragility curves shown in Figure 8.1. Each fragility curve represents the probability for one of the five methods of repair. The probability that a joint will exhibit no damage for a given demand is the difference of the probability of at least Method of Repair 0 will be required from 100%. A joint at this given demand will

have the same probability that the loss estimate will be zero. For the range of joint demand considered here, all joints will have some chance of exhibiting no damage, however small.

The probability of exceeding a method of repair carries over into the loss estimate. For example, for a given joint strain demand of 0.0023, the probabilities of exceeding methods of repair 0,1,2,3, and 4 respectively are 86%, 51%, 46%, 33%, and less than 1%. The loss estimate for this joint has an 86% chance of being the cost associated with Method of Repair 0. The entire cost of repair for this joint should not be assessed using the unit cost for Method of Repair 0. This will overestimate the cost for Method of Repair 0 and grossly underestimate the cost for methods of repair 1, 2 and 3 as zero. Instead, the percentage of each method of repair is multiplied by the job cost for the method of repair. Equation 8.1 describes the assessment in equation form.

$$\text{cost / joint} = \sum_{i=0}^{4} \%_i \times \$_i \tag{8.1}$$

where i is the method of repair, % is the probability of exceeding the damage requiring the method of repair, and $ is the cost per joint of the method of repair.

8.4.2 Markups

The cost per joint is adjusted for specific conditions with the markups discussed in Section 7.3. For this building, the conditions for markup include the building location, accessing the joint, moving materials to stories above the ground floor, repeating the same repair numerous times, mobilization, and post-earthquake delays. An increase of 25% for difficult access is included in the unit cost defined for each method of repair in Section 7.4. The markup factors listed here are from the National Estimator 32, unless otherwise specified.

Two markups must be applied to the unit cost per joint. The additional cost of moving material above the ground floor is 1% per story. A reduction is applied for repair work done repeatedly in the same building. If the same method of repair is required by more than 20% of the joints, a reduction of 20% is applied. Since the process for determining the cost per joint does not assign a single method of repair to each joint, determining if the cost qualifies for the reduction is difficult. To simplify the process, a median method of repair is selected for each joint. The median method must have at least

as much of a chance of being required as not. More clearly, the probability of exceeding the damage requiring the method of repair must be greater than 50% so that the probability of the joint not exhibiting this damage is less than 50%. The highest method of repair meeting this criterion is considered the median method.

The job cost is the sum of the cost per joint for all the joints included in the assessment and is adjusted for three conditions. Each condition is a factor of the cost adjusted for the previous condition. First, the building is located in the San Fernando Valley, just north of the city of Los Angeles. The area modification factor for Los Angeles is 26%. Second, mobilization is 10% of the job cost or $50,000. And third, the post-earthquake conditions may increase the cost by as much as 50%. The building is located in a congested area where labor and equipment will be in severe demand after an earthquake so the maximum increase is appropriate. Equation 8.2 describes the job cost adjustment for order in which the markups are applied.

$$Job\ Cost = M_3\left\{M_2\left[M_1\sum_{j=1}^{n}\left(\cos t/_{jo\,\mathrm{int}} \times M_{access} \times M_{repeat\ repair}\right)\right]\right\} \tag{8.2}$$

Finally, the overhead, profit, and contingency are evaluated and added to the job cost for the quoted contract price. Equation 8.3 describes the cost adjustments in equation form.

$$Contract\ \mathrm{Pr}ice = M_{contingency}\left(M_{overhead+profit} \times Job\ Cost\right) \tag{8.3}$$

8.5 Moderate Earthquake Demand

The maximum joint strain demand due to the moderate earthquake demand are as small as 0.0001 at the top story and range to 0.0009 on the second story.

The assessment of job cost is described for the joint sustaining the largest joint strain demand. The joint is labeled E-W24. The joint is located on the third story so the cost per method of repair is increased by 2% as discussed in Section 8.4.2. The probability model indicates a 76.2% chance the joint will exhibit the damage requiring Method of Repair 0. The probability of the joint having no damage is 23.8%. The cost of Method of Repair 0 is calculated using the price per SF of the low end finish defined in Section 7.4.1. The cost of completing Method of Repair 0 for this joint at this probability

is $13.86. This cost will be reduced by 80% if the method is repeated several times in the frame.

The joint strain demand of all the joints in one E-W perimeter frame must be investigated to determine if the cost for this method of repair qualifies for the 20% reduction discussed in Section 8.4.2. The median method of repair is determined for each joint using the criteria defined in the previous section. For joint E-W24, the probability of damage requiring methods of repair 1, 2, 3, and 4, respectively are 39.2%, 35.3%, 21.6%, and less than 1%. Thus, the median method of repair for joint E-W24 is Method of Repair 0 and is one of the numbers of joints whose median method of repair is the number before the parenthesis shown below:

0) 55 joints
1) none
2) none
3) none
4) none

The Method of Repair 0 qualifies for the reduction since more than 20% of the joints per frame, or 12 joints, require this method. The cost for joint E-W24 can now be evaluated for the probability of each method of repair and the appropriate reductions.

For the entire E-W perimeter frame, the cost of labor, materials, and equipment is described per method of repair. The cost for Method of Repair 0 is $661. The cost for Method of Repair 1 is $959. The cost for Method of Repair 2 is $57. The cost for Method of Repair 3 is $9.987M including the cost of shoring. The cost of Method of Repair 4 is $1,242 including the cost of shoring.

8.5.1 Contract Price

The estimate for each of the E-W perimeter frames is $9.99M. This estimate includes labor, materials, and equipment. The adjustment of the job cost is applied as described by Equations 8.2 and 8.3. The cost of both perimeter frames is considered the economic impact of damage sustained by the structural components of the building. Additional cost due to damage to nonstructural elements, the building contents, and the damage sustained by the interior column-slab frames are not included.

Labor, Materials, and Equipment $19.98M

Location (26%) $5.19M

Mobilization (10%) $2.52M

Post-Earthquake Conditions (50%) $13.8M

Total Job Cost $41.54M

Overhead and Profit (18%) $7.48M

Contingency (10%) $4.90M

Contract Price $53.92M

8.5.2 Downtime

The downtime before this building is fully operational is estimated using Table 7.1. The time per joint is calculated using Equation 8.1. The time for Method of Repair 0 is 42.4 hours. The time for Method of Repair 1 is 20.2 hours. The time for Method of Repair 2 is less than one hour. The time for Method of Repair 3 is 15 hours. The time for Method of Repair 4 is less than one hour. The total time for the job is increased by the three markups discussed in Section 8.4.2.

The total downtime for the completion of all the methods of repair is 162 hours. Assuming 8 hour workdays and 5 day weeks, at least 21 days or 4 weeks should be allotted for the repair of the E-W perimeter frames of the building.

8.6 Severe Earthquake Demand

The maximum joint strain demand due to the severe earthquake demand are as small as 0.0001 at the top story and range to 0.0277 on the third story. The highest strains are in the same locations as for moderate earthquake demand, but the values throughout the frame are larger and indicate a higher extent of damage.

The assessment of job cost is described for the joint sustaining the largest joint strain demand. The joint is labeled E-W32. The joint is located on the third story so the cost per method of repair is increased by 3% as discussed in Section 8.4.2. The probability model indicates a 97.8% chance the joint will exhibit the damage requiring Method of Repair 0. The probability of the joint having no damage is a very low 2.2%. The cost of Method of Repair 0 is calculated using the price per SF of the low end finish defined in Section 7.4.1. The cost of completing Method of Repair 0 for this joint at this probability is $17.99. This cost will be reduced by 80% if the method is repeated several times in the frame.

The joint strain demand of all the joints in one E-W perimeter frame must be investigated to determine if the cost for this method of repair qualifies for the 20% reduction discussed in Section 8.4.2. The median method of repair is determined for each joint using the criteria defined in the previous section. For joint E-W32, the probability of damage requiring methods of repair 1, 2, 3, and 4, respectively are 78.6%, 74.6%, 68.3%, and 34.3%. Thus, the median method of repair for joint E-W32 is Method of Repair 3 and is one of the numbers of joints whose median method of repair is the number before the parenthesis shown below:

0) 55 joints
1) 5 joints
2) 11 joints
3) 35 joints
4) none

The methods of repair 0 and 3 qualify for the reduction since more than 20% of joint per frame, or 12 joints, require this method. The cost for joint E-W32 can now be evaluated for the probability of each method of repair and the appropriate reductions.

For the entire E-W perimeter frame, the cost of labor, materials, and equipment is described per method of repair. The cost for Method of Repair 0 is $850. The cost for Method of Repair 1 is $1800. The cost for Method of Repair 2 is $112. The cost for Method of Repair 3 is $23.4M including the cost of shoring. The cost of Method of Repair 4 is $7.2M including the cost of shoring.

8.6.1 Contract Price

The estimate for each of the E-W perimeter frames is $30.61M. This estimate includes labor, materials, and equipment. The adjustment of the job cost is applied as described by Equations 8.2 and 8.3. The cost of both perimeter frames is considered the economic impact of damage sustained by the structural components of the building. Additional cost due to damage to nonstructural elements, the building contents, and the damage sustained by the interior column-slab frames are not included.

Labor, Materials, and Equipment $61.22M

Location (26%) $15.92M

Mobilization (10%) $7.71M

Post-Earthquake Conditions (50%) $42.43M

Total Job Cost $127.28M

Overhead and Profit (18%) $22.91M

Contingency (10%) $15.02M

Contract Price $165.2M

8.6.2 Downtime

The downtime before this building is fully operational is estimated using Table 7.1. The time per joint is calculated using the Equation 8.1. The time for Method of Repair 0 is 54.6 hours. The time for Method of Repair 1 is 37.8 hours. The time for Method of Repair 2 is less than one workday. The time for Method of Repair 3 is 43.9 hours. The time for Method of Repair 4 is 50.3 hours. The total time for the job is increased by the three markups discussed in Section 8.4.2.

The total downtime for the completion of all the methods of repair is 778.6 hours. Assuming 8 hour workdays and 5 day weeks, at least 98 days or 19½ weeks should be allotted for the repair of the E-W perimeter frames of building.

8.7 Uncertainty

The probability model contributes to the uncertainty associated with the earthquake loss defined for the example building. The fragility curves were generated using the damage data for the joint strain demand. As discussed in Section 4.3.4, the data from only two experimental studies is available for this demand. The sample size for each method of repair can be no larger than ten. Despite the small data set, the joint strain demand ranges widely for the damage states grouped into the same method of repair. The result is fragility curves that do not indicate one method of repair for a given demand. In an effort to account for uncertainty, the loss is estimated using the probability as defined in Equation 8.1.

8.8 Conclusion

The same number of joints did not exhibit any damage for both levels of earthquake demand. These joints are location in the same places in the top story. The concentration of high joint demand is in the lower four stories and therefore, the joints

requiring the highest methods of repair are found here. All joints that exhibit some damage require Method of Repair 0.

The moderate earthquake demand caused a high probability of requiring Method of Repair 0. Despite the large number of joint requiring this method, the cost of the Method of Repair 0 relative to the job cost for the entire frame is less than 1%. The bulk of the job cost is the cost of Method of Repair 3. The discrepancy is due to the difference in the unit cost. Even though joint E-W24 had only a 21.6% chance of requiring Method of Repair 3, the cost at this probability was $215,000. Note the cost of shoring must be added every time this repair is needed, thus the cost increases by $1M before adjusting for the probability.

The severe earthquake demand caused a high probability of requiring Method of Repair 3. Of the fifty-five joints exhibiting damage, thirty-five require this repair. Again, the bulk of the job cost is due to the cost for Method of Repair 3. However, the higher joint demand results in higher probabilities on the fragility curves and Method of Repair 4 has a much higher chance of being required than at lower demands. The job cost is more than 23% due to the cost of this repair. Note this repair is required for failed joints. An alternative to repair is to rebuild. The cost for demolishing a reinforced concrete building is $5.74 per SF. For this 66,000 SF building, the cost of demolition is $1.02M after markup.

The adjustment for the repeating repair work is essential to the job cost. Determining the median method of repair for each joint increases the complexity of the assessment of the job cost. However, the reduction for repeating the same method of repair for several joints has a significant impact on the cost of the repair work. Prior to the reduction, the job cost, not including the three markups in Equation 8.2, for the severe earthquake demand was $42.33M per frame. The methods of repair 0 and 3 were required by 55 and 35 joints, respectively. Adjusting the cost for these methods by 80% dropped the job cost to $35.55M. Undoubtedly, a general contractor would make use of this reduction when bidding for the repair project and it should be included here.

Chapter Nine
Conclusions

The previous chapters describe the development of a model for predicting the economic impact of earthquake-induced structural damage of older reinforced concrete beam-column joints. Section 9.1 summarizes the development process. Section 9.2 identifies conclusions that can be drawn from this work. Improvements for the prediction model specific for joints are discussed in Section 9.3. Section 9.4 suggests ways to build on the research results presented here to advance performance-based design and earthquake engineering.

9.1 Summary

The economic impact model presented here links engineering demand parameters that can be predicted using standard structural analysis tools with damage measures that characterize the earthquake response. These damage measures are linked with decision variables that can be used to evaluate earthquake risk by building owners and insurers.

The model development process starts with identification of damage measures specific to the beam-column joints. In Chapter 3, the width of the concrete cracks, the extent of concrete crushing and the failure mechanisms of the joint are the primary measures that 1) characterize the progression of earthquake damage in older beam column joints and 2) may be linked with viable engineering demand parameters and decision variables.

Chapter 4 discusses a series of engineering demand parameters that are appropriate for defining the earthquake load imposed on a joint and indicating damage. Chapter 5 identifies five repair methods from which repair cost and building downtime for repair may be computed. The methods of repair are specific for the damage sustained by the component of interest.

Probability models indicate the probability of exceeding the damage requiring a particular method of repair for a given engineering demand parameter. The data sets used to generate these fragility curves are data points identifying the demand at which a damage state occurs. The relationship between the damage states and the methods of

repair is treated deterministically because structural engineers and general contractors confirmed the appropriate technique. Thus, the probability model predicts the likelihood that a joint will require a specific method of repair. The best fitting distribution function for the data sets is determined using goodness-of-fit tests. Using the best fitting distribution, the fragility curves are generated in Chapter 6 for all considered engineering demand parameters. The same tests determine the best engineering demand parameter for the component.

The cost and building downtime associated with repair of earthquake damage are the decision variables of interest to building owners. They may be used by building owners to evaluate earthquake risk and may be computed given the earthquake induced damage. The economic loss characterized in Chapter 7 is the contract price of the repair work and the downtime for each of the methods of repair identified for use with beam-column joints.

Chapter 8 presents the application of the proposed economic impact model to determine the risk associated with earthquake induced damage of an older reinforced concrete frame structure at moderate and severe earthquake demands.

9.2 Conclusions

The results of this research support a number of conclusions to improve understanding of the prediction of earthquake risk.

1. Four engineering demand parameters were identified as being appropriate for use in predicting earthquake induced joint damage. These parameters are inter-story drift ratio, number of load cycles, a damage index that is a nonlinear function of inter-story drift ratio and number of load cycles, and joint strain. Of these parameters, only drift and the number of load cycles are reported in all of the experimental investigations reviewed for this study. In comparison with drift ratio, joint strain is a demand measure that is independent of beam and column response and thus allows for less uncertainty in applying the damage-prediction model to building frames with different configurations.

2. Earthquake-induced damage sustained by beam-column is characterized by twelve damage states and three failure mechanisms. Each damage state can be linked deterministically to a method of repair. Five methods of repair restore the damaged joint

when used individually or combined. The methods are, in general incremental, so that any damage requiring Method of Repair 1 or higher will require Method of Repair 0 as well.

3. Fragility curves are used to predict the required method of repair for a given engineering demand parameter. Two goodness-of-fit tests determine the most appropriate approach for generating the fragility curves. Four probability distribution functions are compared using the tests and determine the lognormal distribution with parameters evaluated using the Method of Maximum Likelihood is most appropriate.

4. The fragility curves best predict the method of repair when based on a good indicator of damage. The engineering demand parameter determined by the Kolmorogov-Smirnov test to be the best indicator is the nonlinear function of the drift ratio and the number of cycles. However, joint strain is considered independent of the beam and column response and allows for less uncertainty in applying the fragility curves to building frames with different configurations.

5. Cost estimates for methods of repair are necessarily imprecise, because of the large number of potential sources of uncertainty in the work and the variations between jobs. Estimation software provides a starting quote for the labor, materials, and equipment required for each method of repair, but inflating the job cost with markups, such as contingency, is essential to account for the uncertainty.

6. The model was applied to an example existing reinforced concrete building, using joint shear strain as the engineering demand parameter. For a moderate earthquake demand, the model indicated a high probability of requiring Method of Repair 0, cosmetic repair, for most joints in the building. The severe earthquake demand causes greater damage and more than half of the joints require Method of Repair 3. Since temporary shoring is required for Methods of Repair 3 and 4, the job cost increases significantly.

7. The economic impact model is developed step by step so that any step may be updated and improved as the necessary data becomes available. The necessary data is identified in Section 9.3.

9.3 Improvements of the Prediction of the Economic Impact

This report describes the initial development of a model that can be used to predict the dollar loss and downtime resulting from earthquake damage in older reinforced concrete beam-column joints damage. This model development process combines several steps, and at each step in the process, there is an opportunity to include additional information that will improve the model and reduce the uncertainty in the predicted impact of the earthquake damage. The following paragraphs suggest ways in which the model may be improved.

Fragility curves indicating the probability of exceeding a method of repair can be improved by adding additional experimental damage data. Currently, the curves are best for inter-story drift since the data set contains more specimens than the data set for joint strain. Further experimental testing of beam-column joints having these design details and instrumented to measure joint strain would increase the sample size of the data sets and greatly improve the prediction of methods of repair and the reliability of the fragility curves.

Application of the predictive model requires the output of numerical models. The output is an engineering demand parameter defining the structural response of the beam-column joint. The appropriate fragility curve is selected for the given engineering demand parameter. Empirical data from joints of specific design details are used to generate the selected fragility curves. For prediction of the economic impact of the damage sustained by the example building in Chapter 8, the structural response of the modeled joint is assumed to be the same response of the joints from the experimental studies. Calibration of the modeled joint is required to verify this assumption.

Engineers often receive a range of bids from general contractors for the same project. A range of monetary values should accompany each method of repair where this report presents only one base rate cost. More information from professionals from industry is required to generate a distribution of monetary values for the each method. Ultimately, fragility curves should indicate the probability of exceeding a cost for a given method of repair. Data sets would enable generation of the fragility curves and statistical analysis of the uncertainty associated with the cost estimate.

Further investigation of the cost due to nonstructural damage would improve the estimate for earthquake loss. Method of Repair 0 is the cosmetic repair of nonstructural materials. Early in the research, the repair of the material covering the joint was included in the assessment of cost due to structural damage. Initial damage of the joint is considered to trigger damage of the cover material and must be verified by experimental testing. The estimated contract price for the repair work for the example building does not include any repair of damage sustained by the interior column-slab frame or the nonstructural elements.

9.4 Projected Use of Model

The framework for developing the prediction model is applicable to other components. Older beam-column joints are commonly found in buildings on the West Coast. Similarly, a high demand exists for estimating the earthquake risk posed by older reinforced-concrete columns. Development of the model for predicting the economic impact of earthquake induced damage sustained by columns begins with identifying the engineering demand parameters. The displacement demand is readily available in experimental studies done by H. Sezen (2000) and A. Lynn et al (1996). Next, the damage is measured in terms of the extent and direction of cracking and lateral and vertical load capacity. The damage measures are linked to specific methods of repair. Repair of extreme column damage is a method called “can and grout” where the column is encased in a steel sleeve and filled with grout (Coffman and Kapur, 2003). Finally, the cost is estimated using the algorithm presented here.

The objective of the Pacific Earthquake Engineering Research (PEER) Center is to develop probabilistic models predicting and defining earthquake risk. The models are intended to account for the uncertainty in earthquake hazards, nonlinear numerical models, and links between the intensity measure (IM), the engineering demand parameter (EDP), and the decision variable (DV). This approach to predicting earthquake risk is demonstrated by K. Porter et al (2002). Porter uses a Monte Carlo simulation to link the IM to the DV for the Van Nuys building. The economic impact model developed here demonstrates an improved link between the EDP and the DV for the beam-column joints contained in the Van Nuys building in Chapter 8.

List of References

Alire, Daniel, Dawn Lehman, and John Stanton. "Seismic Evaluation of Existing Unconfined Reinforced Concrete Beam-Column Joints." *University of Washington Thesis* (2003).

American Concrete Institute. "Epoxies with Concrete." *ACI SP-21* (1968).

American Concrete Institute. "Building Code Requirement for Reinforced Concrete." *ACI 318-95* (1995).

American Concrete Institute. "Concrete Repair Guide." *ACI 546R-96* (1996).

Bonacci, J.F., and Wight. "Displacement-Based Assessment of Reinforced Concrete Frames in Earthquakes". *ACI SP 162-6* (1996):117-138.

Cheung, Paulay, and Park. "Design of Beam-Column Joints for Seismic Resistance." *ACI SP-123* (1991).

Clyde, Chandra, Chris P. Pantelides, and Lawrence D. Reavely. "Performance-Based Evaluation of Exterior Reinforced Concrete Building Joints for Seismic Excitation." *PEER Report 2000/05* (July 2000).

Coffman, Harvey and Jugesh Kapur. Washington Department of Transportation. In-person interview. (March 2003).

Cole, Jared. T.Y. Lin. In-person interview. (July 2003).

Durrani, Ahmad and James Wight. "Experimental and Analytical Study of Internal Beam to Column Connections Subjected to Reversed Cyclic Loading." *Report UMEE 82R3* (July 1982).

Federal Emergency Management Agency. "NEHRP Guidelines for the Seismic Rehabilitation of Buildings". FEMA-273 (October 1997): 2-5.

Federal Emergency Management Agency. "Repair of Earthquake Damaged Concrete and Masonry Wall Buildings." FEMA 308 (1998): 24-42.

Filiatrault, A. and Isabelle Lebrun. "Seismic Rehabilitation of Reinforced Concrete Joints by Epoxy Pressure Injection Technique". ACI SP 160-3 (December 1996): 73-92.

Haldar, Achintya and Sankaran Mahadevan. Probability, Reliability, and Statistical Methods for Engineering Design. John Wiley & Sons, Inc. (2000).

Hakuto, Shigeru, Robert Park, and Hitoshi Tanaka. “Seismic Load Tests on Interior and Exterior Beam-Column Joints with Substandard Reinforcing Details.” *ACI Structural Journal* 97.1 (January 1997): 11-25.

Hose, Yael, Silva, and Seible. “Development of a Performance Evaluation Database for Concrete Bridge Components and Systems under Simulated Seismic Loads.” *Earthquake Spectra v.16(2)*(2000): 413-442.

Jara, M., Hernandez, Garcia, and Robles. “The Mexico Earthquake of September 19, 1985-Typical Cases of Repair and Strengthening of Concrete Buildings.” *Earthquake Spectra v5(1)* (1989): 175-181.

Joh, O., Goto, and Shibata. “Influence of Transverse Joint and Beam Reinforcement and Relocation of Plastic Hinge Region on Beam-Column Joint Stiffness Deterioration.” *ACI SP-123-8* (1991).

Joh, O., Goto, and Shibata. “Behavior of Reinforced Concrete Beam-Column Joints with Eccentricity.” *ACI SP-123-12* (1991).

Karayannis, C. G., C.E. Chalioris, and K.K. Sideris. “Effectiveness of RC Beam-Column Connection Repair using Epoxy Resin Injections.” Journal of Earthquake Engineering v.2(2) (1998): 217-240.

Lowes, Laura N. "Finite Element Modeling of Reinforced Concrete Beam-Column Bridge Connections." *Dissertation. University of California, Berkeley* (1999).

Lynn, Abraham, Moehle, Mahin, and Holmes. “Seismic Evaluation of Existing Reinforced Concrete Building Columns.” *Earthquake Spectra v.12(4)* (1996).

Mitchell, Denis, DeVall, Kobayashi, Tinawi, and Tso. “Damage to Concrete Structures due to the January 17, 1995 Hyogo-ken Nanbu (Kobe) Earthquake”. *Canadian Journal of Civil Engineering v.23* (1996): 757-777.

Meinheit, Donald and James Jirsa. “The Shear Strength of Reinforced Concrete Beam-Column Joints.” *CESRL Report* (January 1977).

Nakashima, M., K. Ogawa, and K. Inque. “Generic Frame Model for Simulation for Earthquake Responses of Steel Moment Frames.” *Earthquake Engineering and Structural Dynamics v.31* (2001):671-692.

National Estimator 32, software. "National Renovation and Insurance Repair Estimator". *Craftsman Book Company* (2003).

Newman, Alexander. Structural Renovation of Buildings. McGraw-Hill (2001).

Pessiki, S.P., Conley, Gergely, and White. "Seismic Behavior of Lightly-RC Column and Beam-Column Joint Details." *NCEER-90-0014* (1990).

Porter, Keith, Beck, and Shaikhutdinov. "Sensitivity of Building Loss Estimates to Major Uncertain Variables." *Earthquake Spectra v.18* (2002).

Portland Cement Association. "Preliminary Report: The Behavior of Reinforced Concrete Structures in the Caracas, Venezuela Earthquake of July 29, 1967." (1967): 34.

Tasai, A. "Effective Repair with Resin for Bond Failure of RC Members." Proceedings of the 10th World Conference of Earthquake Engineering (1992): 5211-5216.

Runacres, Roger. Contech, Inc. Telephone interview. (February 2003).

Rutherford & Chekene, Consulting Engineers. "Seismic Upgrading Study of the Main Public Library Building San Francisco, CA for the Asian Art Museum at the Civic Center." *Study Report v.1* (September 1992):C.9-C.43.

Savage, Steve. Coughlin, Porter, and Lundeen. In-person interview. (March 2003).

Saxena, Vinita, Deodatis, Shinozuka, and Feng. "Development of Fragility Curves for Multi-Span Reinforced Concrete Bridges." *unpublished MCEER Technical Report* (2000).

Sezen, Halil. "Seismic Behavior and Modeling of Reinforced Concrete column." *Dissertation. University of California, Berkeley* (2002).

Shinozuka, Masanobu, Feng, Lee, and Naganuma. "Statistical Analysis of Fragility Curves." *Journal of Engineering Mechanics* (December 2000).

Shiohara, Hitoshi. "Lifecycle Economic Loss Estimation of R/C frame Structure Subjected to Multiple Earthquake Load Sequences". *US-Japan Workshop of Performance-Based Earthquake Engineering Methodology for Reinforced Concrete Buiding Structures, PEER v.10* (1999):161-173.

Uzmeri, S.M.. "Strength and Ductility of Cast-In-Place Beam-Column Joints." *ACI SP-53-12* (1978).

Walker, Steven, Dawn Lehman, and John Stanton. “Seismic Performance of Existing Reinforced Concrete Beam-Column Joints.” *University of Washington Thesis* (2001).

Zaid, Safaa, Otani, and Shiohara. “Behavior of Reinforced Concrete Beam-Column Connections under EQ Loading.” *University of Tokyo Thesis* (March 2001).

Zhang, Liande and James Jirsa. “A Study of Shear Behavior of Reinforced Concrete Beam-Column Joints”. *PMSFEL Report 82-1* (February 1982).

Appendix A
Design Details of Selected Specimens

Table A.1: Design details for the selected interior joint specimens.

Specimen	Joint Surface Area (in^2)	Beam to Column Width (b_b/b_c)	Joint Cross Sectional Area (in^2)	f'c (psi)	Joint Ties	Column Rebar*	Fy (ksi)	Beam Rebar** (bottom)	Fy (ksi)	Anchorage Length (in)	Column Splice Location
PEER 14	*360*	*1.00*	*288*	*4606*	*none*	*4#6 and 4#7*	*73*	*4#5*	*73*	*18*	*none*
PEER 22	*360*	*1.00*	*288*	*5570*	*none*	*8#9*	*78*	*4#7*	*76.5*	*18*	*none*
CD15 14	*360*	*1.00*	*288*	*4322*	*none*	*4#6 and 4#7*	*73*	*4#5*	*73*	*18*	*none*
CD30 14	*360*	*1.00*	*288*	*6171*	*none*	*4#6 and 4#7*	*73*	*4#5*	*73*	*18*	*none*
CD30 22	*360*	*1.00*	*288*	*5533*	*none*	*8#9*	*78*	*4#7*	*76.5*	*18*	*none*
PADH 14	*360*	*1.00*	*288*	*6218*	*none*	*4#6 and 4#7*	*73*	*4#5*	*73*	*18*	*none*
PADH 22	*360*	*1.00*	*288*	*5259*	*none*	*8#9*	*78*	*4#7*	*76.5*	*18*	*none*
PEER 09	*360*	*1.00*	*288*	*9500*	*none*	*8 #6*	*67*	*3 #7*	*67*	*18*	*none*
PEER 15	*360*	*1.00*	*288*	*9500*	*none*	*8 #10*	*67*	*4 #6*	*125*	*18*	*none*
PEER 41	*360*	*1.00*	*288*	*5000*	*none*	*10 #9*	*67*	*6 #9*	*67*	*18*	*none*
P2	*384*	*0.88*	*256*	*5000*	*none*	*4 #10 S*	*66.2*	*2 #9*	*70*	*16*	*above joint*
P3	*384*	*0.88*	*256*	*4000*	*none*	*6 #8 S*	*66.2*	*2 #9*	*70*	*16*	*above joint*
P4	*384*	*0.88*	*256*	*4000*	*none*	*8 #7 S*	*70.5*	*2 #9*	*70*	*16*	*above joint*
P5	*384*	*0.88*	*256*	*4000*	*2 #3*	*8 #7 S*	*75.1*	*2 #9*	*77*	*16*	*above joint*
P6	*384*	*0.88*	*256*	*3750*	*6 #3*	*8 #7 S*	*62*	*2 #9*	*77*	*16*	*above joint*
P7	*384*	*0.88*	*256*	*3000*	*none*	*4 #10 S*	*73*	*2 #8 E*	*69*	*12*	*above joint*
P8	*384*	*0.88*	*256*	*3000*	*none*	*4 #10 S*	*66.8*	*2 #6 E*	*69*	*12*	*above joint*
P9	*384*	*0.88*	*256*	*4000*	*none*	*4 #10 S*	*66.8*	*2 #8 E*	*60*	*12*	*above joint*
M II	*324*	*0.85*	*234*	*6060*	*2 #4*	*8 #10*	*65.1*	*3 #8*	*70.3*	*18*	*none*
X1	*235.13*	*0.77*	*203.06*	*4646.7*	*2 #4*	*8 #8*	*60*	*4 #6*	*50*	*14.25*	*none*
X2	*235.13*	*0.77*	*203.06*	*4863.3*	*3 #4*	*8 #8*	*60*	*4 #6*	*50*	*14.25*	*none*
X3	*235.13*	*0.77*	*203.06*	*4400*	*2 #4*	*4 #7*	*48*	*3 #6*	*50*	*14.25*	*none*
JXO-B1	*162.604*	*0.67*	*139.24*	*3901*	*3 #2*	*14 #4*	*58.6*	*3 #4*	*58.6*	*11.8*	*none*
JXO-B2	*162.604*	*0.50*	*139.24*	*3268.7*	*3 #2*	*14 #4*	*58.6*	*3 #4*	*53.8*	*11.8*	*none*
JXO-B8-LH	*162.604*	*0.93*	*139.24*	*3429.3*	*3 #2*	*14 #4*	*58.6*	*3 #4*	*53.8*	*11.8*	*none*

Table A.2: Design details for the selected exterior joint specimens.

Specimen	Joint Surface Area (in^2)	Beam to Column Width (b_b/b_c)	Joint Cross Sectional Area (in^2)	f'c (psi)	Joint Ties	Column Rebar*	Fy (ksi)	Beam Rebar** (bottom)	Fy (ksi)	Anchorage of Beam Rebar	Column Splice Location
C 2	288.0	0.89	216.0	6700	none	8 #7	68.1	4 #9	65.9	90degree bendinto joint core	above joint
C 4	288.0	0.89	216.0	5940	none	8 #7	68.1	4 #9	65.9	90degree bendinto joint core	above joint
C 5	288.0	0.89	216.0	5370	none	8 #7	68.1	4 #9	65.9	90degree bendinto joint core	above joint
C 6	288.0	0.89	216.0	5820	none	8 #7	68.1	4 #9	65.9	90degree bendinto joint core	above joint
U 2	300.0	0.8	225.0	5015	none	8 #8	48.6	2 #9	50.6	90degree bendinto joint core	none
U 6	300.0	1	225.0	5360	8 #4	8 #8	49.3	2 #9	51.5	90degree bendinto joint core	none
U 7	300.0	1	225.0	4460	4 #4	8 #8	49.3	2 #9	51.1	90degree bendinto joint core	none
U 8	300.0	1	225.0	3820	8 #4	8 #8	56.5	3 #9	51.1	90degree bendinto joint core	none
O 7	349.8	0.65	321.8	4500	1 #4	4 #8	44.7	2 #8	44.7	90degree bend out of joint core	none

Table A.3: Response of the selected specimens vary due to variety of values for the peak shear stress and constant axial load during testing.

Specimen	Peak Shear Stress Ratio (stress/f'c)	Axial Load Ratio % (load/column gross capacity)	Bond Strength Ratio (h_c/b_d)
PEER 14	*0.16*	*10.9*	*28.8*
PEER 22	*0.20*	*9.0*	*20.6*
CD15 14	*0.18*	*11.6*	*28.8*
CD30 14	*0.14*	*8.1*	*28.8*
CD30 22	*0.21*	*9.0*	*20.6*
PADH 14	*0.15*	*8.0*	*28.8*
PADH 22	*0.22*	*9.5*	*20.6*
PEER 09	*0.13*	*10.0*	*20.6*
PEER 15	*0.19*	*10.0*	*24.0*
PEER 41	*0.17*	*10.0*	*16.0*
P2	*0.19*	*27.3*	*14.2*
P3	*0.21*	*34.2*	*14.2*
P4	*0.20*	*34.2*	*14.2*
P5	*0.22*	*34.2*	*14.2*
P6	*0.19*	*36.5*	*14.2*
P7	*0.19*	*45.6*	*12.0*
P8	*0.19*	*45.6*	*16.0*
P9	*0.15*	*9.8*	*12.0*
M II	*0.25*	*24.8*	*18.0*
X1	*0.20*	*5.8*	*19.0*
X2	*0.19*	*5.6*	*19.0*
X3	*0.16*	*5.4*	*19.0*
JXO-B1	*0.12*	*14.6*	*23.60*
JXO-B2	*0.24*	*16.7*	*23.60*
JXO-B8-LH	*0.19*	*16.7*	*23.60*
C 2	*0.15*	*10*	*16*
C 4	*0.16*	*25*	*16*
C 5	*0.19*	*25*	*16*
C 6	*0.17*	*10*	*16*
U 2	*0.12*	*46.1*	*11.56*
U 6	*0.14*	*43.1*	*11.56*
U 7	*0.16*	*51.8*	*11.56*
U 8	*0.22*	*60.5*	*11.56*
O 7	*0.045*	*0*	*17.94*

Appendix B

Joint Strain Derived From the Curvature Measurements

Joint strain can be measured by removing the flexural response of the beams and columns and the slip due to bond loss. The drift is a measure of the beam and column end displacements. The curvature of the beams and column contribute to the end displacement. If the length of the beams and columns are instrumented for measurement of the curvature, this method of deriving the joint strain is possible. However, defining the value of the bond slip is very difficult. For method of deriving the joint strain defined in this paper, the slip is included with the deformation of the joint. This can be seen in the equation B.1

$$\begin{aligned} \Delta_{jo\,\mathrm{int}+slip} = \\ \Delta_{demand} - \Delta_{column\ flexure} - \Delta_{beam\ flexure} = \\ \Delta_{demand} - \left(\Delta_{top\ column} - \Delta_{bottom\ column}\right) - \left(\Delta_{right\ beam} - \Delta_{left\ beam}\right) \end{aligned} \qquad \text{B.1}$$

The flexural response is evaluated using the curvature measurements of the beams and columns. The curvature, $\phi = \frac{\theta}{x}$, is obtained from previous experiments where the change in length over various segments of the columns and beams was measured.

The component is divided into segments along which the curvature is measured. Each segment has a length, x and height, h. The deformation is the difference of the elongation of the top and the bottom of the segment, Δt and Δb, respectively. If the section is assumed to elongate on both ends of the measured segment, the deformation is measured according to equation B.2.

$$\theta = \frac{\Delta b - (-\Delta t)}{h} \qquad \text{B.2}$$

However, if the deformation of the section assumed to be fixed on one end and elongated on the other end, the deformation is reduced by one half as shown in equation B.3. This is the case for the evaluation of the curvature of the beams and columns where the end attached to the joint is assumed to be fixed.

$$\theta = \frac{\frac{\Delta b}{2} - \frac{-\Delta t}{2}}{h} = \frac{\Delta b - (-\Delta t)}{2 * h} \qquad \text{B.3}$$

The angle, β, is the rotation due to the curvature over the segment and is evaluated as follows:

$$\beta_i = \phi_i x_i \qquad \text{B.5}$$

Using the curvature measurements, the deformation in the columns and beams due to flexure can be evaluated. The overall deflection, or story drift, is a function of the flexure of the columns and beams, the deformation of the joint, and the slip due to bond degradation in the beam reinforcement. Thus, the deformation due to flexure can be removed from the story drift and the remaining deformation is attributed to the joint deformation plus the slip. The column and beam flexure is calculated using the curvature measurement to determine the rotation and ultimately the deflection of the component ends due to flexure.

$$\Delta_{beam} = \left\{ \frac{1}{2}\beta_i x_i + \left(\beta_i + \frac{1}{2}\beta_{i+1} \right) x_{i+1} + \left(\beta_i + \beta_{i+1} + \frac{1}{2}\beta_{i+n} \right) x_{i+n} \right\} * \frac{L_{column}}{L_{beam}} \qquad \text{B.6}$$

$$\Delta_{column} = \left\{ \frac{1}{2}\beta_i x_i + \left(\beta_i + \frac{1}{2}\beta_{i+1} \right) x_{i+1} + \left(\beta_i + \beta_{i+1} + \frac{1}{2}\beta_{i+n} \right) x_{i+n} \right\} \qquad \text{B.7}$$

These equation are applicable to the specimens tested at the University of Washington. The data from these tests provided the curvature measurements and the inter-story drift representing the entire test. A response hysteresis based on these measurements is developed for specimen PEER 22 and is shown in figure 4.1. The damage states are marked at the joint demand at which they were observed.

Appendix C

Determining best Engineering Demand Parameter

Table C.1: Data Set One: Kolmogorov-Smirnov test results comparing the engineering demand parameters. Note sample size for uncertainty.

	Repair Groups	0	1	2	3	4
Sample Size		20	16	24	15	11
Critical Value	α=0.05	0.2941	0.3273	0.26934	0.3376	0.3912
Drift		-0.3911	0.22645	0.90322	1.2801	1.3315
	ζ	0.55037	0.61897	0.34107	0.42914	0.50772
	K-S, Dn	0.1639	0.1786	0.17497	0.20468	0.25574
	P(Dn<Dna)	0.61593	0.64276	0.41792	0.50707	0.41041
Cycles	λ	1.1658	0.81475	2.1224	2.5993	3.1251
	ζ	0.986	1.3471	1.1775	1.2021	1.263
	K-S, Dn	0.18557	0.16485	0.19201	0.15759	0.30088
	P(Dn<Dna)	0.45515	0.73815	0.30588	0.81671	0.22578
F(Drift, Cycles)	λ	2.1027	2.483	3.1604	3.4596	3.5759
	ζ	0.48081	0.34702	0.17333	0.17497	0.14698
	K-S, Dn	0.22515	0.18724	0.10956	0.31566	0.15279
	P(Dn<Dna)	0.23009	0.58266	0.92044	0.079691	0.94133
Sample Size		5	10	10	9	1
Critical Value	α=0.05	0.5633	0.4093	0.4093	0.4300	0.9750
Joint Strain	λ	-8.8626	-6.1251	-5.7635	-4.8735	-3.1817
	ζ	2.6085	3.1994	3.2836	2.8692	6.8715
	K-S, Dn	0.3176	0.3451	0.2933	0.3861	0.5000
	P(Dn<Dna)	0.6039	0.1454	0.3002	0.1025	0.8438

Table C.2: Data Set Two: Kolmogorov-Smirnov test results comparing the engineering demand parameters. Note sample size for uncertainty. The nonlinear function of the story drift and number of cycles provides the best fit, $P(D_n<D_n^a)$ value.

	Repair Groups	0	1	2	3	4
Sample Size		25	25	25	22	11
Critical Value	α=0.05	0.2641	0.2641	0.2641	0.2809	0.3912
Drift	λ	-0.2318	0.4180	0.9167	1.2809	1.3315
	ζ	0.6183	0.4853	0.3407	0.3614	0.5020
	K-S, Dn	0.1279	0.1648	0.1833	0.1476	0.2533
	P(Dn<Dna)	0.7800	0.4690	0.3369	0.6891	0.4224
Cycles	λ	0.8218	1.5683	2.1722	2.7615	3.1251
	ζ	1.1255	1.4507	1.1792	0.9217	1.0891
	K-S, Dn	0.2074	0.1402	0.1885	0.1661	0.2725
	P(Dn<Dna)	0.2057	0.6765	0.3046	0.5396	0.3329
F(Drift, Cycles)	λ	2.1691	2.7422	3.1763	3.4821	3.5759
	ζ	0.4773	0.4595	0.1870	0.1721	0.1470
	K-S, Dn	0.2250	0.1534	0.1051	0.2186	0.1528
	P(Dn<Dna)	0.1376	0.5621	0.9323	0.2141	0.9413
Sample Size		10	10	10	9	1
Critical Value	α=0.05	0.4093	0.4093	0.4093	0.4300	0.9750
Joint Strain	λ	-7.1110	-6.1251	-5.7635	-4.8735	-3.1817
	ζ	3.2142	3.1994	3.2836	2.8692	6.8715
	K-S, Dn	0.1998	0.3451	0.2933	0.3861	0.5000
	P(Dn<Dna)	0.7719	0.1454	0.3002	0.1025	0.8438

Table C.3: Data Set Three: Kolmogorov-Smirnov test results comparing the engineering demand parameters. Note sample size for uncertainty. The nonlinear function of the story drift and number of cycles provides the best fit, $P(D_n<D_n^a)$ value.

	Repair Groups	0	1	2	3	4
Sample Size		4	4	8	12	11
Critical Value	α=0.05	0.6239	0.6239	0.4543	0.3754	0.3912
Drift	λ	-0.8998	0.2322	0.9517	1.2217	1.3315
	ζ	0.4881	0.5747	0.4526	0.2999	0.3053
	K-S, Dn	0.3405	0.3171	0.2161	0.3259	0.1681
	P(Dn<Dna)	0.6429	0.7282	0.7991	0.1243	0.8858
Cycles	λ	0.2291	0.7997	1.9700	2.6728	3.1251
	ζ	0.8457	1.1721	1.4016	0.9129	0.6412
	K-S, Dn	0.3568	0.3359	0.2894	0.1775	0.1773
	P(Dn<Dna)	0.5837	0.6598	0.4435	0.8044	0.8436
F(Drift, Cycles)	λ	1.5637	2.5233	3.1980	3.4419	3.5759
	ζ	0.4223	0.2772	0.2108	0.1871	0.1470
	K-S, Dn	0.3227	0.3439	0.1974	0.3182	0.1528
	P(Dn<Dna)	0.7080	0.6305	0.8776	0.1417	0.9413
Sample Size		2	4	8	8	1
Critical Value	α=0.05	0.8419	0.6239	0.4543	0.4543	0.9750
Joint Strain	λ	-10.9745	-8.6064	-5.0924	-4.2255	-3.1817
	ζ	2.8760	3.7631	2.5240	2.1107	2.4931
	K-S, Dn	0.3413	0.2892	0.2664	0.4017	0.5000
	P(Dn<Dna)	0.9226	0.8237	0.5508	0.1123	0.8438

Appendix D
Questions and Answers from Personal Interviews

Questions presented to industry professionals:

Confirming Repair Techniques:

1. Are there additional repair techniques that should be considered?
2. Residual deformation has been associated with repair techniques #2 and #3 when higher levels of damage are anticipated. At what drift level would the residual deformation be (a) ignored, (b) corrected, and (c) cause the building to be replaced?
3. How significantly do the environmental conditions affect material selection for a RC component in a building where cladding and other non-structural elements provide protection?
4. Are these repair techniques appropriate for beam-column joints as well as columns?
5. Are there sub-divisions within the repair techniques listed above that are associated with substantially different costs?
6. A variety of application processes accompany these repair techniques, e.g. Vacuum versus High-pressure injection. Why would a more expensive process be selected?

Linking Correct Repair Technique to Damage in Joints:

7. What damage measures would trigger use of Repair Technique #1 - epoxy injection?
8. What damage measures would trigger use of Repair Technique #2 - patching? Diagonal or vertical cracks $\geq$ 0.04" or 0.75"? Onset of spalling?
9. What damage measures would trigger use of Repair Technique #3 – replacement of joint? Onset of significant spalling? Loss of bond strength within the joint? First sign of buckling of reinforcing steel?
10. What damage measure would result in an unrepairable joint? Significant buckling of longitudinal reinforcing steel? Fracture of transverse reinforcing steel? Fracture of longitudinal reinforcing steel? Fracture of multiple longitudinal reinforcing bars?

Linking Correct Repair Technique to Damage in Columns:

For the column considered to exhibit a flexural response mechanism,

11. What damage measures would trigger use of Repair Technique #1 - epoxy injection? Horizontal (flexural) cracks ≥ 0.75"? Horizontal (flexural) cracks distributed over a height extending 50% of the column cross-section depth?
12. What damage measures would trigger use of Repair Technique #2 - patching? Horizontal (flexural) cracks ≥ 2 mm? Horizontal (flexural) cracks distributed over a height extending 50% of the column height? Onset of spalling? Onset of significant spalling?
13. What damage measures would trigger use of Repair Technique #3 – replacement of column? First sign of buckling of reinforcing steel? Significant buckling of longitudinal reinforcing steel?
14. What damage measures would result in an unrepairable column? Fracture of transverse reinforcing steel? Fracture of longitudinal reinforcing steel? Fracture of multiple longitudinal reinforcing bars?

For the column considered to exhibit a brittle (shear or bond-failure) response mechanism,

15. What damage measures would trigger use of Repair Technique #1 - epoxy injection? Visible diagonal cracking? Sources indicate that shear cracks >0.04" can not be repaired using epoxy injection. Is this true for vertical cracks as well?
16. What damage measures would result in an unrepairable column? What is the appropriate repair for the onset of the shear or bond-failure mechanisms? Shear mechanism is defined by diagonal cracking over 67% of the column depth and crack width > 0.08". Bond-failure is cracks extending vertically over 67% of column depth and crack width > 0.08".

Defining Loss due to Repair:

17. Loss has been defined as the unit cost of material, unit cost of equipment, and the unit cost of personnel plus the amount of downtime in terms of days. Is this the same definition loss used for estimation in practice?
18. Is it possible to set-up rules to estimate the start-up cost of the repair technique. Start-up cost would include mobilization and demolition to the extent required for the level of damage. For example, how can I estimate the start-up cost associated with epoxy injection of 10 columns versus 100 columns?
19. Is it possible to estimate the cost of the architectural finish?
20. What is the per-unit material cost associated with the repair technique? Will this vary substantially if the concrete crack widths are 0.05 in. versus 0.2 in.? Or if the height of spalling on a concrete column is 12 inches versus 24 inches?
21. How long will it take to accomplish repair of a single unit and what would be the labor rate? Will repair time vary substantially if there are 10 units versus 100 units?
22. Can the building be occupied while repair is accomplished?

Interview with S. Savage:

Comments regarding questions:

1. Question 1: Repair methods are complete.
2. Question 2: For steel, correction of residual deformation depends on type of system. For concrete, correction of residual deformation is not possible. The offset may be within the limits of the building code and could be ignored.
3. Question 4: Repair methods for columns in addition to those provided are wrapping, ie. jacketing. A combination of epoxy injection and jacketing would be most applicable in damage seen in figure (Hakuto ext.)
4. Question 7: When determining the "trigger" damage state for a repair method, analysis of capacity is best. If not possible, then repair will be recommended.
5. Question 11: Determining "trigger" for repair of flexural response of column requires analysis, if available, to determine amount of inelastic response already used. Flexural cracks will require less amount of repair.
6. Epoxy resin injection: Lower bound crack width is 1/16".
7. New concrete: Remove damaged joint core by jackhammering.
8. Question 12: Patching of damaged concrete can be used until crushing of concrete occurs. Not jacketing of flexural response should be required.
9. Questions 13 & 14: Enlargement due to concrete crushing repaired with jacket. Must be observant of stiffness changes and shear force capacity after repair for future analysis.
10. Cost effiency: Jacketing is best if several columns are to be repaired. Replacement is best if only one column is damaged.
11. Question 15: The "trigger" for replacement or jacketing of brittle response of column is when the cracks get into middle third of column. Cracks just at end (seen in figure (Sezen)) would require replacing or jacketing.
12. Cost increases: Replacement of column requires shoring. This increases the cost beyond that expected for jacketing.
13. Question 17: Cost of repair is determined by contractors.
14. Question 18: Developing rules for start up cost would involve establishing a $/ft^2$ cost based on quantity of components.
15. Must specify the following for estimate from general contractor:
    a. Close environment (office) versus open environment
    b. Vintage
    c. Quality
    d. Type of use
    e. Partitioning material will drive cost

Interview with H. Coffman and J. Kapur:

Comments regarding cost:

1. Contributing factors to cost
    a. Lack of contractors
    b. Lack of labor
    c. Lack of equipment
2. Traffic control
    a. High tolerance - allow work to be done during day
    b. Low tolerancce - require work to be done at night at time and a half

Comments regarding repair:

3. Epoxy resin injection
    a. Use when crack width is >1mm (0.025")
    b. Potential corrosion of rebar
    c. May use if smaller crack lends to reduced capacity
    d. Lineal ft. of cracks to determine amt./ cost of adhesive
    e. **Cost is $10/ft**.
4. Spalling
    a. paint rebar with epoxy to prevent corrosion
    b. place chicken wire after spalled concrete is removed.
5. Steel jacketing
    a. Square column may be repaired with circular can and filled with grout
    b. Cost is $1000/ft.
6. Damage specific to bridge
    a. Little experience with damage caused by EQ in Washington, however may be comparable to damage due to scour.
    b. concetrated in superstructure
    c. Shoring is done immediately to prevent additional damage and continue use of bridge
    d. Monitoring of cracks with crack gauges to decide if repair is neccessary.
    e. Restoring residual deformation can be done using jacks and rollers.
    f. column
        i. cracking at cover indicates cracking through width
        ii. chip off cover concrete if
            1. core into core to test for internal damage
            2. hammer test yields spalling
        iii. crushing and cracking of core
            1. remove substantial amt. of concrete
            2. replace concrete
7. Note that our repair method #3 is considered repair level #1 for WSDOT. Prior to that, the damage is not severe enough.

Appendix E
Determining Best Distribution

Table E.1: Kolmogorov-Smirnov test results for the four considered distributions.

	Repair Groups	0	1	2	3	4
Critical Value	α=0.05	0.294	0.327	0.264	0.338	0.375
Lognormal	λ	-0.433	0.253	0.935	1.293	1.337
	ζ	0.513	0.493	0.352	0.309	0.264
	K-S, D_n	0.190	0.175	0.154	0.336	0.168
	$P(D_n<D_n^a)$	0.428	0.668	0.554	0.052	0.856
Normal	μ	0.780	1.409	2.610	3.693	3.841
	σ	0.428	0.740	0.948	1.169	1.033
	K-S, D_n	0.226	0.237	0.148	0.323	0.185
	$P(D_n<D_n^a)$	0.226	0.288	0.610	0.068	0.761
Weibull	k	1.912	2.005	2.986	3.462	4.132
	w_1	0.879	1.590	2.924	4.106	4.230
	K-S, D_n	0.455	0.656	1.000	1.000	1.000
	$P(D_n<D_n^a)$	0.000	0.000	0.000	0.000	0.000
Beta	q	1.250	1.250	1.250	2.000	2.000
	r	2.750	2.750	2.750	2.000	2.000
	K-S, D_n	0.640	0.906	1.000	1.000	1.000
	$P(D_n<D_n^a)$	0.000	0.000	0.000	0.000	0.000

Table E.2: Chi-Square test results for the best two of four consider distributions.

Repair Groups	0	1	2	3	4
Error Lognormal	3.4	2.357	4.46	10.08	2.0402
Error Normal	7.89	3.916	3.79	11.46	1.4813
Critical Value	5.99	5.991	5.99	5.991	5.991
Bins	#	#	#	#	#
1	5	7	10	1	4
2	11	6	4	8	2
3	1	1	9	1	2
4	1	0	0	1	0
5	2	2	2	4	4
Total	20	16	25	15	12

Table E.3: Chi-Square test results for the best of the methods of evaluating the parameters of the lognormal distribution.

Repair Groups	0	1	2	3	4
Error Lognormal (Moments)	3.4	2.357	4.46	10.08	2.0402
Error Lognormal (Maximum Likelihood)	3.55	2.259	3.06	6.762	0.4982
Critical Error Value	5.99	5.991	5.99	5.991	5.991
Bins	#	#	#	#	#
1	5	7	10	1	4
2	11	6	4	8	2
3	1	1	9	1	2
4	1	0	0	1	0
5	2	2	2	4	4
Total	20	16	25	15	12

Appendix F
Modeling of Beam-Column Joints in OpenSEES

Theiss, Adam. *University of Washington MSCE candidate* (2003).

The numerical output is generated using the data gathered from a University of Washington investigation of the Holiday Inn hotel in Van Nuys, CA. A model of the building was developed and a displacement controlled pushover analysis was undertaken using OpenSEES. The two dimensional model simplified the building to an interior gravity frame that was rigidly joined to an exterior moment frame. The frames consisted of elastic beams and columns with plastic behavior focused in hinges at the ends of the elements. The joint elements used in the model were based on a scissors model. This type of joint model consists of a rotational spring that is introduced to act as the joint that constrains the otherwise independent column and beam. The joint is the pivot point and the columns and beams are the blades of the scissors. The material models that were used to model the joint, concrete, and steel behavior were developed to take into account issues such as lack of confining reinforcement in elements and joints, torsion, shear, and splice failures.

Additional references:

Paspuleti, Chaitanya. “Seismic Analysis of An Older Reinforced Concrete Structure.” *University of Washington Thesis* (2002).